MRI for Technologists

4712-302 Musculoskeletal MRI

PROGRAM INFORMATION

MRI for Technologists is a training program designed to meet the needs of radiologic technologists entering or working in the field of magnetic resonance imaging (MRI). These units are designed to augment classroom instruction and on-site training for radiologic technology students and professionals planning to take the review board examinations, as well as to provide a review for those looking to refresh their knowledge base in MR imaging.

Original Release Date: **May 2004**
Material Review Date **June 2018**
Expiration Date: **August 1, 2021**

This material will be reviewed for continued accuracy and relevance. Please go to www.icpme.us for up-to-date information regarding current expiration dates.

OVERVIEW

The skill of the technologist is the single most important factor in obtaining good quality diagnostic images. A successful MRI examination is the culmination of many factors under the direct control of the technologist.

Musculoskeletal MRI introduces the learner to the basic imaging requirements for high-quality image acquisition, technical considerations, advanced MSK MRI applications, upper and lower extremity anatomy, and common pathology. Scan protocols are included.

After completing this educational material, the reader should be able to:

- Effectively balance the parameters of spatial resolution, signal-to-noise ratio, and image contrast to optimize image detail
- Properly position the patient and area of interest to ensure diagnostic images
- Explain the indications for and differences between arthrography and contrast-enhanced imaging
- Discuss advanced MSK MRI applications
- Reduce metal artifact in the imaging of prosthetic joints
- Describe and discuss upper and lower extremity anatomy and pathology
- Apply appropriate planes of acquisition for each area of interest

Thomas Schrack, BS, ARMRIT
Manager, MR Education and Technical Development
Fairfax Radiological Consultants
Fairfax, VA

Currently serving as Manager of MR Education and Technical Development at Fairfax Radiological Consultants in Fairfax, VA, Thomas Schrack served as Adjunct Faculty Instructor for Northern Virginia Community College from more than 10 years, teaching MR physics and clinical procedures. He serves on the Board of Examiners of the American Registry of Magnetic Resonance Imaging Technologists (ARMRIT) and in 2013 was elected to the Board of Directors. Mr. Schrack is also the Co-Founder and Program Director of the Tesla Institute of MRI Technology, a school offering certification in MRI for radiologic technologists and others interested in entering the field of MRI.

Mr. Schrack is the author of *Echo Planar Imaging: An Applications Guide,* GE Healthcare, 1996, and contributing author, *Magnetic Resonance Imaging in Orthopaedics & Sports Medicine* with David Stroller, MD, 1997. Working with International Center for Postgraduate Medical Education, Mr. Schrack has authored or co-authored several units of the *MRI for Technologists* series, including *MRI Systems and Coil Technology, MR Image Postprocessing and Artifacts, Patient and Facility Safety in MRI, MRI Contrast Agent Safety, Advanced MRI Neurological Applications, MRI of the Brain and Spine, Musculoskeletal MRI, Clinical Magnetic Resonance Angiography, MRI of the Body, and Cardiac MRI.*

Mr. Schrack is a graduate of The Pittsburgh NMR Institute, James Madison University, and Northern Virginia Community College.

EDUCATIONAL CREDIT

This program has been approved by the American Society of Radiologic Technologists (ASRT) for 3.5 hours ARRT Category A continuing education credit.

HOW TO RECEIVE CREDIT

Estimated time to complete this activity is 3.5 hours. The posttest and evaluation are required to receive credit and must be completed online.

- In order to access the posttest and evaluation, enroll in the online course at icpme.us
- Read the entire activity either online or download and print the pdf.
- Log in to your account at icpme.us to complete the posttest and evaluation, accessible through the course link in your account.
- A passing grade of at least 75% is required to be eligible to receive credit.
- You may take the test up to three times.
- Upon receipt of a passing grade, you will be able to print a certificate of credit from your online account.

SPONSORED BY

icpme
Your Partner in Medical Education

SUPPORTED BY AN EDUCATIONAL GRANT FROM

Bayer HealthCare
Pharmaceuticals

FDA Drug Safety Communication: FDA warns that gadolinium-based contrast agents (GBCAs) are retained in the body; requires new class warnings

https://www.fda.gov/Drugs/DrugSafety/ucm589213.htm Accessed June 14, 2018.

05-16-2018 Update

In addition to approving the updated prescribing information concerning the gadolinium retention safety issues described in the Drug Safety Communication below, FDA has also approved new patient Medication Guides for all GBCAs.

Health care professionals and patients can access the patient Medication Guides according to the GBCA drug name* on the Medication Guides webpage, or the latest prescribing information by searching in Drugs@FDA.

All MRI centers should provide a Medication Guide the first time an outpatient receives a GBCA injection or when the information is substantially changed. In general, hospital inpatients are not required to receive a Medication Guide unless the patient or caregiver requests it. A health care professional who determines that it is not in a patient's best interest to receive a Medication Guide because of significant concerns about its effects may direct that it not be provided to that patient; however, the Medication Guide should be provided to any patient who requests the information.†

*The brand names of the GBCAs can be found in Table 1 below.
†For more information on distribution of Medication Guides, see the Guidance Document, the Drug Info Rounds Video, or the Code of Federal Regulations at 21 CFR 208.26.

This is an update to the FDA Drug Safety Communication: FDA identifies no harmful effects to date with brain retention of gadolinium-based contrast agents for MRIs; review to continue issued on May 22, 2017.

12-19-2017 Safety Announcement

The U.S. Food and Drug Administration (FDA) is requiring a new class warning and other safety measures for all gadolinium-based contrast agents (GBCAs) for magnetic resonance imaging (MRI) concerning gadolinium remaining in patients' bodies, including the brain, for months to years after receiving these drugs. Gadolinium retention has not been directly linked to adverse health effects in patients with normal kidney function, and we have concluded that the benefit of all approved GBCAs continues to outweigh any potential risks.

However, after additional review and consultation with the Medical Imaging Drugs Advisory Committee, we are requiring several actions to alert health care professionals and patients about gadolinium retention after an MRI using a GBCA, and actions that can help minimize problems. These include requiring a new patient Medication Guide*, providing educational information that every patient will be asked to read before receiving a GBCA. We are also requiring manufacturers of GBCAs to conduct human and animal studies to further assess the safety of these contrast agents.

GBCAs are used with medical imaging devices called MRI scanners to examine the body for problems such as cancer, infections, or bleeding. GBCAs contain gadolinium, a heavy metal. These contrast agents are injected into a vein to improve visualization of internal organs, blood vessels, and tissues during an MRI, which helps health care professionals diagnose medical conditions. After being administered, GBCAs are mostly eliminated from the body through the kidneys. However, trace amounts of gadolinium may stay in the body long-term. Many GBCAs have been on the market for more than a decade.

Health care professionals should consider the retention characteristics of each agent when choosing a GBCA for patients who may be at higher risk for gadolinium retention (see Table 1 listing GBCAs). These patients include those requiring multiple lifetime doses, pregnant women, children, and patients with

inflammatory conditions. Minimize repeated GBCA imaging studies when possible, particularly closely spaced MRI studies. However, do not avoid or defer necessary GBCA MRI scans.

Patients, parents, and caregivers should carefully read the new patient Medication Guide* that will be given to you before receiving a GBCA. The Medication Guide explains the risks associated with GBCAs. Also tell your health care professional about all your medical conditions, including:

- If you are pregnant or think you might be pregnant
- The date of your last MRI with gadolinium and if you have had repeat scans with gadolinium
- If you have kidney problems

There are two types of GBCAs based on their chemical structures: linear and macrocyclic (see Table 1 below). Linear GBCAs result in more retention and retention for a longer time than macrocyclic GBCAs. Gadolinium levels remaining in the body are higher after administration of Omniscan (gadodiamide) or OptiMARK (gadoversetamide) than after Eovist (gadoxetate disodium), Magnevist (gadopentetate dimeglumine), or MultiHance (gadobenate dimeglumine). Gadolinium levels in the body are lowest after administration of Dotarem (gadoterate meglumine), Gadavist (gadobutrol), and ProHance (gadoteridol); the gadolinium levels are also similar across these agents.

*The Medication Guide will be posted once it is approved.

Table 1. FDA-Approved GBCAs*

Brand name	Generic name	Chemical Structure
Dotarem†	gadoterate meglumine	Macrocyclic
Eovist	gadoxetate disodium	Linear
Gadavist†	gadobutrol	Macrocyclic
Magnevist	gadopentetate dimeglumine	Linear
MultiHance	gadobenate dimeglumine	Linear
Omniscan‡	gadodiamide	Linear
OptiMARK‡	gadoversetamide	Linear
ProHance†	gadoteridol	Macrocyclic

*Linear GBCAs result in more gadolinium retention in the body than macrocyclic GBCAs.
†Gadolinium levels remaining in the body are LOWEST and similar after use of these agents.
‡Gadolinium levels remaining in the body are HIGHEST after use of these agents.

To date, the only known adverse health effect related to gadolinium retention is a rare condition called nephrogenic systemic fibrosis (NSF) that occurs in a small subgroup of patients with pre-existing kidney failure. We have also received reports of adverse events involving multiple organ systems in patients with normal kidney function. A causal association between these adverse events and gadolinium retention could not be established.

We are continuing to assess the health effects of gadolinium retention in the body and will update the public when new information becomes available. We are requiring the following specific changes to the labeling of all GBCAs:

- A *Warning and Precaution*
- Changes related to gadolinium retention in the *Adverse Reactions, Pregnancy, Clinical Pharmacology*, and *Patient Instructions* sections

We urge patients and health care professionals to report side effects involving GBCAs or other medicines to the FDA MedWatch program.

4712-302

Musculoskeletal MRI

*Please note: items in **bold** can be found in the glossary.*

After completing this material, the reader should be able to:

- Effectively balance the parameters of spatial resolution, signal-to-noise ratio, and image contrast to optimize image detail
- Properly position the patient and area of interest to ensure diagnostic images
- Explain the indications for and differences between arthrography and contrast-enhanced imaging
- Discuss advanced MSK MRI applications
- Reduce metal artifact in the imaging of prosthetic joints
- Describe and discuss upper and lower extremity anatomy and pathology
- Apply appropriate planes of acquisition for each area of interest

OVERVIEW

Musculoskeletal (MSK) magnetic resonance imaging (MRI) is the evaluation of muscles, bones, and joints in the body using MRI technology. While it may appear that advanced technical developments in MR applications have centered on neurological and body imaging techniques, there is no application in MR that requires greater spatial resolution than MSK imaging and none where positioning of the area of interest is so critical. In fact, there is arguably no MR application that requires more from both the MR system and the technologist than MSK. No application has enjoyed as many benefits of hardware and software development, including advances in image reconstruction speed, gradient slew rate, surface coil development, and pulse sequence design as MSK MRI.

MSK MR imaging is a demanding application. The imaging of large muscles and gross bony pathologies does not typically require extreme detail because these pathologies are large, like muscle tears and bony tumors, and their contrast mechanisms are well known. Conversely, MSK MRI of the joints requires exquisite detail. The anatomical structures of joints are extremely small, often only a few millimeters. Whether a small partial tear of the labrum in the hip or a small medial meniscal tear in the knee, the pathologies being evaluated with MR joint imaging are not only small but subtle, with varying degrees of contrast compared to normal tissue.

The key to MSK MR imaging, specifically joint imaging, is in *seeing detail.* In order to obtain the greatest detail in MSK MRI, all of the system's imaging components must be carefully adjusted. To obtain the highest visible detail in the MR image, the technologist must thoroughly understand the elements of spatial resolution, signal-to-noise ratio, and image contrast, as well as the complexities and ramifications of surface coil selection, proper anatomical positioning, and optimal protocol selection, all balanced to acquire the required diagnostic images within a reasonable scan time.

BASIC REQUIREMENTS

The primary requirements for a highly diagnostic MR image are spatial resolution, signal-to-noise ratio and image contrast.

Spatial resolution is the ability to resolve finely detailed or small structures within an MR image and is determined by the number and size of the voxels in an image. It is the singular most important requirement in MSK joint imaging and yields essential anatomical detail on the MR image.

Spatial resolution is the singular most important requirement in MSK joint imaging

Signal-to-noise ratio (SNR) is the maximizing of recorded radiofrequencies emitted from the patient while minimizing electronic and background noise frequencies. SNR is affected by several components such as static magnetic field strength, surface coils, the number of signal averages or excitations, and voxel size.

Image contrast is the ability to discern one tissue type from another, for example, fat from muscle or cortical bone from bone marrow. Optimal contrast is obtained through proper pulse sequence selection and parameter selection.

All three of these elements — spatial resolution, SNR, and image contrast — are interdependent. At times they complement each other, while at other times they counter each other. *Yet, a deficiency in any one of these three elements cannot be compensated for by the other two.* For example, high SNR cannot compensate for poor detail and, likewise, high anatomical detail cannot compensate for poor image contrast.

Again, spatial resolution is the most critical of these three elements in MSK MR joint imaging. Image contrast and SNR are the foundations upon which spatial resolution, and therefore anatomical detail, rests.

Spatial Resolution

Spatial resolution determines image sharpness and detail. The higher the spatial resolution, the sharper the anatomical detail. Spatial resolution is the product of the number and sizes of the voxels in the image, that is, *the smaller the voxel size, the higher the spatial resolution*.

There are three ways to decrease voxel size and increase spatial resolution: increase the phase and/or frequency-encoding steps, decrease the field of view, or decrease slice thickness (**Figures 1-3**).

For a fixed field of view (FOV), increasing the number of phase or frequency-encoding steps decreases the voxel size in the x, y dimensions. Conversely, for a fixed number of phase and frequency-encoding steps, decreasing the FOV also decreases the voxel size in the x, y dimension. Decreasing the slice thickness decreases the voxel size in the z dimension.

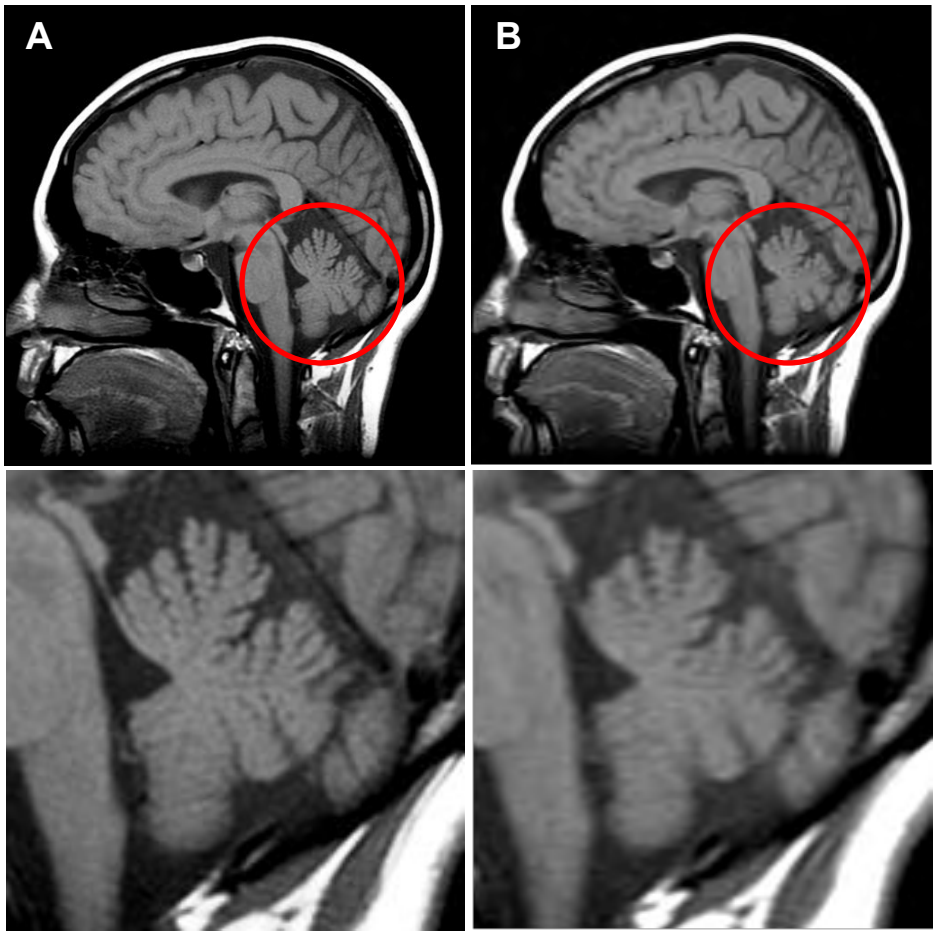

Figure 1. Sagittal brain images demonstrating the effect of voxel size on spatial resolution. (A) Image acquired with 288 phase-encoding steps. (B) Image acquired with 128 phase-encoding steps.

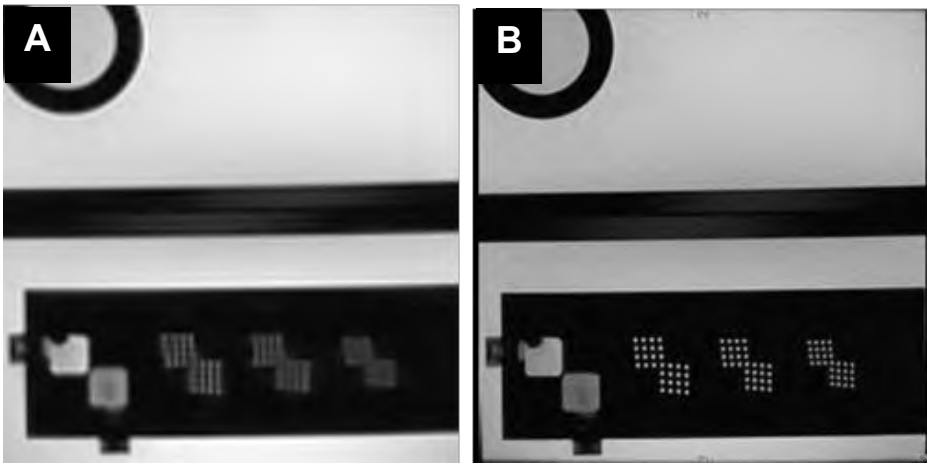

Figure 2. Phantom images demonstrating the effect of field of view on spatial resolution. (A) Image was acquired with a 24cm FOV. (B) Image was acquired with a 12cm FOV.

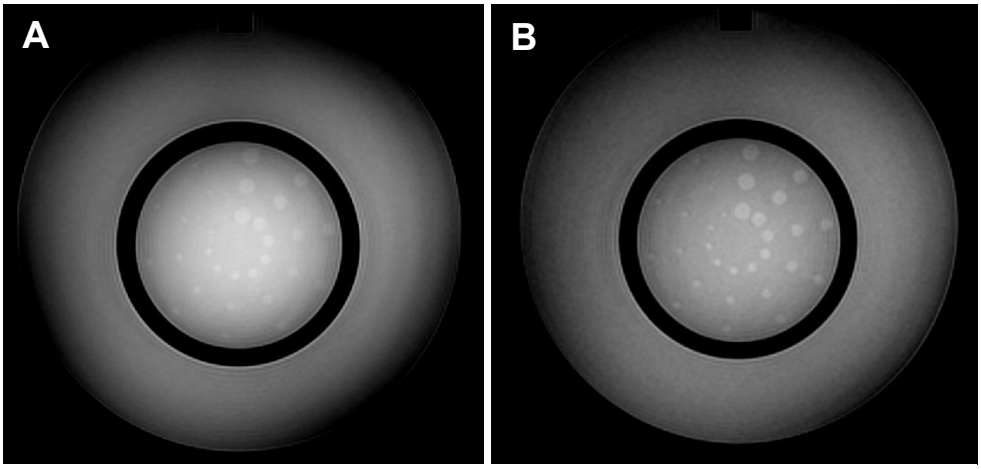

Figure 3. Phantom images demonstrating the effect of slice thickness on spatial resolution. (A) Image acquired with a 5.0mm slice thickness. (B) The same slice location acquired with a 2.5mm slice thickness

An important caveat is that as *voxel size decreases, SNR also decreases*. Therefore, SNR considerations must be taken into account when decreasing voxel size in order to obtain higher spatial resolution.

Signal-to-Noise Ratio

SNR is determined by maximizing **RF signals** emitted from the patient while minimizing noise from sources such as equipment electronics and noise inherent in the patient body. The SNR of an MR image is a summation of the SNR in all of the individual voxels within the image, that is, *the greater the SNR per voxel, the greater the overall SNR of the image.*

The great demands for increased spatial resolution with MSK MR imaging saps the SNR from the image. Obtaining adequate SNR is of paramount importance for "seeing" the spatial resolution of the image.

Understanding the differences between SNR and spatial resolution can be confusing. Consider a painting in a well-lit gallery. The painting is sharp, highly intricate, and detailed. The detail of the painting is not only apparent but is also fixed. If the light in the room were to be dimmed or turned off, the details of the painting still exist yet cannot be seen as clearly. The painting, then, represents spatial resolution, and the lighting in the room represents SNR. The question then becomes how to increase the SNR in order to appreciate the spatial resolution of the image (**Figure 4**).

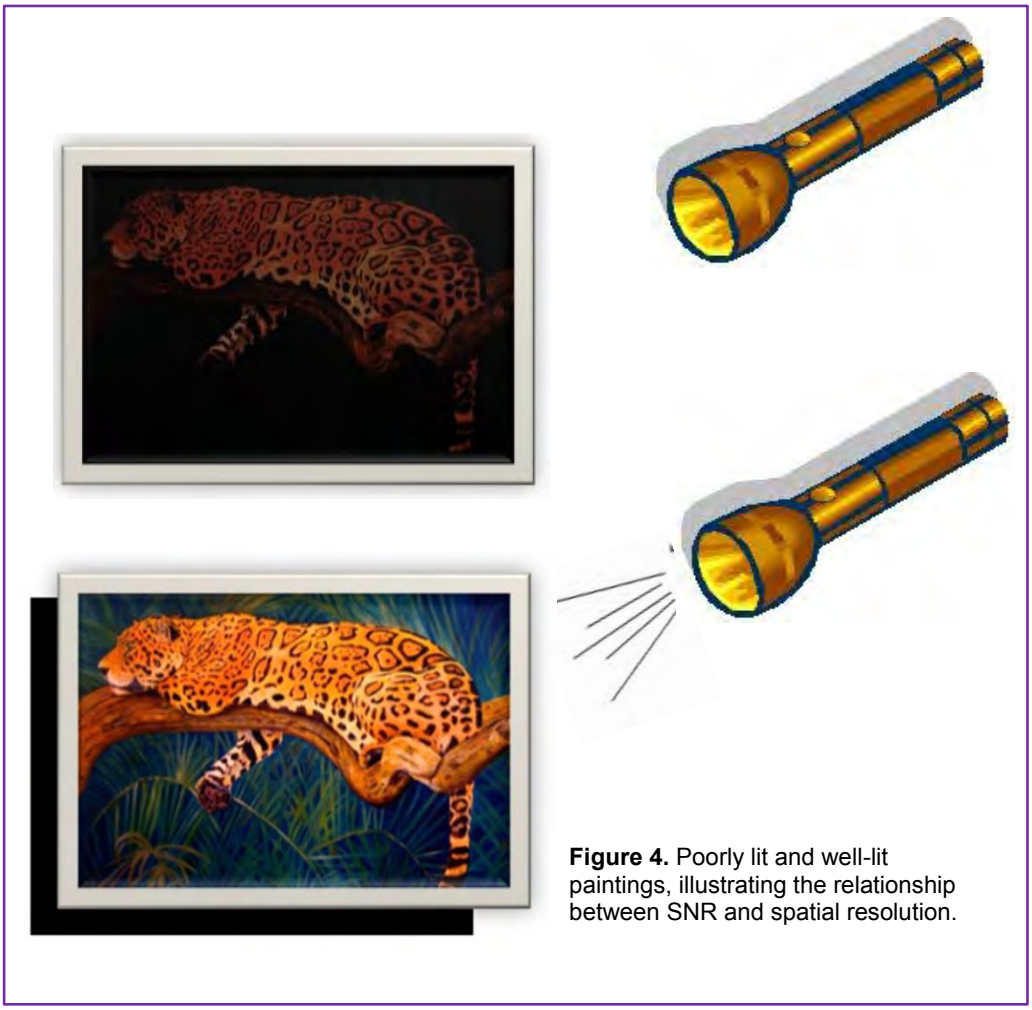

Figure 4. Poorly lit and well-lit paintings, illustrating the relationship between SNR and spatial resolution.

There are many ways to increase the SNR of an image. Some methods require significant changes in imaging parameters to visually appreciate the increase in SNR. Some methods increase scan times (increasing NEX/NSA) while, paradoxically, others actually decrease spatial resolution (increasing slice thickness and/or FOV). And other means may be fiscally challenging, as in purchasing an ultra-high field MRI system.

FIELD STRENGTH

The higher the magnetic field strength of the MR system, the higher the inherent SNR. The increase in SNR is fairly proportional to increases in field strength. For example, an increase in field strength from 1.5T to 3.0T is virtually two times greater (**Figure 5**). For this reason alone, MSK MR imaging is an application that has benefited directly from the proliferation of 3.0T imaging systems in the clinical setting.

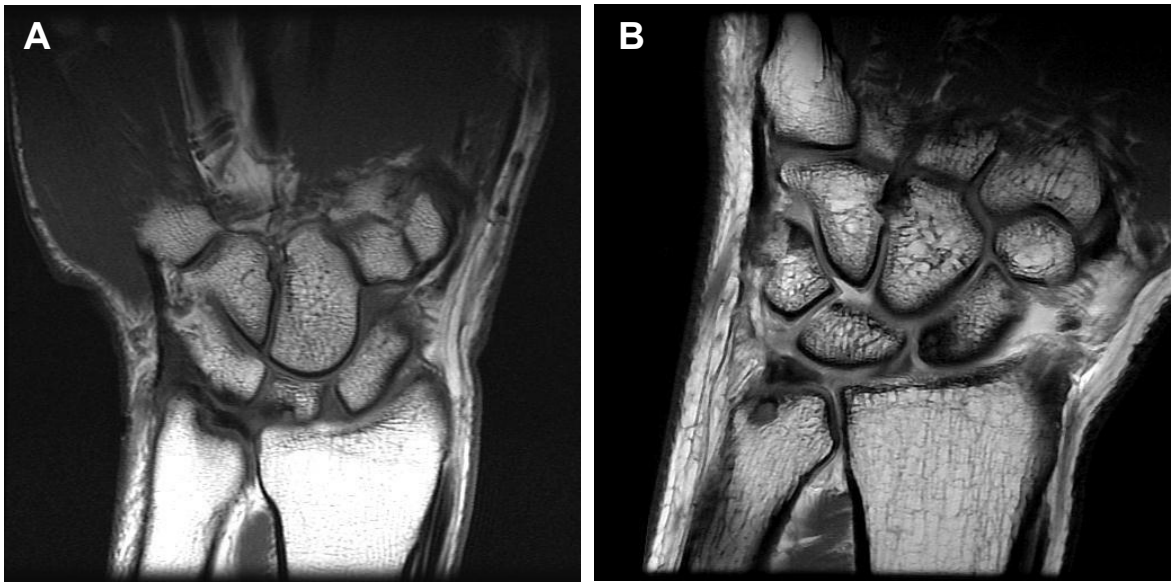

Figure 5. Signal-to-noise comparison. (A) Coronal PDW wrist image acquired at 1.5T at 3.0mm slice thickness with 2 NEX/NSA. (B) Coronal PDW wrist image acquired at 3.0T with a 1.6mm slice thickness and only 1 NEX/NSA.

HIGHER CHANNEL PHASED-ARRAY AND SPECIALLY DESIGNED PHASED-ARRAY COILS

Phased-array coil technology has revolutionized all of MR imaging. As a general rule, the smaller the surface coil, the greater the SNR for the area of sensitivity of the coil. The obvious caveat is that a smaller surface coil provides less coverage than a larger one. Fortunately phased array technology provides the coverage of a single larger coil while yielding the SNR benefit of several smaller coils. When coupled with increased numbers of RF receivers, phased-array coil elements can be even smaller and more numerous within each coil, yielding the benefit of even greater SNR. That is, a phased-array coil with 16 smaller elements coupled with 16 RF receivers yields higher SNR than same phased-array coil with only 8 elements, and even greater SNR compared to a 4-element phased-array coil (**Figure 6**).

In addition to phased arrays coils that yield higher SNR, specialized phased-array coils are available, such as the hand-wrist array that further boost SNR by allowing close placement to the area of interest and provide custom molding to better cover and immobilize the body part.

Advanced phased-array coil design coupled with 3.0T imaging provide high spatial resolution MR imaging with high SNR within reasonable scan times.

Figure 6. 8-channel phased array wrist coil. *Courtesy of Siemens.*

High-quality diagnostic MSK imaging is possible on lower field strength systems. However, magnetic resonance physics dictates that, *all factors remaining equal,* an image obtained at 3.0T will have almost 2x greater SNR than the same image obtained at 1.5T. In order to obtain the same diagnostic quality at lower field strengths, the imaging time must increase dramatically. Why?

Other Factors That Can Increase SNR

Other factors that can have an effect on SNR:

- **Increasing TR** (time to recovery; recovery time)**.** This increases SNR but also increases scan time and, more importantly, can greatly affect the desired image contrast.
- **Decreasing TE** (echo time).This increases SNR but more importantly can adversely affect image weighting.
- **Increasing FOV.** This increase boosts SNR by placing more excited spins within each voxel. Of course, this also decreases spatial resolution at the same time and therefore can be counterproductive.
- **Increasing slice thickness.** As with increasing FOV, increasing slice thickness boosts SNR by placing more excited spins within each voxel. Again, this can decrease spatial resolution at the same time and therefore can be counterproductive.
- **Decreasing phase and/or frequency-encoding steps.** Decreasing phase encoding increases SNR by enlarging the size of individual voxels, thereby placing a greater number of excited spins within each voxel in the same manner as increasing slice thickness. Likewise, voxel enlargement also decreases spatial resolution at the same time and also risks being counterproductive.
- **Increasing the number of signal averages or excitations** (NSA/NEX)**.** Increasing the NSA/NEX increases SNR. *A 2x increase in NSA/NEX yields a 40% increase in SNR but doubles scan time as a result.* The SNR increase is not proportional, as increasing NSA/NEX also increases noise but to a lesser extent.

In order to appreciate an increase in SNR using any of these methods, the human eye needs approximately a 20% increase in SNR. To appreciate an increase in SNR, then, one needs to increase the NSA/NEX by at least 50%. Because a 3.0T magnet has about 2x more inherent SNR than at 1.5T, the NSA/NEX must be virtually doubled on a 1.5T system to obtain the same SNR at 3.0T (all other variables remaining the same) (**Table 1**).

Effect of increasing...	Spatial Resolution	SNR	Scan Time	Comments
TR	___	↑	↑	Be sure that TR range fits CONTRAST requirements
TE	___	↓	___	Be sure TE range fits CONTRAST requirements
Field of View	↓	↑	___	Too small FOV may cause aliasing
Slice Thickness	↓	↑	___	Slice thicknesses too thick may cause partial volume effects
Phase Matrix	↑	↓	↑	
Frequency Encoding	↑	↓	___	Increasing FREQ steps will increase echo spacing (ESP) and cause FSE blurring and EPI distortion
NEX/NSA	___	↑	↑	Increased NEX can reduce some motion artifacts
Receive Bandwidth	___	↓	___	Decreasing RBW too much increases ESP and causes FSE blurring and EPI distortion and decreases slice/TR; decreasing RBW also increases chemical shift artifacts at fat/water interfaces

Table 1. The effect of operator-controlled imaging parameters.

Image Contrast

Acquiring good image contrast between tissues in MSK MR imaging can be complicated. For example, skeletal bone is composed of bone marrow and **cortical bone**. Cortical bone appears black (extremely **hypointense**) on all imaging sequences, while marrow cavity has a variable appearance depending upon the marrow type (fatty vs **hematopoietic**). Muscle tissue has intermediate signal intensity (**isointense**) on all sequences. Tendons and ligaments are generally hypointense on all sequences with the exception of the quadriceps tendon and triceps tendon which normally show striations within the substance of the tendon. Fatty tissue is very **hyperintense** on short TE imaging (**T1-weighted** [T1W] and **proton density-weighted imaging** [PDW]) and can remain hyperintense, though not to the same degree on long TE imaging as with **T2 weighted-imaging** (T2W).

Pulse sequence selection and implementation vary widely not only by manufacturer but by facility. However, image contrast requirements are fairly uniform. MSK MR imaging typically consists of short TE non-fat-suppressed imaging and intermediate TE fat-suppressed imaging.

Guidelines for achieving the desired image contrast:

- **Short TE non-fat-suppressed imaging** can be either T1W or PDW imaging. The choice is determined by the radiologist or facility preference, but most facilities that perform a lot of MSK MRI favor PDW imaging. This sequence provides a great degree of spatial resolution as well as SNR compared to T1W imaging in approximately the same imaging time.
- **Intermediate TE fat-suppressed imaging** consists of a TE range of 35-55msec and is desirable compared to T2W fat-suppressed imaging. Intermediate PDW imaging with fat suppression provides excellent contrast between hypointense ligaments and tendons against hyperintense fluid in joint spaces. Intermediate TE also avoids the SNR loss of long-TE (90-120msec) T2W imaging yet maintains excellent contrast and preserves high detail.
- **Fat-suppressed imaging** is by far the most common parameter in MSK MR imaging, crossing all facilities as to its use and importance. Suppressing fat signal is essential for distinguishing between hyperintense signal from fluid, blood, or inflammatory response from hyperintense fat signal. There are two ways to achieve fat suppression: frequency-selective (chemical) fat suppression and STIR imaging.
    - **Frequency-selective fat suppression** is the application of a RF pulse at the resonant frequency of fat. The RF pulse saturates the signal from fat, preventing it from recovering its longitudinal magnetization without affecting the signal from water. Fat suppression is used in conjunction with intermediate-TE PDW imaging to make fluid and **edema** more conspicuous against a darker background. Chemical fat suppression is also widely used for postcontrast T1W imaging.

      The main drawback of frequency-selective fat suppression is the potential for inhomogeneous suppression of fat signal. This is especially true when a curved surface is being scanned or when the anatomy in question is far from isocenter of the magnet, such as the shoulder. Also frequency-selective fat suppression techniques are not always available on mid- and low-field strength magnets because the **chemical shift** between fat and water is too narrow, preventing the precise application of the frequency-selective RF pulse.
    - **STIR (short-tau or short-T1 inversion recovery) imaging** produces better homogeneous fat suppression because it is not as sensitive to field inhomogeneities as the frequency-selective technique. With STIR imaging, a slice selective 180^0 RF pulse (the “IR pulse”) is applied to the area of interest, inverting all the spins in the slice to the z-axis. A time delay, called TI for **time to inversion**, is set by the operator from the application of the IR pulse until data acquisition. That time delay is set to the **null point** of fat, which is ~ 150msec at 1.5T and ~190msec at 3.0T (**Figure 7**).

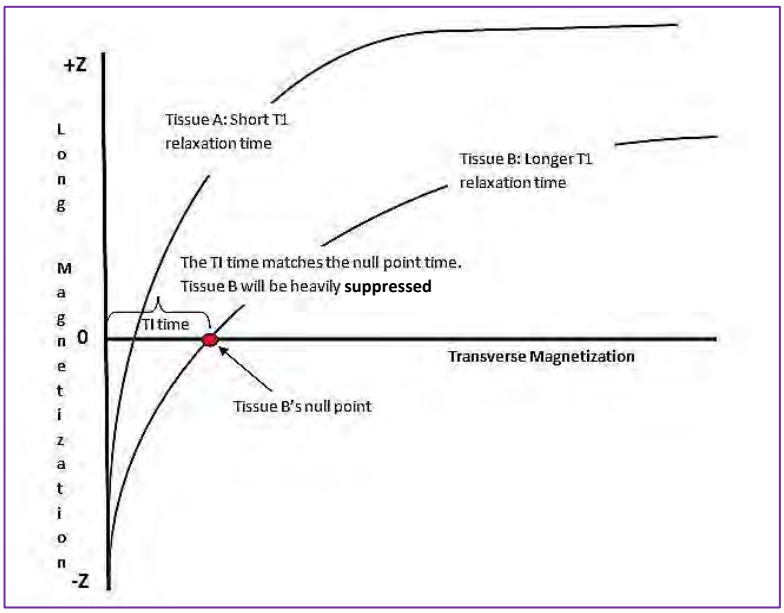

Figure 7. T1 inversion recovery relaxation curve demonstrating tissue null points and resulting in maximum signal suppression.

However, STIR imaging cannot be used as a post-gadolinium injection imaging as the signal from the gadolinium can also be suppressed. Also, STIR imaging can be inherently lower in SNR compared to frequency-selective PDW imaging. In addition, longer TR periods are often required in STIR imaging, which can dramatically increase scan time compared to frequency-selective PDW imaging. Still, the contrast of the STIR imaging is so robust it remains an integral part of most MSK imaging protocols. Many imaging facilities employ a balanced approach to fat-suppression imaging, using both STIR and frequency-selective PDW at key points in the imaging process (**Figure 8**).

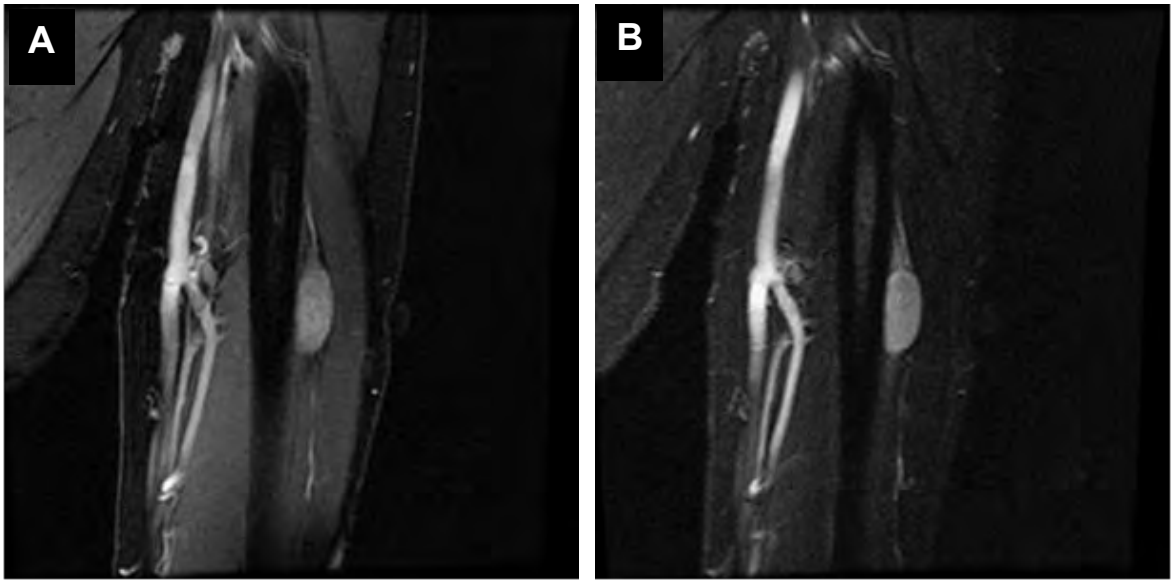

Figure 8. Left humerus of a 51-year-old male demonstrating a benign peripheral nerve tumor, most likely a schwannoma. (A) Chemical fat-suppression technique. (B) Same slice location utilizing a STIR fat-suppression technique.

2D and 3D Imaging Applications

In the quest for ever-increasing spatial resolution in MSK imaging, the debate about 2D versus 3D acquisitions can arise. Although the issue is often answered by the preferences of the interpreting radiologist and facility, there are advantages and disadvantages to acquiring 2D vs 3D images.

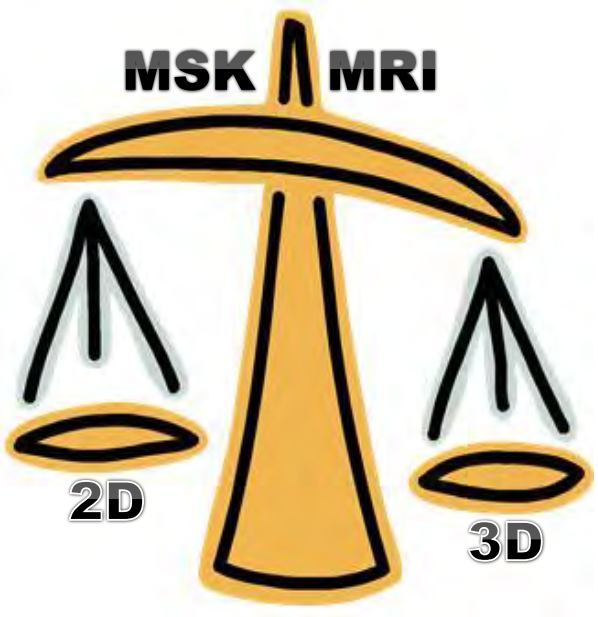

3D imaging acquisitions excite a thick slab of information instead of a single, thin slice. The thick slab increases SNR dramatically compared to 2D acquisitions (all other factors remaining the same) because the abundance of excited spins within the slab can be orders of magnitude greater than for a thinner 2D slice. A second set of phase-encoding steps in the slice-select direction reconstructs the slab into individual and extremely thin slices, often sub-millimeter in thickness, which provides very high spatial resolution. If the reconstructed slice thickness is equal to the voxel size in both the phase and frequency directions, the voxels are termed **isotropic**, which allows the reformation of the slab data into any plane desired. However, there are disadvantages to this approach.

The extra set of phase-encoding steps in the slice-select direction significantly increases scan time. To reduce this increase, the vast majority of 3D sequences are gradient-echo-based (GRE). The sequences can be T1-weighted sequences using a spoiler pulse to eliminate residual transverse magnetization, or they can be T2* (star)-based to provide brighter signal intensity in fluids. Regardless of the weighting, a GRE-based T1W 3D image has a slightly different appearance in muscle and bone compared to a spin-echo-based (SE) T1W 2D image. Moreover, a T2*-based 3D sequence is highly sensitive to magnetic susceptibility effects that can lead to excessive dephasing in interfaces of high-and-low magnetization, such as cyst and cortical bone.

Advances in gradient power and phased-array coils, however, now provide the ability to acquire 2D slices in extremely thin slices, often less than 2.0mm. High-element phased-array coils and the use of 3.0T imaging systems provide high SNR. SE-based 2D sequences provide contrast characteristics with which many radiologists are familiar, providing high spatial resolution in a reasonable scan time. However, because 2D data sets are not composed of isotropic voxels, that is, the same size in all three dimensions, they cannot be reformatted with any useful image quality.

TECHNICAL CONSIDERATIONS OF MSK IMAGING

Appearance of Musculoskeletal Structures on MRI

As in body MR imaging, musculoskeletal structures with an abundance of hydrogen spins produce strong MRI signals, while those with little or no water molecules produce little to no MRI signal.

For instance, bone marrow contains an abundance of water molecules attached to fat and therefore produces a strong MRI signal, appearing hyperintense on pulse sequences that are not fat-suppressed. By contrast, cortical bone is almost exclusively comprised of calcium and little water so appears hypointense on MRI.

Like cortical bone, ligaments and tendons have very little water and generally appear dark on all MR sequences. The exceptions are the quadriceps and triceps tendons, which normally show striations within the bulk portion of the tendon that contain water and therefore will produce stronger MR signal, providing useful tissue contrast within these specific tendons.

Muscle demonstrates intermediate signal intensity and thus generally appears isointense. The contrast of all of these tissues — ligaments, tendons, muscle, bone marrow, and cortical bone — will change in the presence of inflammatory responses such as infection, injury, and neoplasm. Optimal visualization of the anatomy and pathological process requires an imaging approach that includes high resolution imaging, various imaging weightings, the use of fat suppression techniques and, at times, the administration of gadolinium-based contrast agents.

Importance of Positioning

MSK imaging is the only MRI application that relies heavily on body positioning. Neurologic and body applications require the patient be in a simple supine position or, in some cases like breast imaging, in the prone position. The patient's body, whether feet-first or head-first, simply needs to be straight. This is not the case with MSK imaging. While there are MSK MRI exams that require the patient to be straight and flat for imaging, for example a large muscle of a long bone, most MSK exams require precise positioning.

Imaging of the shoulder, elbow, wrist, hip, knee, and ankle all require specific positioning before the onset of imaging. The first localizing series on all these areas must be carefully scrutinized to ensure the joint is positioned correctly. If the positioning is inaccurate, the technologist must re-position the patient before proceeding. Specific positioning techniques will be reviewed under each area of anatomy.

Patient Comfort

Patient comfort is absolutely essential for obtaining a high-quality image. Because MSK imaging requires ultra-high spatial resolution to visualize very fine detail, any **motion artifact** due to patient movement will have a detrimental effect on diagnostic quality. Therefore, patient comfort is essential as anatomic positioning is not always as comfortable in MSK imaging as the simple supine position used with other MR applications.

For MSK MRI, the patient must maintain positioning so that the anatomy of interest is closest to the **isocenter** of the magnet. This position can often be difficult to maintain, particularly for the obese and elderly. Time and effort should be made to make the patient as comfortable as possible. Placing pillows and wedge sponges to support the head, neck, and areas of the body will assist in keeping the patient comfortable and relaxed throughout the exam.

As with all MR imaging, hearing protection is as much an essential safety requirement as it is for the comfort of the patient.

Patient History

Obtaining a thorough patient history is important in any MRI examination but especially in MSK imaging. A complete history will not only guide the radiologist when interpreting the exam but direct the imaging process in real time.

For example, an imaging requisition that notes the patient's chief complaint as "hand and wrist pain" is often too general a description to proceed. Hand and wrist pain are symptoms of both carpal tunnel syndrome and arthritis, but their imaging protocols are vastly different. Asking the patient about the cause of the pain, for example, due to trauma versus a more gradually increasing pain over a period of time is usually sufficient information for determining the appropriate imaging protocol.

Obtaining a complete history ensures not only appropriate protocol selection but acquisition of diagnostic images. The following information is necessary to determine the appropriate imaging protocol:

- Cause and date of onset of pain
- Current range of motion
- Specific location of pain (place marker on area)
- Past history of surgery in the area of interest
- Swelling or visible changes

- Specific to knee:
  - Difficulty climbing stairs
  - "Popping" or grinding when knee is bent
  - Knee weakness (may indicate cruciate ligament pathology)
- Specific to elbow, wrist, or hand:
  - Pain generating in forearm or hand. Posterior or anterior hand pain (may indicate ulnar or radial nerve pathology)

MR Arthrography

Much like x-ray arthrography, MR arthrography is a procedure that increases intra-articular contrast to better visualize small labral or tendon tears.

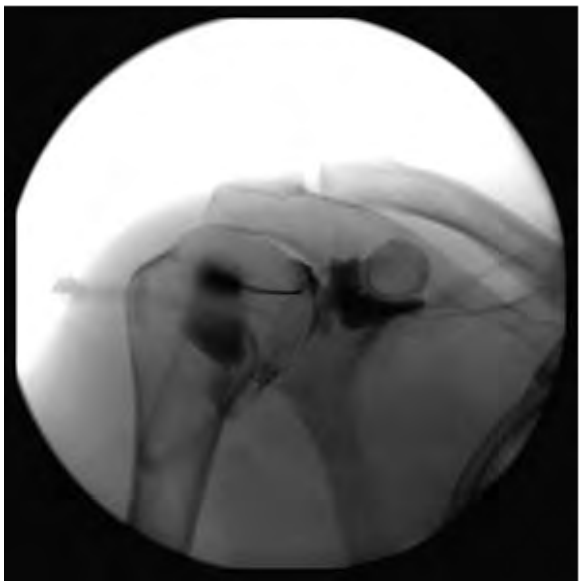

Figure 9. Fluoroscopic image of needle placement and contrast injection into the shoulder joint capsule before undergoing MRI examination.

MR arthrography consists of a mixture of **radiopaque** contrast material, a diluted gadolinium-based contrast agent (GBCA), and saline injected directly into the joint under fluoroscopic guidance. The radiopaque dye allows the visualization of needle placement and confirms that the joint space has been accessed (**Figure 9**). The GBCA provides the contrast mechanism under MR visualization. The saline provides volume to distend the joint space, allowing separation between a small tear from normal tissue (**Figure 10**).

MR arthrography is most often used to evaluate small tears in the shoulder and hip. However, arthrography can also be used to evaluate small tears in the ankle, wrist, and even toes.

Arthrography performed using chemical fat suppression (frequency-selective) makes gadolinium contrast highly conspicuous against hypointense background, significantly aiding in the visualization of small tears.

MR arthrography is an invasive procedure that carries some risk of infection, albeit small, at the injection site. Usually 1-2ml of GBCA is greatly diluted in a saline solution. Although the GBCA solution is not injected into the blood stream, patients contraindicated for GBCAs should not undergo MR arthrography.

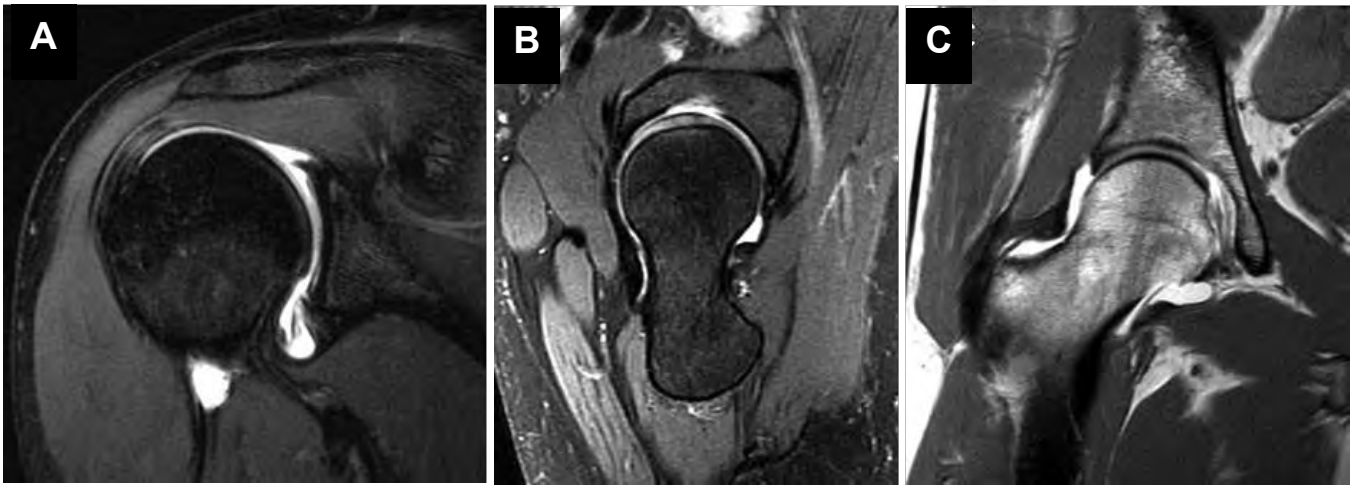

Figure 10. MR shoulder and hip arthrography. (A) Oblique-coronal T1W with fat suppression of the shoulder. (B) Oblique-sagittal PDW with fat suppression of the hip. (C) Coronal PDW without fat suppression of the hip.

ADVANCED MUSCULOSKELETAL MRI APPLICATIONS

The median age of the US population has been increasing each year. According to the US Census Bureau, between 2005 and 2015, the population of those 65 and older in the US will increase by 28%. By 2025, this age group will make up almost 20% of the US population, compared with 10% in 1975.[1] On the other end of the age spectrum, teenaged sports-related injuries are on the increase with as many as 2.0-3.5 million injuries reported annually.[2,3] As both these patient population groups increase, so too will the need to evaluate, diagnose, and treat injuries, diseases, and degeneration of the joints.

To address the growing demand for advanced musculoskeletal imaging, two MSK-specific applications have emerged: cartilage T2 mapping, a useful diagnostic tool for visualizing and staging cartilage damage and rehabilitation, and metal artifact suppression techniques, which aid in the evaluation of continued pain in joint replacements.

Cartilage T2 Mapping

Healthy cartilage — the stiff but flexible connective tissue found in many areas of the body such as joints, ears, and nose — contains little water. In T2W imaging, this lack of water significantly increases the speed of T2 decay, resulting in hypointense signal on imaging. Cartilage is made up of **collagen**, the primary protein of connective tissue in the body. Areas of collagen degeneration or injury in a joint result in an increase in water to the damaged area that will decrease the speed of T2 decay. The contrast difference, however, between healthy and damaged cartilage may be difficult to visualize with a single TE value, particularly with intermediate or long TE values (50msec-100msec). Imaging the area of damaged cartilage with a series of *increasing* TE values permits a mapping of the areas of rapid T2 decay (healthy cartilage) compared to a areas of prolonged T2 decay (damaged cartilage).

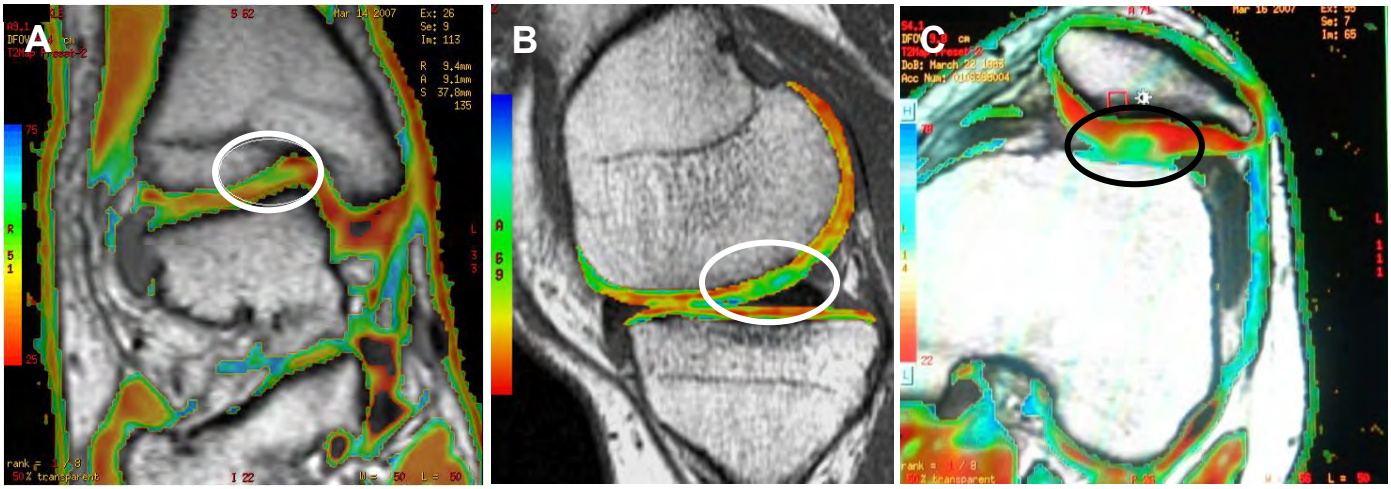

Figure 11. T2 cartilage mapping demonstrating cartilage damage. (A) Coronal view of the ankle. (B) Sagittal view of the knee. (C) Axial view of the knee.

Using a cartilage T2 mapping technique, an individual slice of damaged joint cartilage is imaged multiple times with the same TR but with successively increasing TE values, for example, from 20msec to 120msec, resulting in several images of the exact same location. Analysis software compares the rate of T2 decay on a voxel-by-voxel basis and produces a color-coded composite image. The color map demonstrates rapid T2 decay as warmer colors of orange to red and prolonged T2 decay in cooler colors of green to blue (**Figure 11**).

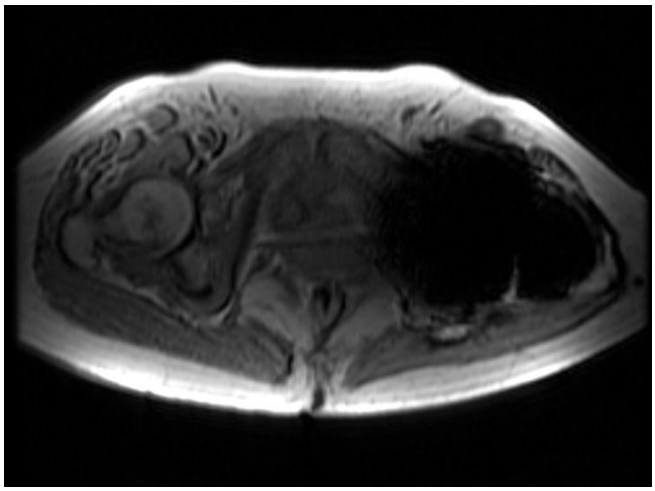

Figure 12. Typical metal artifact from a hip replacement prosthesis. Note the area of signal void encompasses an area far beyond the boundaries of the prosthesis itself.

Potential uses for T2 cartilage mapping include assessment of early cartilage degeneration as well as the evaluation of articular cartilage following autologous osteochondral grafts, the grafting of cartilage from another part of the body to the damaged joint in order to “grow” new cartilage.

Metal Artifact Suppression

In MRI, any metal near the area of interest greatly disrupts the **homogeneity** of the magnetic field near the location of the metal, creating a significant degree of artifact. Water protons near the metal will experience a magnetic field that is vastly different than water protons far from the area of metal. Thus precessional frequencies of protons near the metal are far outside the required **Larmor frequency** and as a result never produce an MR signal (**Figure 12**).

The extent of artifact is determined by the amount of metal and its composition. Iron by far produces the most magnetic field disturbance and therefore the greatest amount of artifact. Imaging near an area of metal also increases the potential for heating as metal efficiently absorbs radiofrequency energy. Though extremely rare, excessive heating of a metal implant can lead to a patient burn and is an obvious safety concern.

In MSK MRI the presence of metal is common and often found within the area of interest. Artifacts produced by oral braces, spinal fusion hardware, as well as joint implants will seriously affect imaging quality.

METAL ARTIFACT REDUCTION SEQUENCE

Artifacts from metal are a type of **magnetic susceptibility** effect, which is simply the degree to which a tissue can be magnetized in the MR system. Remember that metal cannot become magnetized in an MRI system like normal body tissue can be. Moreover, protons in the tissue in the near vicinity of the metal will also fail to become magnetized. The artifact on an MR image from metal cannot be eliminated, but it can be reduced.

Metal artifact reduction techniques (MARS) are available on every MR system. The degree to which a MARS technique can be used varies from manufacturer to manufacturer. For example, the manipulation of the **receive bandwidth** (RBW) is a critical part of utilizing a MARS technique, but not all manufacturers allow the operator full manipulation of the RBW. Therefore, obtaining an optimal MARS series is far more difficult on an MR system that does not allow manipulation of the RBW.

A MARS technique can be used with different pulse sequences such as FSE/TSE or STIR. By using a metal artifact reduction sequence, magnetic susceptibility artifacts can be reduced in the following ways:

- **Using an MR system with a lower field strength.** Magnetic susceptibility effects, including metal-induced artifacts, increase with field strength. If possible, image the patient using an MR system with a lower field strength.
- **Avoiding gradient-echo-based pulse sequences.** Susceptibility-related artifacts are exacerbated by gradient-echo-based pulse sequences due to the inability of GRE-based sequences to correct for dephasing caused by **T2'** (prime) effects. Recall that dephasing caused by T2' as well as true T2 yields weighting that is T2*.
- **Increasing the echo train length of fast/turbo spin-echo pulse sequences.** Using a 180^0 refocusing RF pulse, spin-echo-based pulse sequences correct for T2' effects and reduce susceptibility-based artifacts like metal artifacts. By increasing the number of 180^0 refocusing RF pulses (increasing the echo train length [ETL]), a greater reduction in T2' effects can be achieved.

However, there are pitfalls. As ETL increases, particularly for short-TE fast/turbo spin (FSE/TSE) imaging, image blur may increase. A general rule of thumb: whatever the protocol offers as a "typical" ETL, double it; for example, if the typical ETL is 7, increase it to 14.

- **Increasing the receive bandwidth.** Susceptibility-induced artifacts increase as the duration of the frequency-encoding gradient increases (also called "readout"). As the receive bandwidth increases, the required duration of the frequency-encoding gradient decreases. The result is reduced metal-induced artifact.

  Caution must be taken in this approach because increasing the RBW while decreasing the duration of the frequency-encoding gradient also reduces signal-to-noise ratio. Doubling the RBW reduces the SNR in the same proportion as halving the NEX/NSA. To offset the reduction in SNR, it may be necessary to increase the NEX/NSA, thereby increasing scan time.
- **Decreasing voxel size by increasing phase-encoding steps.** Increasing the phase-encoding steps increases spatial resolution. While increasing the phase-encoding steps has no *direct* effect on metal-induced artifact, the increased spatial resolution does sharpen the boundary between areas of artifact and unaffected areas of tissue signal.
- **Utilizing STIR imaging to obtain fat suppression.** Chemical fat suppression techniques are not effective in the presence of metal implants. However, fat suppression is extremely important in the evaluation of patients with joint replacements. STIR fat suppression is a highly effective method for suppressing fat signal.

Even with artifact-reducing methods, the artifact from metal will always present, and the greater the amount of metal, the greater the degree of artifact beyond the boundary of the metal itself. In other words, the more metal present near the area of interest, the more artifact will "plume" to tissue close to the metal. Nowhere is this more evident than when imaging a prosthetic hip or knee (**Figure 13**).

Hip and knee replacement surgeries grow in number each year as the median population age grows. According to CDC statistics, there are now 719,000 knee replacements and 332,000 hip replacements performed each year in the United States.[4-5]

Because of the artifacts caused by the metal portions of these replacement prosthetics, performing MRI examination of these joints was virtually unheard of until 2010. However, as this patient cohort grows, the need for evaluating post-operative complications has also grown. Complications include infection, continued joint pain, and tissue inflammation from debris from joint interface friction. Not surprisingly, then, MR imaging of both knee and hip replacements has become the most rapidly growing application in MSK MRI.

With the increasing need for MR evaluation of knee and hip replacements, the demands for higher image quality with greater emphasis on artifact reduction has increased as well, resulting in the development of more advanced sequences for metal artifact reduction.

ADVANCED PULSE SEQUENCES FOR METAL ARTIFACT REDUCTION

The need to reduce metal-induced artifact has led to the development of specialized sequences that attempt to reduce the metal artifact plume to the exact boundaries of the implant itself.

Three methods for significantly reducing metal artifact have been developed: variable angle tilting, slice-encoding metal artifact correction, and multi-acquisition variable resonance imaging combination.

VARIABLE ANGLE TILT

Recall that spins from tissues near metal lose their resonant frequency due to disruptions in the local magnetic field because of the presence of metal. The longer the frequency-encoding gradient (readout) is collecting data, the greater potential for spins to fall outside the resonant frequency range and thus become misregistered and create a distortion in the image.

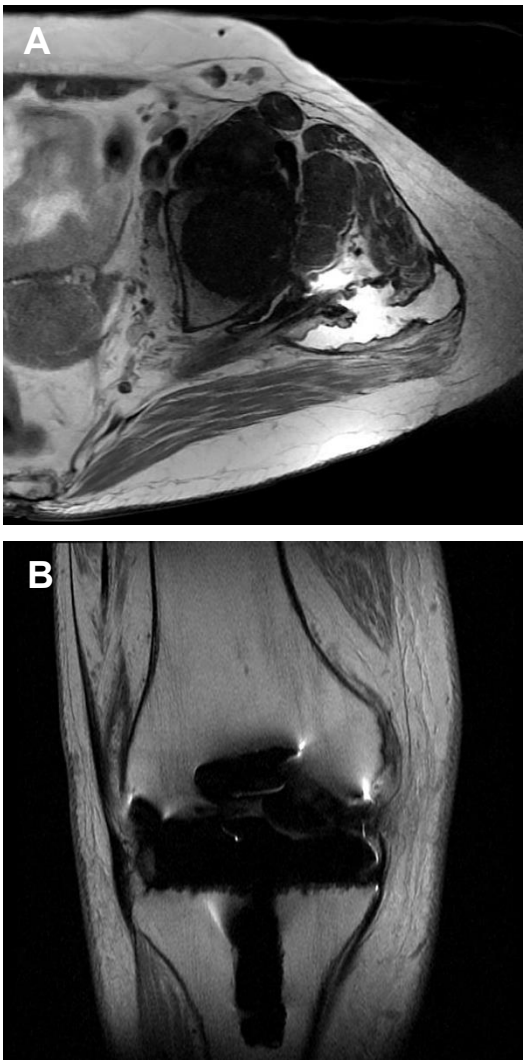

Figure 13. Metal-artifact-reduction (MARS) sequence. (A) Axial PDW non-fat-suppressed MARS image of the left hip. The use of extremely wide receiver bandwidth (=/-100Khz) in conjunction with a very high imaging matrix (512x384) aids in reducing but not eliminating the metal artifact. (B) Coronal PDW of the knee with end-plate replacements. Image B utilizes the MARS technique of 19ETL, +/-84kHz, and 512x384 frequency/phase matrix.

The variable angle tilt method (VAT) applies the slice-encoding gradient during frequency encoding, changing the resonant frequency of spins that are outside the receive bandwidth range and bringing them back to within the RBW range. The result is an imaging slice with a reduction in distortions caused by metal in the area of interest (**Figure 14**).

The disadvantages of this method are that VAT can produce blurring artifacts in the images, which limits its scope and effectiveness. VAT is most effective when the amount of metal comprises only a small area of the overall imaging volume. With larger metal implants such as hip and knee replacements, VAT may be of limited use.[6]

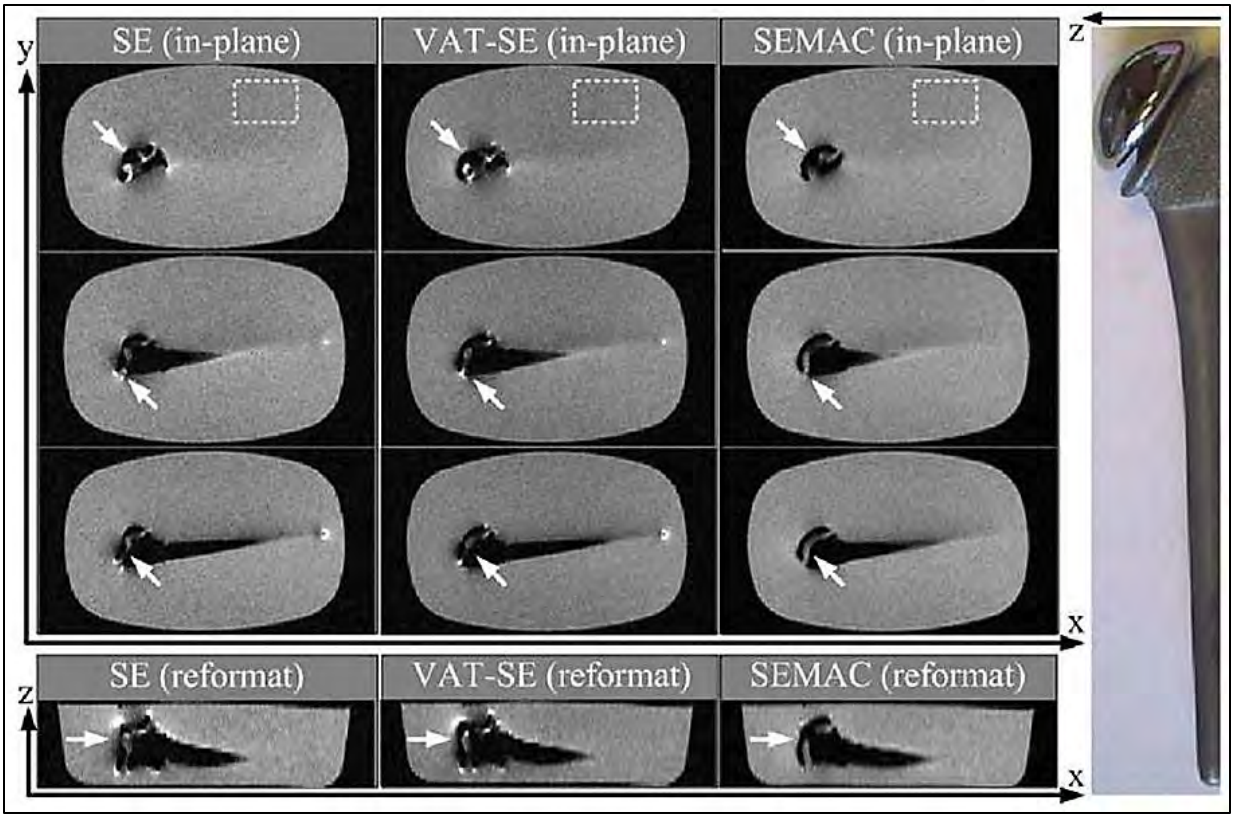

Figure 14. Comparison of the phantom results obtained from the SE sequence, the VAT-SE sequence, and the SEMAC technique. The first three rows show the comparison of the in-plane results. The dashed boxes in the first row select an uniform region for SNR evaluation of the different techniques. Despite partial correction of the distortions in the results obtained with the SE sequence, the VAT-SE sequence still suffers from uncorrected through-plane distortions, which occlude the features of the cobalt-chrome head of the prosthesis (noted by arrows). In contrast, the SEMAC technique correctly reproduces the shape and fine details of the prosthesis. The improvement produced by the SEMAC technique can also be clearly visualized by comparing the reformatted results in the bottom row. With the elimination of almost all metal-induced distortions, the rounded shape of the implant head is recovered. *Courtesy of Wenmiao Lu, PhD, Biomedical Imaging Center, University of Illinois, Urbana-Champaign.*

SLICE-ENCODING METAL ARTIFACT CORRECTION

Slice-encoding metal artifact correction (SEMAC) is an imaging mode that increases the effectiveness of VAT by adding phase-encoding steps in the slice-select direction in much the same way a 3D acquisition is performed. Recall that in a 3D MR acquisition, a shallow amplitude slice-encoding gradient is applied so that a thick “slab” of data is excited. A single phase-encoding step is performed after each slab excitation. The frequency-encoding gradient is applied, just as with a 2D acquisition. At this point in the sequence, a second set of phase encoding is done in the slice-select direction to generate multiple thin slice images.

Using SEMAC, however, the extra phase-encoding steps are not applied over the entire volume but over a distinct slice. Because the phase encoding is stepped and therefore extremely rapid, spins are not sensitive to off-resonant effects as with frequency encoding of much longer duration. The extra phase encodings are not used to produce thinner slices but rather to spatially encode spins that are distorted in the slice-select direction due to the close proximity of metal.

SEMAC furthers the process of bringing off-resonant spins back into the RBW range. SEMAC is inherently low in SNR on a per-slice basis and requires the summation of slices to yield an image that is of adequate SNR.[7] See **Figure 14** for a comparison of VAT and SEMAC sequences of a prosthetic hip.

Multi-Acquisition Variable Resonance Imaging Combination

Multi-acquisition variable resonance imaging combination (MAVRIC) is a 3D FSE-based sequence. As with all FSE sequences, an RF echo train is applied to rapidly fill *k*-space. Like other 3D methods, an extra set of phase-encoding steps is applied in the slice-select direction to spatially encode individual slices in 3D FSE. In MAVRIC, the echo train is **interleaved** within each TR period with alternating and unique spectral transmission frequencies (in typical FSE echo trains, all transmission frequencies are identical) (**Figures 15 and 16**).

Multiple and unique *transmission* frequencies yield multiple and unique *receive* frequencies. Typically the spectral transmit bandwidth range is +/- 12 kHz offset from the resonant transmission frequency. The multiple spectral transmission/ receive frequencies allow the capture of off-resonant spins, and any frequencies outside the spectral bandwidth are not recorded. Each of the unique series of spectral receive frequencies is placed or "binned" in a separate area of memory. For example, for a range of 16 different spectral transmission/receive frequencies, there would be 16 bins of frequencies for each image. Each bin is reconstructed into an image free of metal artifact in the slice direction and nearly free of artifact in the frequency direction.

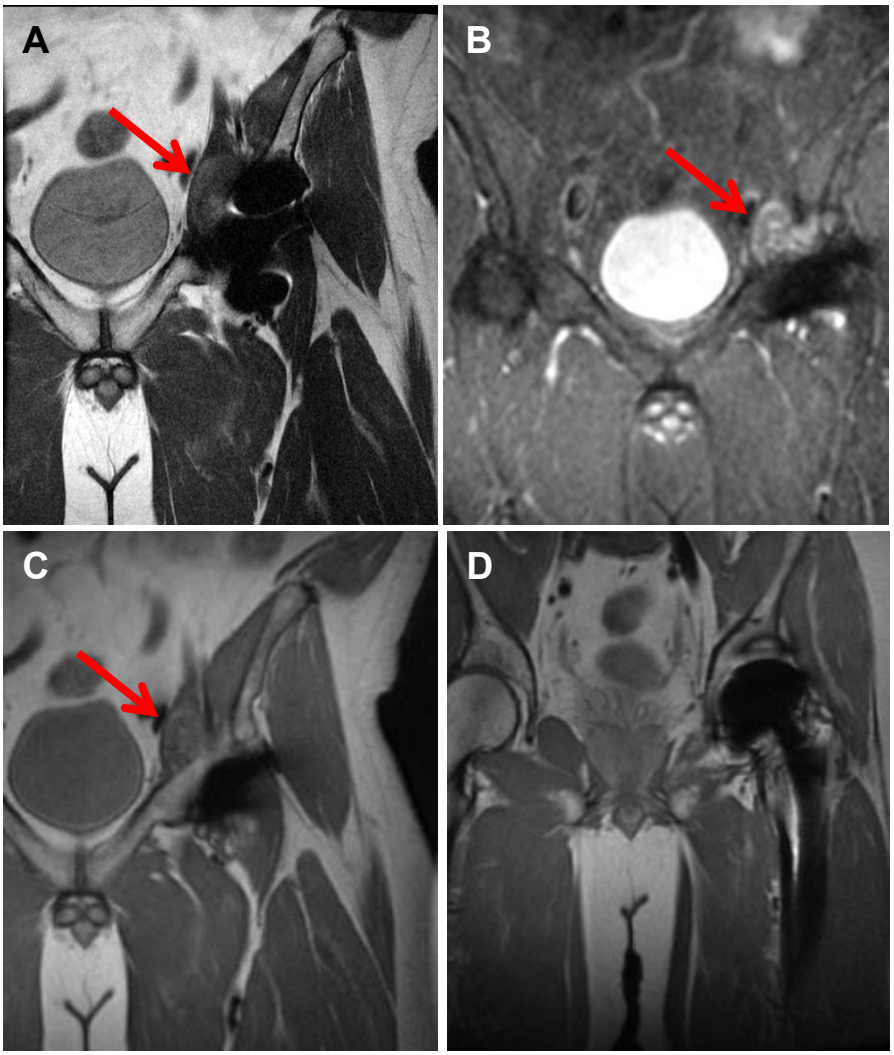

Figure 15. (A) Coronal FSE. (B) MAVRIC IR. (C and D) MAVRIC moderate echo time. Images demonstrate an adverse local tissue reaction in a patient with a recalled hip implant. The solid adverse reaction (arrows) is better visualized on the MAVRIC images. (D) Note the ability to further define the neck of the arthroplasty. *Courtesy of Hollis Potter, MD, Weill Medical College of Cornell University, New York, NY*

During image reconstruction, all binned images are combined into a single image that is nearly free of the plume artifact around the implant. In essence, the metal artifact is restricted to the shape of the implant itself.[8]

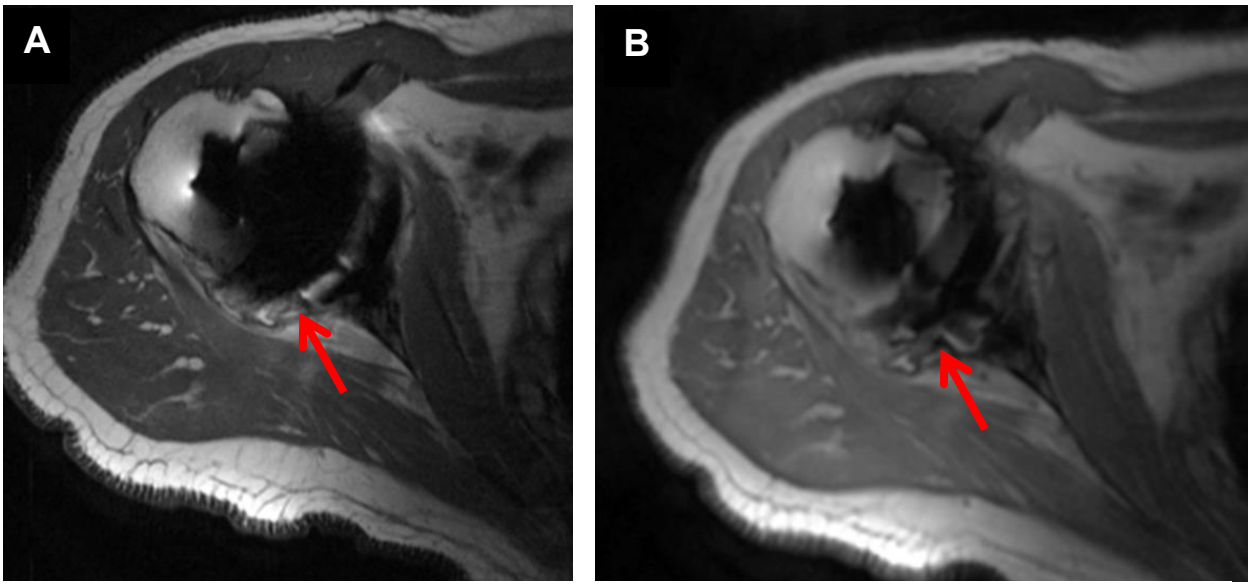

Figure 16. (A) Axial FSE and (B) MAVRIC images in a patient following total shoulder arthroplasty. The interface of the glenoid component is obscured on the FSE but clearly demonstrated on the MAVRIC, where loosening of the component is evident (arrows). *Courtesy of Hollis Potter, MD, Weill Medical College of Cornell University, New York, NY.*

UPPER EXTREMITY IMAGING — THE SHOULDER

Anatomy of the Shoulder

After the knee, the shoulder is the mostly commonly image joint in MRI. The bony structure of the shoulder consists of two main sections: the humerus and glenoid. The humerus has a smooth articulating surface at the superior medial portion of the bone. The greater tuberosity is located laterally, while the smaller lesser tuberosity is located anteriorly. These tuberosities help to form a shallow groove, the bicipital groove, where the biceps tendon is located as it travels along this portion of the humerus.

The glenoid is located on the lateral aspect of the scapula. It is normally **anteverted** with respect to the coronal plane of the body. Bony protuberances on the glenoid include the supra- and infraglenoid tubercles. The supraglenoid tubercle is the attachment site for the biceps tendon, superior glenohumeral ligament, and middle glenohumeral ligament. The infraglenoid tubercle is the attachment site for the long head of the triceps tendon. Lining the articular surface of the humerus and glenoid is a thin layer of **hyaline articular cartilage.** See **Figure 17** for a general overview of shoulder anatomy.

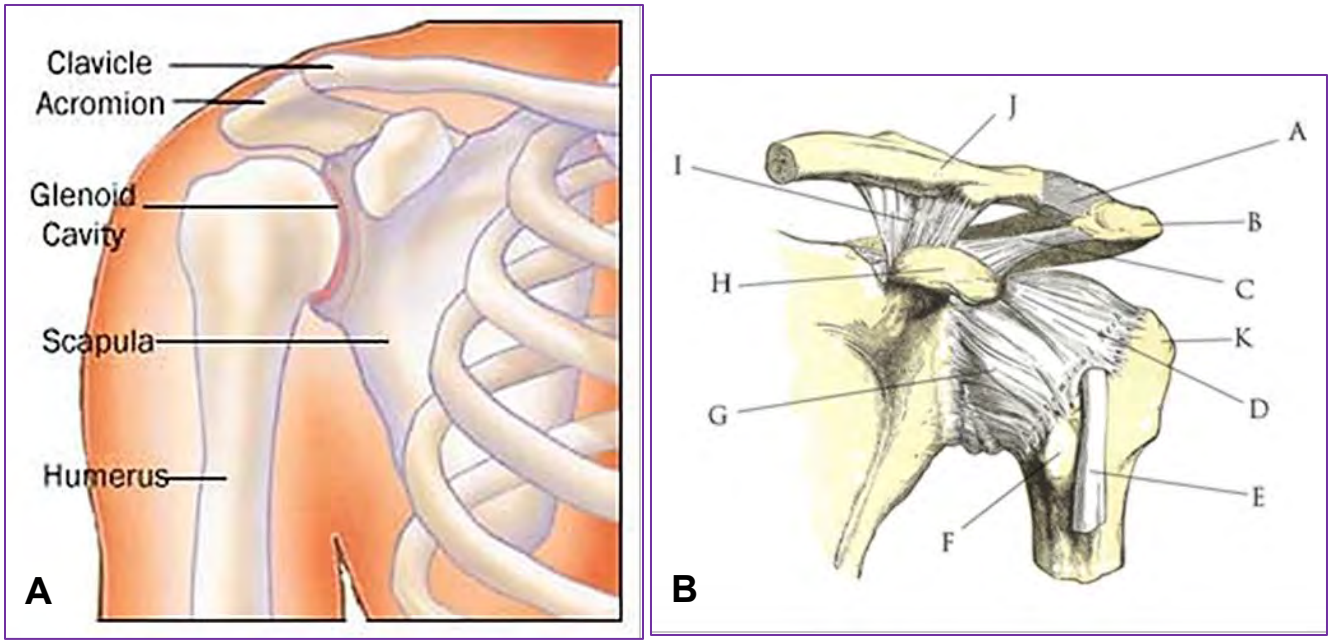

Figure 17. Shoulder anatomy. (A) Available at: Wikimedia Commons Rotator Cuff. (B) Anatomy of the left shoulder and acromioclavicular joints and the proper ligaments of the scapula. *Courtesy of AidMyRotatorCuff.com* .Available at: Wikimedia Commons.

A. Superior acromioclavicular ligament
B. Acromion
C. Coraco-acromial ligament
D. Coraco-humeral ligament
E. Biceps tendon
F. Lesser tuberele
G. Capsular ligament
H. Coracoid process
I. Coraco-clavicular ligament
J. Clavicle
K. Greater tuberele

The glenohumeral joint is inherently unstable due to the shallow glenoid cavity and the round humeral head. Surrounding soft tissue structures provide the stability of the joint. These structures include the rotator cuff, the labrum which lines the glenoid, capsular ligaments, and ligaments outside of the joint space such as the coracohumeral ligament (connecting coracoid process to humeral head) and the coracoacromial ligament (connecting the coracoid process to the acromion).

ROTATOR CUFF

The rotator cuff is made of up the supraspinatus (superior), infraspinatus, teres minor (both posteriorly located), and the subscapularis (anteriorly located) tendons, which insert on the greater tuberosity, while the subscapularis tendon inserts at the lesser tuberosity. The supraspinatus muscle arises within a **fossa** of the scapula. The muscle is obliquely oriented from posteromedial to anterolateral at an angle of 45º to the coronal plane. The tendon is also obliquely oriented and attaches to the anterior greater tuberosity just posterior to the attachment of the coracohumeral ligament.

The infraspinatus and teres minor tendons insert inferior to the supraspinatus tendon on the greater tuberosity. The subscapularis tendon arises in an anterior fossa of the scapula. The tendon of the subscapularis has multiple slips and forms a long attachment to the lesser tuberosity. The interval between the anterior aspect of the supraspinatus tendon and the superior portion of the subscapularis tendon is called the rotator cuff interval. The intra-articular portion of the biceps tendon can be found within this space, as well as the coracohumeral ligament and the superior glenohumeral ligament. The subacromial subdeltoid bursa lies deep to the acromioclavicular joint and deltoid muscle and superficial to the tendons of the rotator cuff. This bursa does not communicate with the glenohumeral joint because it is separated by an intact rotator cuff. If the rotator cuff is torn, then fluid from the glenohumeral joint can communicate with this bursa.

Figure 18. Magic angle demonstrated in the ankle. (A) Axial T1W. (B) T2W. Note the high signal in the peroneal tendon on the T1W image (arrow) not seen on T2W. *Courtesy of Nancy Major, MD.*

BICEPS TENDON

The biceps tendon has two segments, a short head and a long head. The short head originates from the coracoid process, while the long head has striations of tendinous tissue originating from the superior labrum as well as the supraglenoid tubercle. At the point where the biceps tendon attaches to the supraglenoid tubercle, the biceps tendon is **intra-articular**. The tendon is contained within the bicipital groove, the **extra-articular** location, by the transverse ligament (subscapularis tendon). A **synovial sheath** surrounds the extra-articular portion of the tendon, which is continuous with the glenohumeral joint. A small amount of fluid around the tendon and within the tendon sheath is normal when a shoulder joint **effusion** is present or when intra-articular contrast agent has been administered (arthrography).

The normal appearance of shoulder tendons is uniformly hypointense on T2-weighted imaging sequences**.** The phenomenon called **magic angle** (**Figure 18)** can falsely increase signal in the tendons that course 55º to the bore of the magnet on short TE sequences; this phenomenon will be discussed in the ankle section.

GLENOID LABRUM

A ring of fibrous tissue, the labrum, deepens the shallow glenoid (**Figure 19**). The labrum is conventionally divided into six quadrants, best seen on oblique-coronal images. The six quadrants are:

- superior labrum
- anterosuperior
- anteroinferior
- posterosuperior
- posteroinferior (best seen best on axial images)
- inferior labrum (best seen with joint distension)

The anterosuperior portion of the labrum has a loose attachment to the glenoid. The more inferior portion of the labrum is more tightly adherent. The integrity of the labrum is best assessed in the presence of fluid distension, whether from a joint effusion or the administration of a contrast agent.

Anatomic variations exist in the anterosuperior portion of the labrum. A sublabral recess is a vertical cleft formed between the superior labrum and the articular rim of the glenoid and best seen on oblique-coronal images. This recess is at the level of the intra-articular biceps tendon and anterior to the biceps attachment.

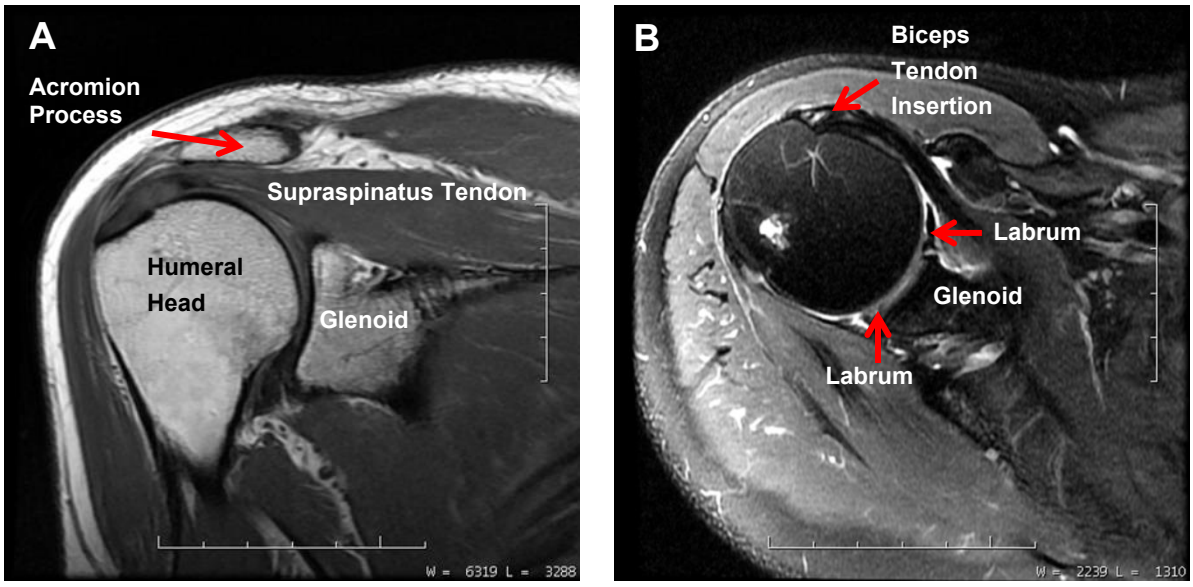

Figure 19. (A) Oblique-coronal PDW shoulder image. (B) Oblique-axial intermediate-TE PDW shoulder image with chemical fat suppression.

The sublabral foramen is a hole created by the lack of attachment of the anterosuperior labrum to the glenoid. Inferiorly, the labrum will attach normally to the glenoid. Occasionally, there can be a complete lack of formation of the anterior labrum, which is associated with a thick, cord-like middle glenohumeral ligament. This anatomic variation is called a Buford complex.

The normal appearance of the glenoid labrum is triangular in shape but can occasionally be round in contour. The glenoid labrum is generally low in signal on all imaging sequences. The posterior labrum is often smaller than the anterior labrum. The hyaline articular cartilage can separate the labrum from the underlying bony glenoid; this cartilage can appear to have intermediate signal between the labrum and underlying glenoid on imaging, mimicking a labral tear.

GLENOHUMERAL LIGAMENTS

The glenohumeral ligaments help maintain glenohumeral stability and are located superiorly, medially, and inferiorly to the glenoid fossa. The superior glenohumeral ligament is best seen on axial images immediately adjacent to the concavity of the coracoid process. The middle glenohumeral ligament is also best seen on axial images. When fluid is present in the joint, the entire extent of the middle glenohumeral ligament can be seen. Oblique-sagittal images can elucidate the entire course of the middle glenohumeral ligament located posterior to the subscapularis tendon. The inferior glenohumeral ligament is the largest of the glenohumeral ligaments and is the primary stabilizer of the joint with both an anterior and posterior band. The anterior band is responsible for **avulsion** of the anterior glenoid labrum during shoulder dislocation.

Shoulder Positioning

The shoulder is positioned with the arm down by the side, with the exception of abduction external rotation (ABER) views; refer to the shoulder protocol found at the end of this material. The hand is rotated to a neutral position so that the patient is comfortable and the arm is stable and stationary. While external rotation is required in radiography of the shoulder, it is not required for MRI. Complete external rotation can become uncomfortable for the patient over the course of the exam and cause motion. Internal rotation (back of the hand to the body) should be strictly avoided as the humeral head will rotate, making the supraspinatus tendon difficult to visualize (**Figure 20**).

In addition to the position of the hand, the elbow and humerus should be supported and level with the shoulder joint. Position the patient on the unaffected side on the table to bring the affected shoulder as close to isocenter of the magnet as possible where the magnetic field is most homogeneous and yields the best image quality regardless of pulse sequence.

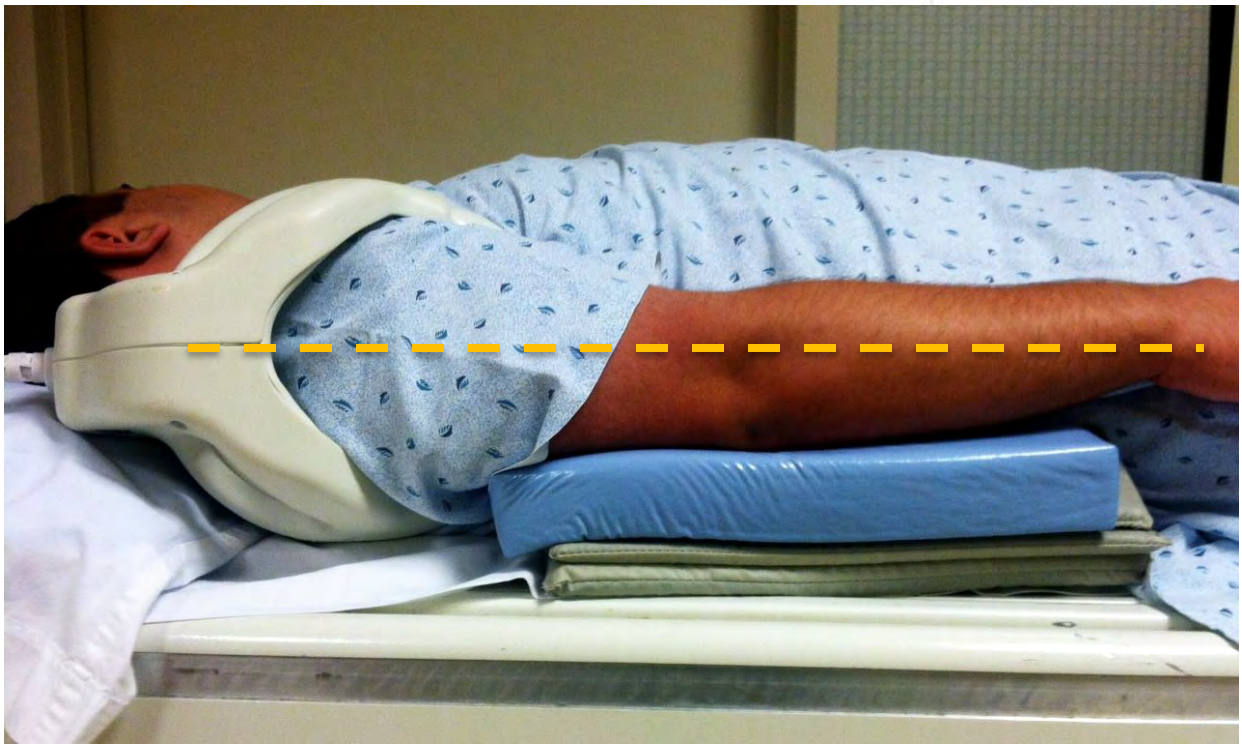

Figure 20. Shoulder positioning: Position the affected side as close to the center of the table as possible. Place support sponges under the humerus, elbow, and proximal forearm to position the humerus into a single plane as well as provide comfort and stability to the patient.

Planes of Acquisition

Shoulder imaging is typically acquired in the axial plane, oblique-coronal, and oblique-sagittal planes. (Arthrography of the shoulder involves additional planes of the acquisition, outlined later.)

After securely positioning a phased-array shoulder coil over the affected shoulder, a 3-plane localizing scout series is performed. In the axial plane, the imaging coverage includes the acromioclavicular (AC) joint superiorly through the glenoid and humeral head into the proximal humeral shaft (**Figure 21**).

The coronal plane is prescribed off the axial view and is obliqued to be *parallel* to the supraspinatus tendon, covering the entire humeral head into the scapular girdle. In the oblique-coronal plane, the supraspinatus can be seen in its entirety. The sagittal plane is also prescribed off an axial view and is obliqued to be *perpendicular* to the oblique-coronal plane.

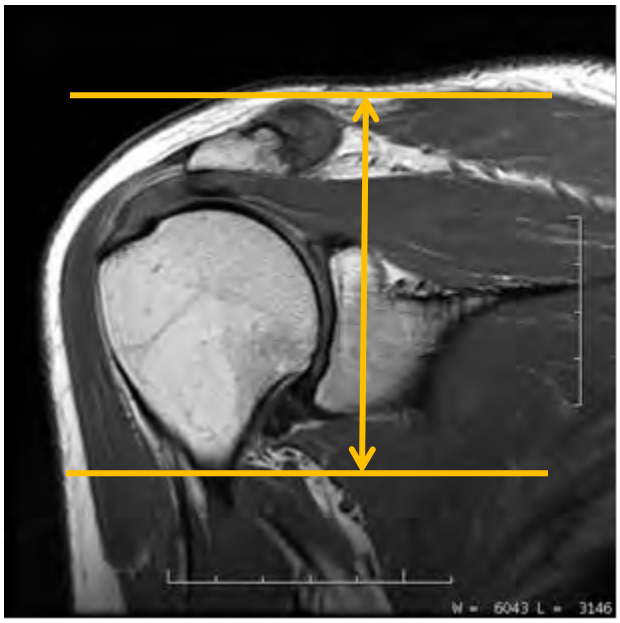

Figure 21. For axial imaging of the shoulder, the imaging is typically orthogonal axial with coverage through the AC joint through the glenoid fossa into the proximal humeral shaft.

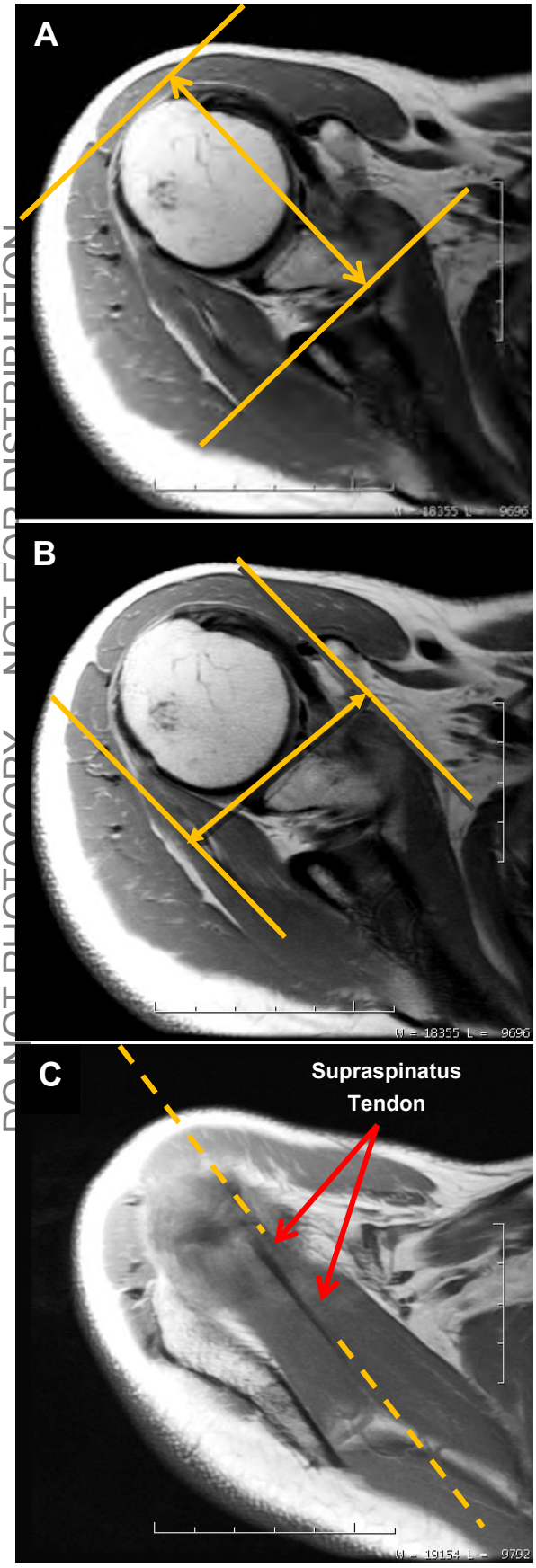

The oblique-sagittal coverage is through the entire humeral head and through the glenoid fossa (**Figure 22**). Oblique-sagittal images allow easy assessment of muscle atrophy, as well as an additional view of the rotator cuff tendon and the intra-articular biceps tendon.

The far lateral location of the shoulder to the rest of the body means the shoulder is rarely near isocenter of the magnet. In many cases, particularly with larger athletes, the shoulder can be close to the side of the magnet bore. To obtain the highest possible magnetic field homogeneity, use local shimming capabilities of the MR system. This is particularly true when utilizing chemical fat saturation techniques.

MR Shoulder Arthrography

Recall that MR arthrography is performed when fluid is instilled into the joint space prior to the MR examination, most often using a dilute gadolinium solution. The presence of gadolinium increases signal intensity on T1-weighted images. To allow the gadolinium solution to be more conspicuous and distinguish it from fat, the application of chemical fat suppression helps evaluate the locations of the gadolinium solution to readily diagnose pathology.

Partial thickness rotator cuff tears and labral tears are more easily identified when injecting gadolinium solution into the joint space. In some institutions, MR arthrography in the shoulder is used routinely, while in others the technique is reserved for use in postoperative patients and patients with joint instability.

Figure 22.(A) Oblique-sagittal imaging of the shoulder is *perpendicular* to the supraspinatus tendon. Coverage is completely through the humeral head and through the glenoid fossa. (B) Oblique-coronal imaging of the shoulder is *parallel* to the supraspinatus tendon. Coverage is completely through the humeral head and through the supraspinatus tendon. (C) The angle for oblique-coronal imaging and oblique-sagittal imaging of the shoulder should be *parallel and perpendicular* to the supraspinatus tendon easily seen on the axial images.

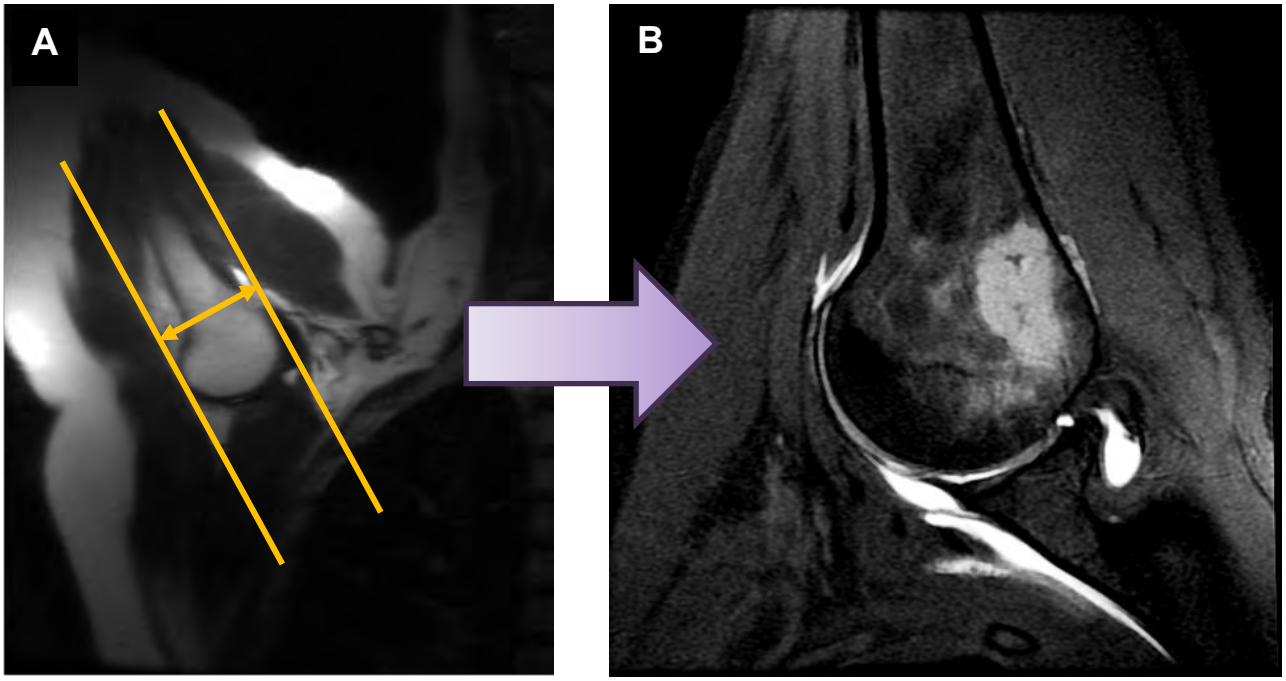

Figure 23. MR shoulder arthrogram ABER prescription. Position the patient's arm over the head and stabilize for comfort and immobilization. (A) Prescribe sagittal views from the coronal scout view (B) for the resultant image.

In addition to standard imaging of the shoulder, two other sets of images are typically acquired in MR shoulder arthrography.

The first is the abduction external rotation view, which is performed with the patient's arm placed over the head and the elbow bent to 90^0. The surface coil is rotated around the shoulder to ensure adequate coverage and signal capture. A localizing scout view is obtained to yield a coronal image with an oblique-sagittal series prescribed through the humeral head (**Figure 23**).

The other additional series is a radial scan. Recall that a radial series is one in which all slices share a common center point, with the slices prescribed in a circular fashion instead of the more typical parallel slice alignment. To obtain optimal views of the labrum, a series of concentrically centered slices are prescribed from an oblique-sagittal image near the glenoid fossa (**Figure 24**). Both ABER and the radial scans are performed as fat-suppressed series.

In addition to using magnetic field shimming tools, the use of spatial saturation pulses graphically placed over the apex of the lung can reduce breathing motion that creates respiratory ghosting image artifacts.

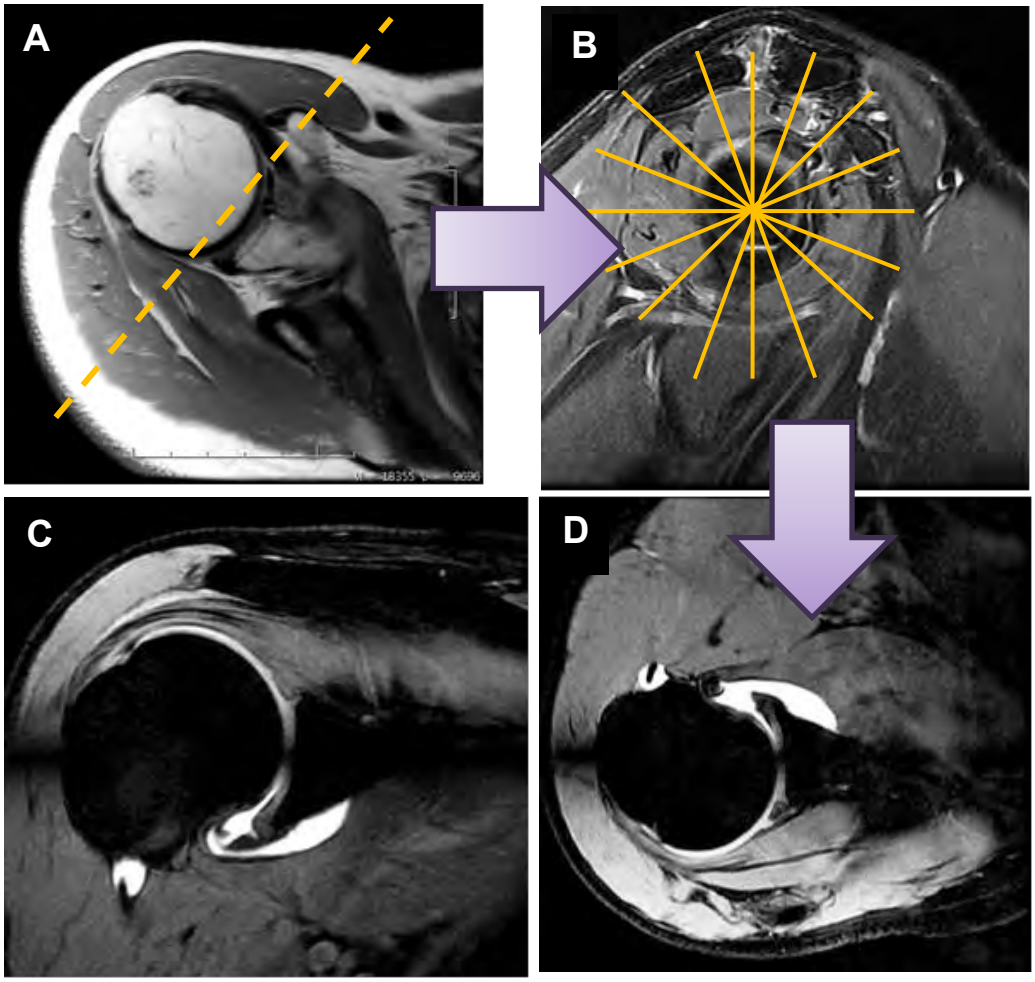

Figure 24. MR shoulder arthrogram radial prescription. (A) Select an oblique-sagittal image that is most proximal to the glenoid fossa. (B) Prescribe the radial series off that oblique-sagittal view. (C, D) Examples of the resultant series.

Common Pathology

Within the rotator cuff a **myxoid** degeneration can take place from chronic microtears called **tendinopathy** and **tendinosis**. Partial tears can occur on the articular or bursal side of the tendon, though they are most common along the articular surface. With partial tears, fluid signal will be seen within the substance of the tendon. A full thickness tear is identified by fluid visualized through the tendon from the joint space into the overlying bursa (**Figure 25**). The ends of the tendon will be surrounded by fluid in a full thickness tear. In a completely torn tendon, it is important to note the amount of retraction as well as associated muscle atrophy, best seen on oblique-sagittal T1-weighted images.

Biceps tendon pathology can also occur in association with rotator cuff pathology. Abnormal signal will be identified within the substance of the biceps tendon on the T2-weighted image. In addition, the size of the tendon can be altered. Tenosynovitis is diagnosed when the fluid in the biceps tendon sheath is out of proportion to what is identified within the joint space.

Figure 25. 67-year-old male. Coronal PDW of the shoulder with fat suppression demonstrating a 1cm full thickness tear of the rotator cuff.

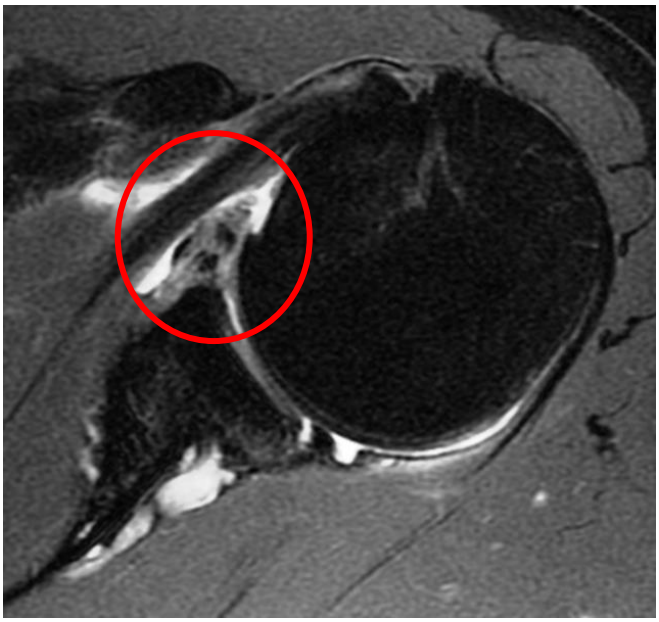

Figure 26. 45-year-male. Oblique-axial PDW shoulder image with fat suppression demonstrating an anterior labral tear.

Labral pathology can also occur in conjunction with rotator cuff tears or in isolation. Many anterior labral tears are the result of an anterior shoulder dislocation. The labrum may be detached from the underlying glenoid or torn through the substance of the labrum. Posterior labral tears can result from dislocations or from activities that increase the force of the humeral head against the glenoid posteriorly, for example, when engaging in a bench press (**Figure 26**).

UPPER EXTREMITY IMAGING — THE ELBOW

Anatomy of the Elbow

The anatomy of the elbow is straightforward; however, the complexity of motion requires consistency in imaging techniques for every single exam.

The elbow is capable of flexion, extension, pronation, and supination. The bony structures that make up the elbow joint are the humerus, which has two bony protuberances — the medial and lateral epicondyles — and the radius and ulna (**Figure 27**).

The humerus articulates with the ulna and radius, and the radius and ulna articulate with each other. A thin rim of hyaline articular cartilage lines the joint **articulations**. The radius and ulna each have a bony protuberance responsible for insertion sites of key structures; the radius has the radial tuberosity that receives the biceps tendon, while the ulna has the ulnar tuberosity for the brachialis tendon and the coronoid process (an anteriorly projecting portion of the proximal ulna).

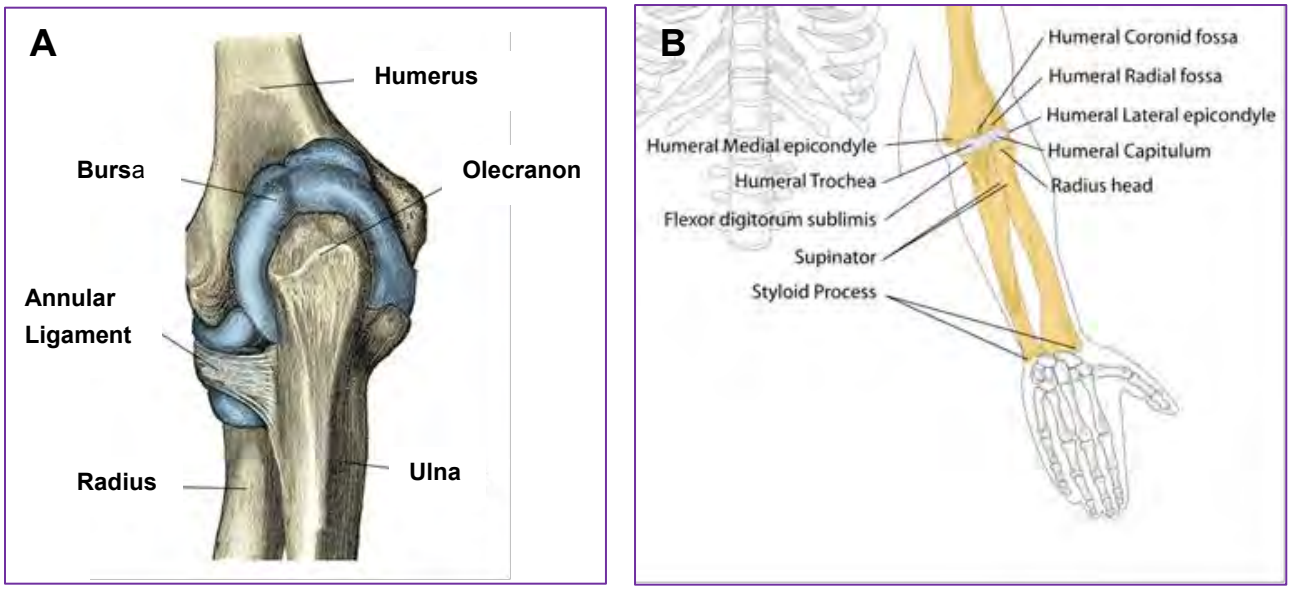

Figure 27. Elbow anatomy. (A) Available at: Wikimedia Commons Bursa of Elbow Joint. (B) Available at: Wikimedia Commons Human Arm Bones.

The structures around the elbow include the common flexor tendon and pronator muscles that arise from the medial epicondyle and the common extensor tendon and supinators that arise from the lateral epicondyle.

The primary function of the biceps tendon is to be a strong flexor of the elbow; it also serves as a supinator of the elbow (**Figure 28**). The biceps tendon around the elbow does not have a tendon sheath, unlike the tendon at the shoulder. A long portion of the biceps tendon is exposed and superficial, thereby rendering it more susceptible to injury.

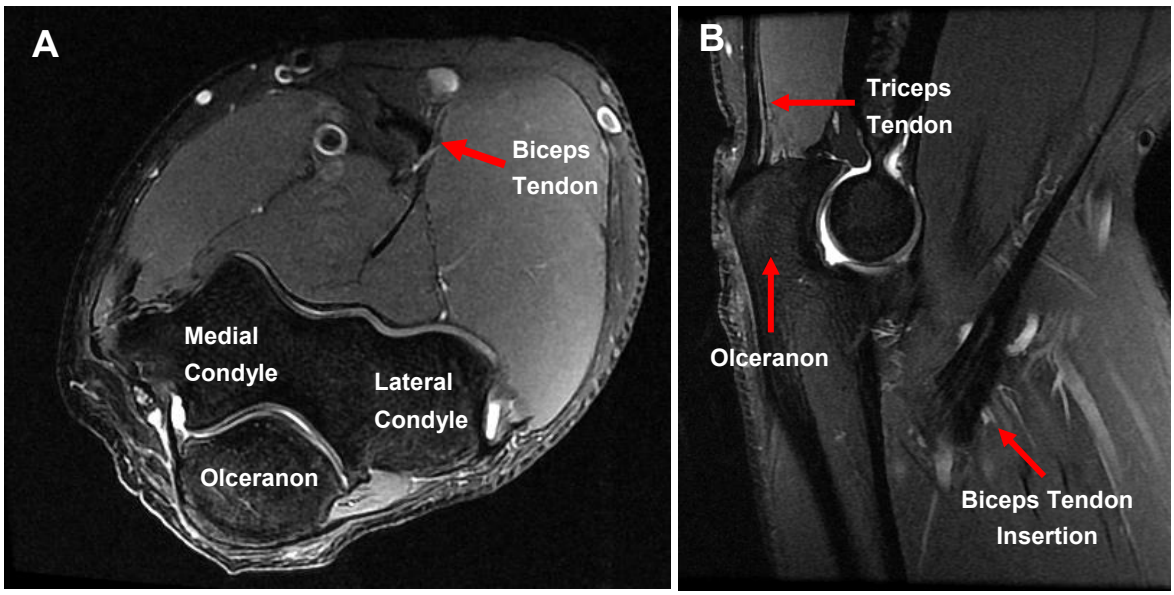

Figure 28. Biceps tendon and insertion point. (A) Axial intermediate-TE PDW image of the elbow with chemical fat suppression. (B) Sagittal intermediate-TE PDW image of the elbow with chemical fat suppression.

The brachialis tendon inserts on the ulna. Most of the tendon of the brachialis is contained within the muscle belly and therefore is not as prone to injury. The brachialis is also a flexor of the elbow.

Figure 29. Elbow positioning with the arm extended overhead and patient in the prone position. This position places the elbow within the magnet's optimal homogeneity near isocenter. While this may not be the most comfortable patient position, it provides the best image quality, particularly when using chemical fat suppression techniques.

The triceps tendon is the primary elbow extender. Like the biceps tendon, it does not have a tendon sheath and consequently on MRI may appear to have high signal within the muscle. This represents adjacent connective tissue and fat that can get between the slips of tendon, creating this signal configuration.

The collateral ligaments provide stability to the joint. The ulnar collateral ligament is located on the medial (ulnar) aspect of the joint, arising from the medial epicondyle of the humerus and inserting onto the sublime tuberacle of the ulna. There are other components of the ulnar collateral ligament that are not necessary for stability and will not be discussed.

The radial (lateral) collateral ligament is comprised of three contiguous bands. The first is the lateral ulnar collateral ligament (LUCL) that arises from the lateral epicondyle and has an oblique course to its insertion on a bony prominence of the ulna. Anterior to this structure is the true radial collateral ligament that blends into the fibers of the lateral ulnar collateral ligament. The third band in this complex is the annular ligament, which wraps around the radial head.

There are three important nerves that surround the elbow: the radial nerve bifurcates into deep and superficial branches, the median nerve located near the anterior branch of the radial nerve, and the ulnar nerve adjacent to the medial epicondyle deep to the ulnar collateral ligament. The close proximity of the ulnar nerve to the ulnar collateral ligament and flexor tendon can lead to damage of the nerve when these structures are injured. Thus, MR examination can be critical for determining the etiology of medial elbow pain. MR **neurography** — MR imaging specific to nerves of the extremities — is used to visualize and assess nerve damage caused by trauma, disease, or surgery.

Elbow Positioning

The elbow, like the shoulder, should be as close to isocenter as possible to ensure the best image quality. If tolerated, position the patient prone or supine with the arm extended overhead and with a phased-array surface coil as close to isocenter as possible. The arm must be straight with no bend in the elbow, and the hand should be in a comfortable and neutral rotation (**Figure 29**).

Figure 30. Elbow positioning with the arm by the side with the patient in the supine position. This position is more comfortable for the patient but places the elbow far from isocenter. In this position, chemical fat suppression may be difficult, particularly for larger patients who cannot move toward the unaffected side to place the elbow closer to isocenter. If chemical fat suppression is not successful, STIR imaging may be an alternative. Note that the forearm and wrist are supported in the same plane, and the wrist is rotated in the optimal neutral position.

Recall that phased-array coils are a series of smaller coils aligned to collect signal data over an area greater than any of the individual coils, yet each individual coil maintains its SNR and is not averaged into all the others. A 16-element phase array coil, for example, provides excellent coverage and SNR. A 32-element coil provides more SNR still. The coil type depends on the manufacturer's coil designs and availability; flexible phased-array coils are common and help boost SNR.

If the patient cannot tolerate positioning with the arm extended, the only alternative is to place the patient supine with the arm down by the side (**Figure 30**). While this position may be more comfortable for the patient, it is the least desirable from an image quality standpoint as the elbow is far from isocenter. Magnetic field homogeneity is not optimal and obtaining robust and uniform chemical fat saturation can be challenging.

Because of the bulky size of some phased-array coils, there may not be sufficient room for the surface coil to be placed at the side of the patient table. In this instance, flex coils may not be a phased-array configuration or lack sufficient coverage to scan the elbow completely and with enough SNR to permit high spatial resolution. As with the shoulder, having the patient move toward the unaffected side may mitigate the issue of being far from isocenter.

The technologist should be prepared to alter the protocol in order to obtain the resolution and contrast required for thoroughly evaluating the elbow. For example, if effective chemical fat saturation is not possible, STIR imaging may be required instead.

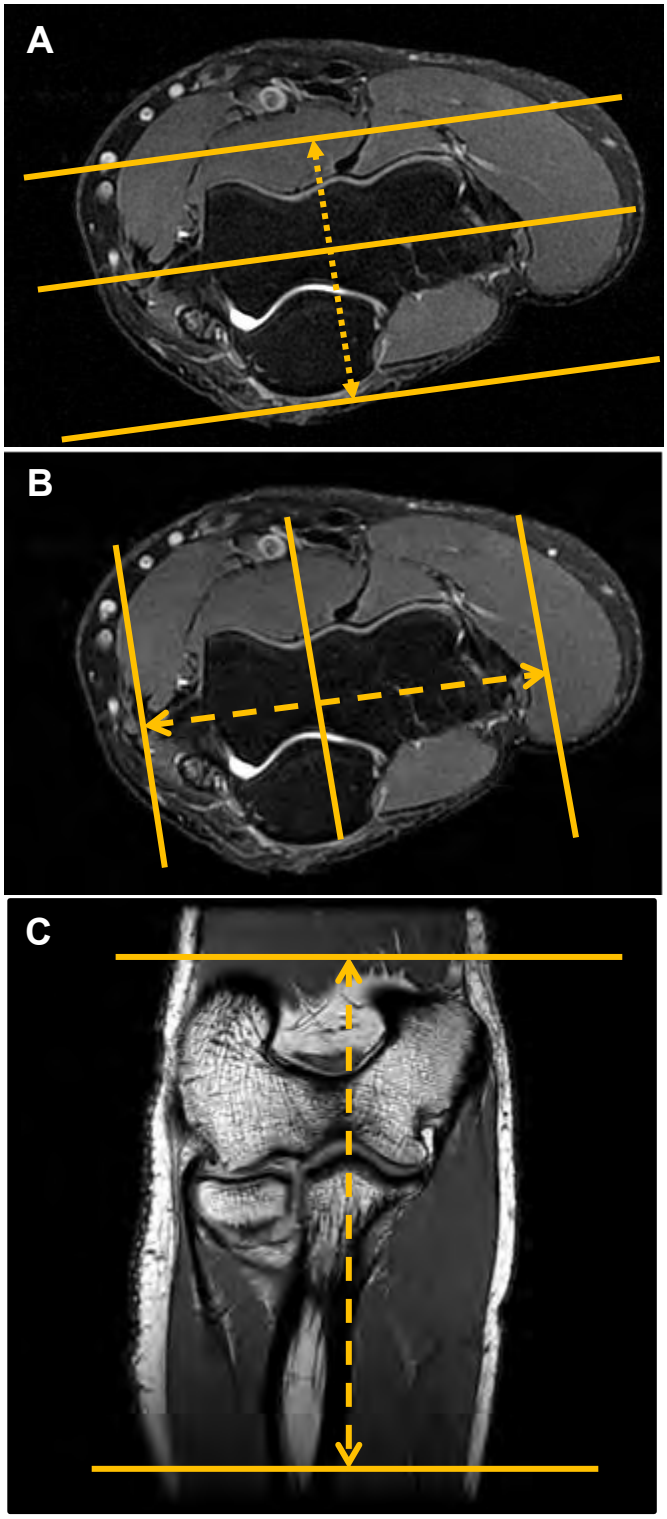

Figure 31. (A) Oblique-coronal elbow. Coverage is parallel to the condyles through the biceps tendon insertion point. (B) Oblique-sagittal elbow. Coverage is perpendicular to the condyles. Coverage is from condyle to condyle including the biceps tendon insertion. (C) Axial elbow. Coverage is from the distal humerus through the radial tuberosity.

Planes of Acquisition

Elbow imaging typically consists of three planes of T1W and intermediate-weighted fat- suppressed imaging. While long-TE imaging (80msec – 100msec T2W) is used in many imaging facilities, a growing trend in imaging with intermediate TEs (40-55msec) is favored by many radiologists. This range of TE, particularly in conjunction with chemical fat saturation, yields higher SNR than long-TE imaging as longer TEs increase the signal decay time. Intermediate TEs also provide exquisite tissue contrast while providing excellent spatial resolution.

In positioning the elbow in the phased-array coil, it is common to place the elbow at the center of the coil. While this may appear to be the correct centering, placement of the elbow at the center of the coil risks incorrectly positioning the biceps tendon insertion point into the radial tuberosity at the very end, or worse, outside the surface coil. The radial tuberosity is an essential evaluation point in the imaging of the elbow. The biceps tendon attaches to the radius at this point and is distal to the elbow. To ensure proper evaluation of the biceps tendon insertion point for tear or rupture, position the center of the coil not on the elbow itself but more distally so that while the elbow is still within the coil and the proximal radius and ulna are also well within imaging range.

Axial imaging is obtained by prescribing slices perpendicular to the long axis of the distal humerus and proximal radius and ulna. Coverage should be from the distal humerus through the biceps insertion point (**Figure 31A**).

Coronal imaging is obliqued to run parallel to the long axis of the humeral lateral and medial condyles. Coverage is through the entire elbow joint as well as the radius and ulna. If ulnar or radial nerve neuropathy is a consideration, coronal coverage also should cover the muscles of the forearm (**Figure 31B**).

Sagittal imaging is obliqued to run perpendicular to the humeral condyles and therefore is perpendicular to the coronal imaging. Slice coverage is from lateral condyle to medial condyle (**Figure 31C**).

Because the structures of the elbow are very small, high spatial resolution is essential. Small FOVs and high imaging matrices are required in all planes. Axial imaging should be no more than 3.0mm. Sagittal and coronal slice thickness should be even thinner, and 1.5mm – 2.5mm thickness is optimal.

MR Elbow Arthrography

The use of an intra-articular contrast medium is extremely helpful when evaluating the ligaments around the elbow, as well as for identifying loose body formation and assessing cartilage defects. Recall that immediately prior to the MRI examination, a contrast solution, usually a dilute gadolinium solution, is injected into the elbow joint. A post-injection elbow MRI exam is done using both high resolution fat-suppressed and non-fat-suppressed imaging techniques (**Figure 32**).

Figure 32. MR arthrogram of the elbow acquired at 2.0mm slice thickness. (A) Oblique-coronal T1W image with chemical fat suppression. (B) Oblique-coronal PDW image without fat suppression.

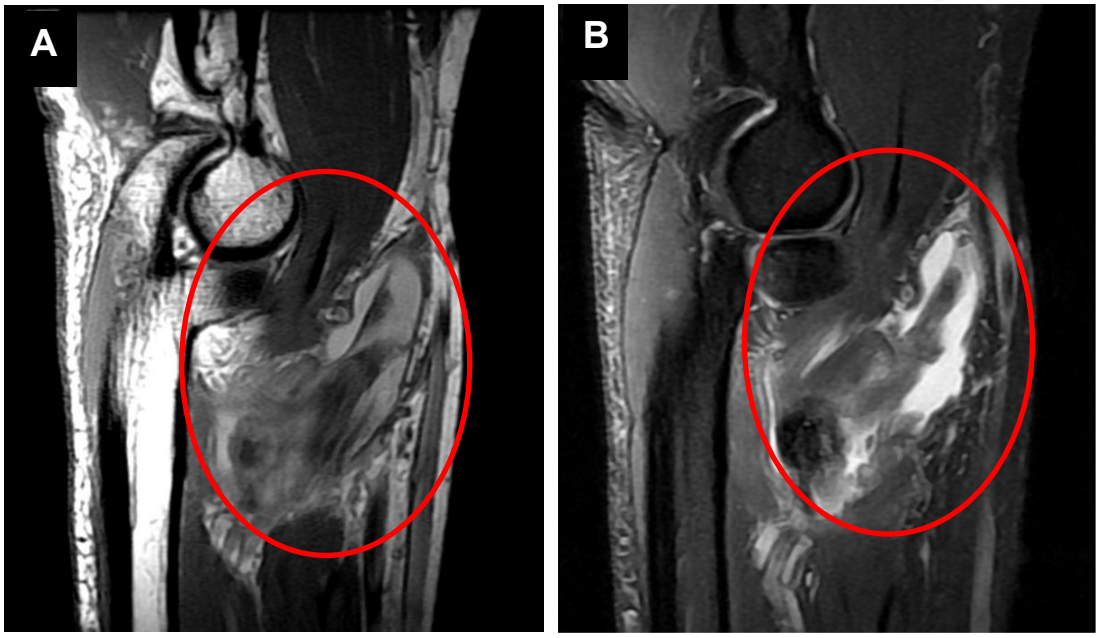

Figure 33. 36-year-old male demonstrating a complete but non-retracted tear of the biceps tendon. (A) Sagittal PDW without fat suppression. (B) Sagittal intermediate-TE PDW with chemical fat suppression.

Common Pathology

One of the more commonly encountered injuries to the elbow is “tennis elbow.” This painful condition is the result of the extensor carpi radialis brevis suffering microtears with healing by scar formation, followed by a cycle of repetitive microtears and healing in a continual process. Abnormal high signal is seen on T2-weighted images within the substance of the tendon. On the medial side of the joint the common flexor tendon can suffer a similar fate. MRI can elucidate the severity of the tear and help guide treatment.

Injuries to the biceps tendon are not as common at the elbow as at the shoulder. When injuries do occur, the biceps tendon can be partially or completely torn, and MRI is an excellent modality for making that distinction. MRI can demonstrate the amount of gap or retraction of the tendon, thus aiding in surgical planning. Injuries to the triceps tendon are unusual; as with the biceps, the amount of the triceps tendon involved in a tear can be determined with MRI, as well as the measurement of the gap and proximal retraction of the tendon (**Figure 33**).

Determination of injury to the ligaments in the elbow joints is vital. When abnormal signal is identified within the tissue, the ligaments may be sprained or completely torn, in which case the free edge of the ligament can be identified since it will be surrounded by high signal. When gadolinium is present in the elbow joint, the contrast solution should flow out around the damaged ligament into the surrounding soft tissues. In the setting of a partial tear of the ulnar collateral ligament, the gadolinium solution is seen between the bone of its insertion site and the overlying intact portion of the ligament. MR arthrography is the modality of choice for evaluating these particular types of injury.

UPPER EXTREMITY IMAGING — THE WRIST

Anatomy of the Wrist

The wrist is composed of eight carpal bones, as well as the distal radius and distal ulna. The relationships between the carpal bones are very important. The wrist is not a single joint, but rather a series of articulations that includes the distal radius with the carpal bones (proximal carpal row), the distal ulna with the proximal carpal row, the distal ulna with the distal radius, the proximal carpal row with the midcarpal row, the midcarpal row with the metacarpals, and the pisiform with the triquetrum (**Figure 34**).

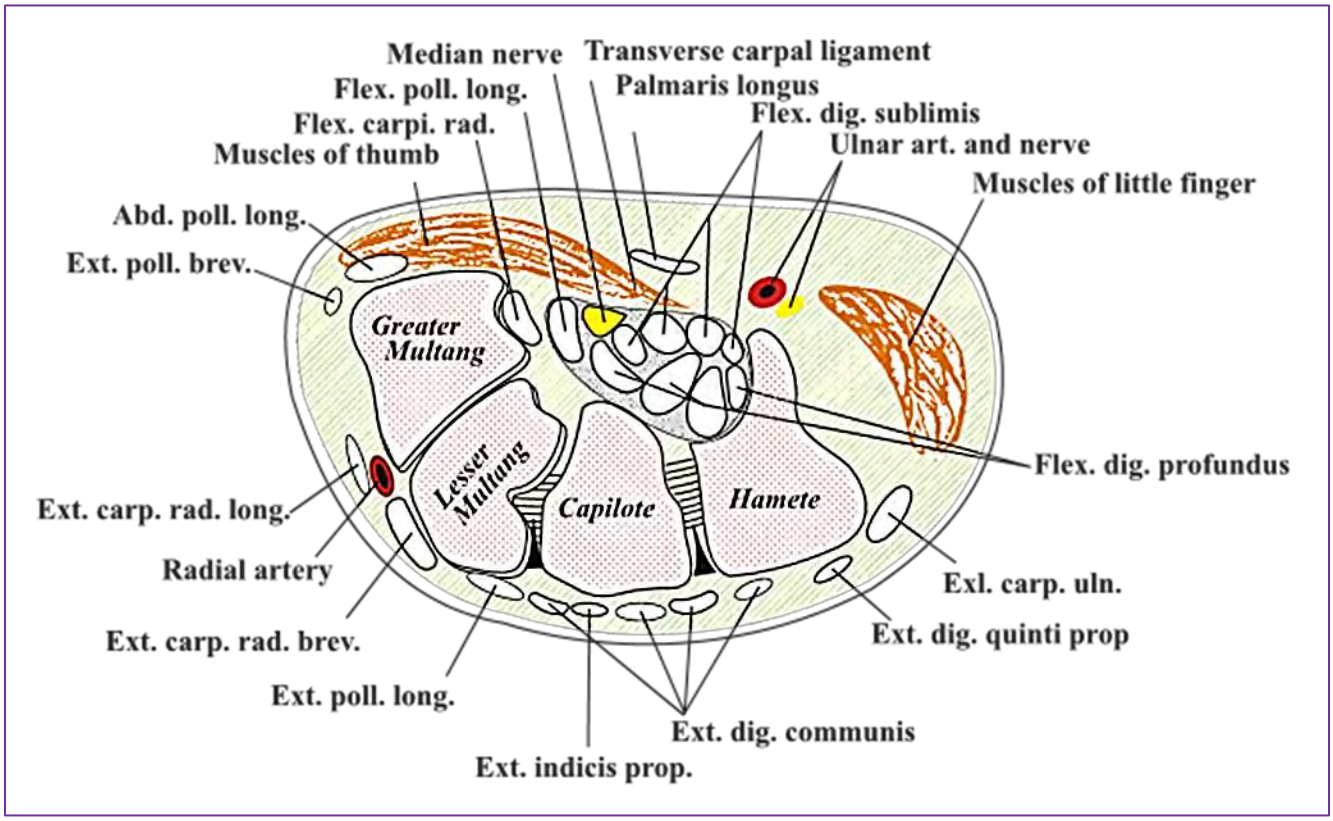

Figure 34. Wrist anatomy. Available at: Wikimedia Commons Carpal-Tunnel.

MR examinations of the wrist are most often performed for evaluating the triangular fibrocartilage complex (TFCC) and intrinsic ligaments. The anatomy of the TFCC is probably the most important soft tissue structure of the wrist since it serves as the primary stabilizer of the wrist and acts as a cushion between the carpus and the distal ulna. The TFCC serves as an extension of the articular surface of the radius, providing a site of insertion for the ulnar-sided carpal bones. Normal-appearing TFCC is uniformly low in signal on all pulse sequences, demonstrated as an elongated triangle on coronal images. The volar aspect (palm side of the hand) of the TFCC attaches strongly to the triquetrum with additional attachments to regions around the lunate. The dorsal aspect of the TFCC is incorporated into the floor of the sheath of the extensor carpi ulnaris tendon (**Figure 35**).

The intrinsic ligaments connect adjacent carpal bones. The most commonly injured and hence the most studied ligaments of the wrist are the scapholunate and lunatotriquetral ligaments that separate the radiocarpal joint space from the midcarpal compartment. They are low in signal intensity on imaging and are a variety of shapes from triangular to blunt in appearance. Their disruption causes communication of the radiocarpal and midcarpal joint spaces.

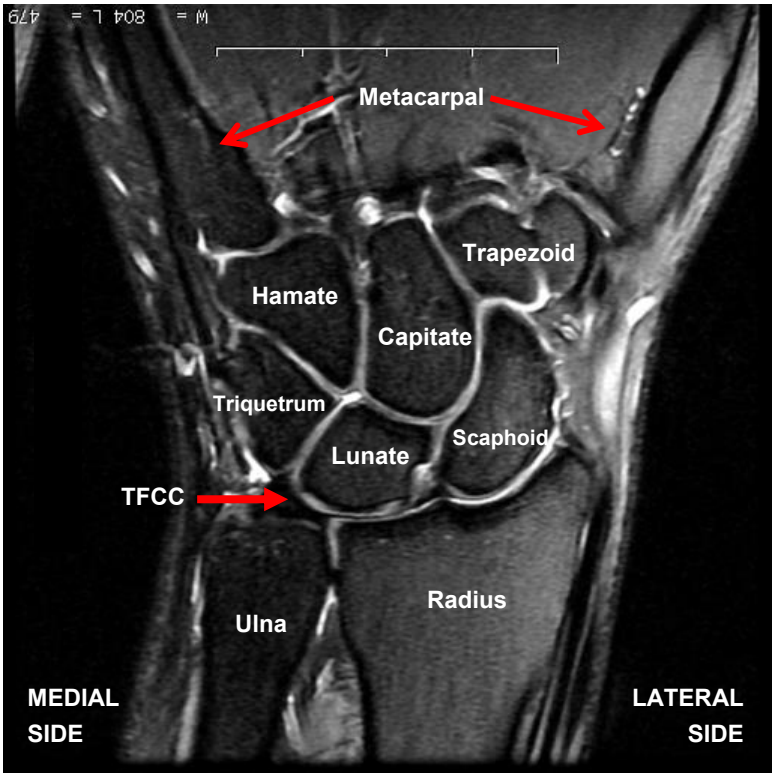

Figure 35. Oblique-coronal view of the wrist using intermediate-weighted TE PDW imaging with chemical fat suppression.

Wrist Positioning

Like the elbow and shoulder, the wrist is best imaged with the arm as close to isocenter of the magnet as possible, usually requiring the patient to be placed prone on the table with the arm extended above the head. The elbow should be as close to straight as possible but some bend is not problematic as long as the elbow is not bent more than 45^0; the wrist should be in a neutral position. This position rotates the ulnar styloid processor medially. With the styloid in the medial-pointing position, the TFCC is most easily visualized (**Figure 36A and B**).

For both the elbow and the wrist, if the patient cannot tolerate a position with the arm extended, imaging with the arm by the side is the only alternative (**Figure 36C**). Position the patient to the unaffected side of the table so that the affected joint is as close to isocenter as possible. Chemical fat suppression techniques may be more difficult far from isocenter. Moreover, with the elbow or wrist by the side, careful use of anti-aliasing techniques may also be required.

Planes of Acquisition

Imaging the wrist can be demanding as, much like the elbow, the wrist is comprised of very small structures. Pathologies such as small microtears require very high spatial resolution and precise oblique prescriptions. Begin with a 3-plane localizing scout series. The axial of this series should be observed closely. The styloid process of the ulna should be away from the radius or in the 3:00 position. If the styloid process is at the 12:00 or 6:00 position, in most cases the elbow is bent at greater than 90^0, and the patient should be re-positioned.

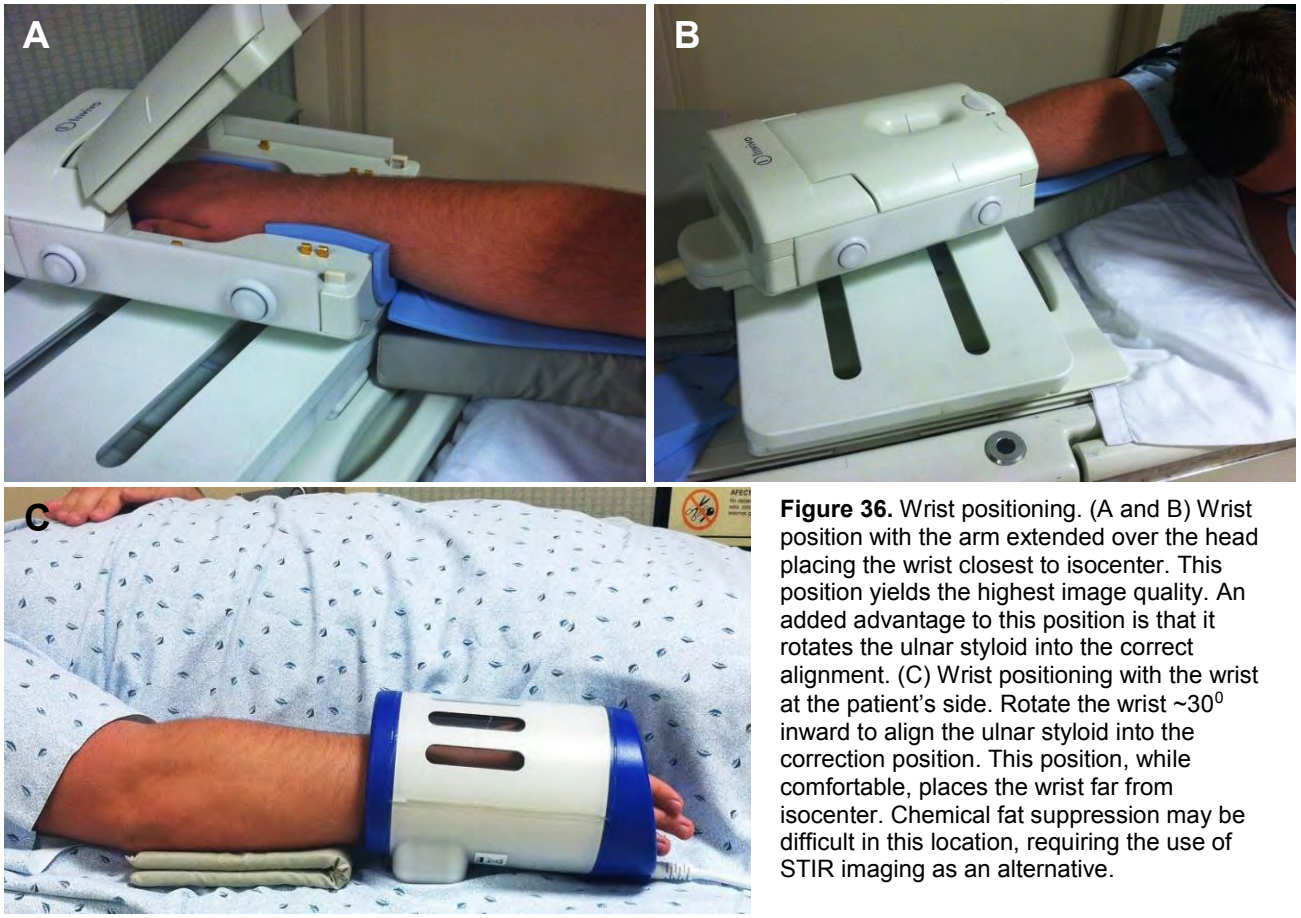

Figure 36. Wrist positioning. (A and B) Wrist position with the arm extended over the head placing the wrist closest to isocenter. This position yields the highest image quality. An added advantage to this position is that it rotates the ulnar styloid into the correct alignment. (C) Wrist positioning with the wrist at the patient's side. Rotate the wrist ~30^0 inward to align the ulnar styloid into the correction position. This position, while comfortable, places the wrist far from isocenter. Chemical fat suppression may be difficult in this location, requiring the use of STIR imaging as an alternative.

Axial imaging is done perpendicular to the long axis plane of the forearm. Coverage is from the distal ulna and radius through all the carpal bones into the proximal metacarpals. Typically both T1W and intermediate TE fat-suppressed imaging are done. The field of view, matrix, and slice thickness are optimized to yield high spatial resolution with a maximum slice thickness of 3.0mm (**Figure 37A**).

The angulation for the sagittal images through the wrist is perpendicular to the angulation of the coronal series. Slice coverage is all of the carpal bones as well as the distal humerus and ulna (**Figure 37B**). Because blood flow is in-plane in the sagittal view, artifacts from flowing blood cascading through the sagittal images can be problematic. The use of **gradient-moment nulling** and spatially selected saturation pulses is recommended.

Oblique-coronal imaging is extremely important as it is in the coronal plane that the TFCC is best visualized. Obtaining the correct angle of obliquity is essential. Prescribe the oblique-coronal images off the axial image that best demonstrates the ulnar styloid process and the radius. The coronal plane should be prescribed through the long axis plane that is made by visualizing a line that runs from the ulnar styloid through the center of the radius. Once the correct angulation is set, prescribe the coronal images to cover all the ligaments of the wrist as well as all the carpal bones. The center point of the field of view should be set to the center of the capitate bone. The slice thickness is thinner than that of the axial images and is usually 2.0mm or less (**Figure 38**).

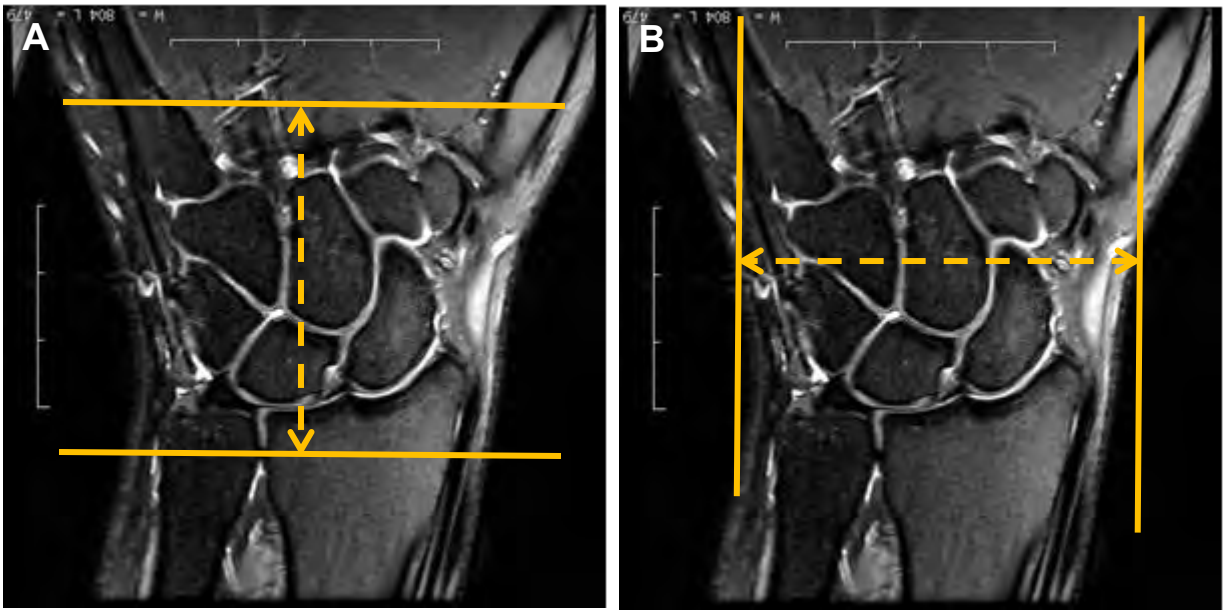

Figure 37. (A) Axial wrist coverage includes the distal radius and ulna through the carpals into the proximal metacarpals. (B) Sagittal coverage includes the carpals and entire distal radius and ulna. The center point for sagittal imaging is the center of the capitate bone.

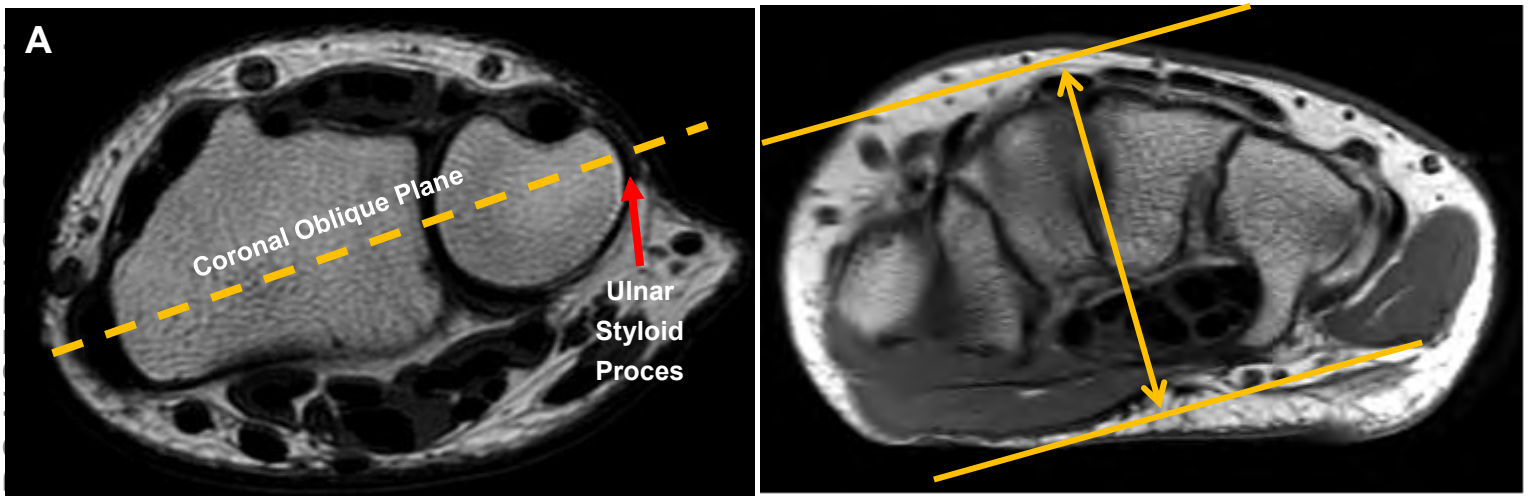

Figure 38. (A) Oblique-coronal imaging of the wrist requires the ulnar styloid be pointed in the medial direction, ensuring the TFCC is aligned for optimal visualization. (B) Coverage of the oblique-coronal wrist must include all ligaments and tendons. As with oblique-sagittal imaging, the center point is the center of the capitate bone.

MR Wrist Arthrography

MR wrist arthrography is used for evaluating the possibility of small tears in the TFCC and for assessing the intrinsic ligaments; identification of gadolinium in the midcarpal row would suggest disruption of one of the intrinsic ligaments (**Figure 39**). However, this information can be readily obtained with conventional MRI, and therefore MR arthrography is not widely used for evaluating the wrist as it is for other joints.

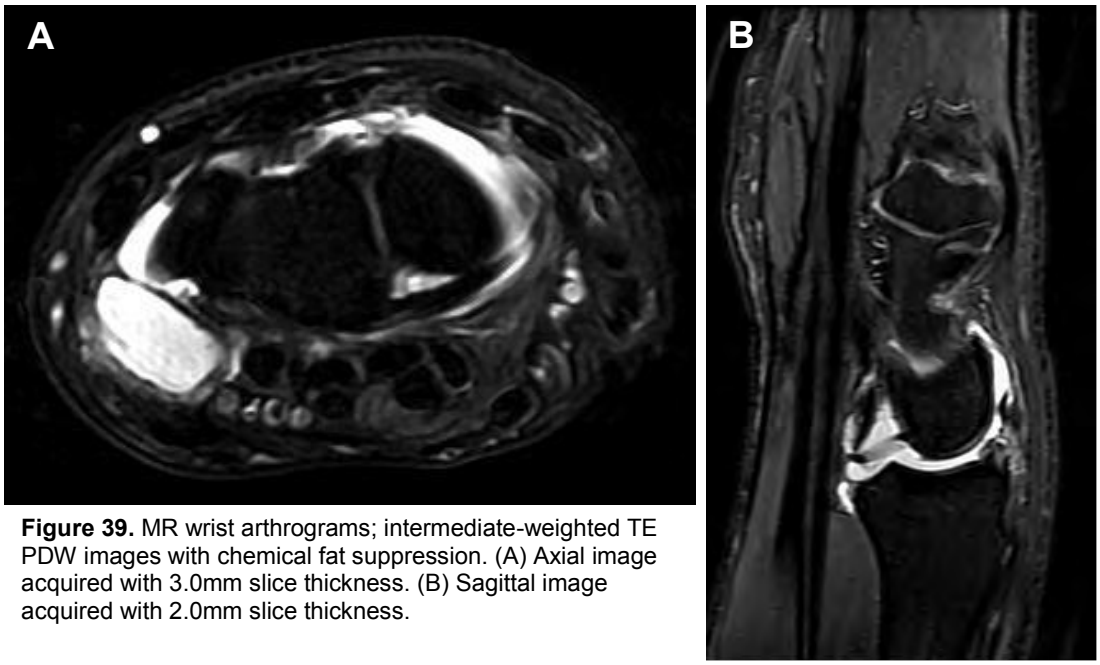

Figure 39. MR wrist arthrograms; intermediate-weighted TE PDW images with chemical fat suppression. (A) Axial image acquired with 3.0mm slice thickness. (B) Sagittal image acquired with 2.0mm slice thickness.

Common Pathology

Common pathologies of the wrist include tears to the TFCC, carpal tunnel syndrome, fracture, degenerative joint disease (DJD), and both rheumatoid and osteoarthritis.

The most common disorders of the TFCC are secondary to degeneration or injury. Degeneration is characterized by intermediate to high signal intensity on T1-weighted images, which becomes low signal on intermediate TE-weighted images. Irregular appearances on MRI include abnormal morphology of the TFCC, a defect in the TFCC, and fluid within the defect; fluid may also be seen in the radio-ulnar joint as a consequence of the TFCC tear. Fluid may also be found underneath the attachment of the TFCC, separating the TFCC from the distal ulna.

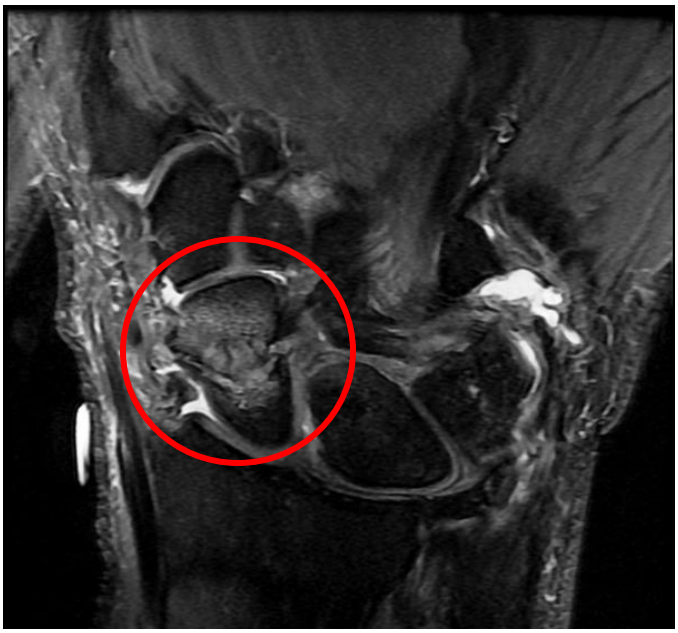

Figure 40. Oblique-coronal PDW image with fat suppression demonstrating a complete fracture of the scaphoid bone of the wrist (circle).

The use of fat suppression is important for identifying abnormal signal within the bones, which can result from either bone contusions or fractures. MRI is useful for identifying a fracture not seen on conventional x-rays, particularly scaphoid fractures and fractures of the hook of the hamate (**Figure 40**).

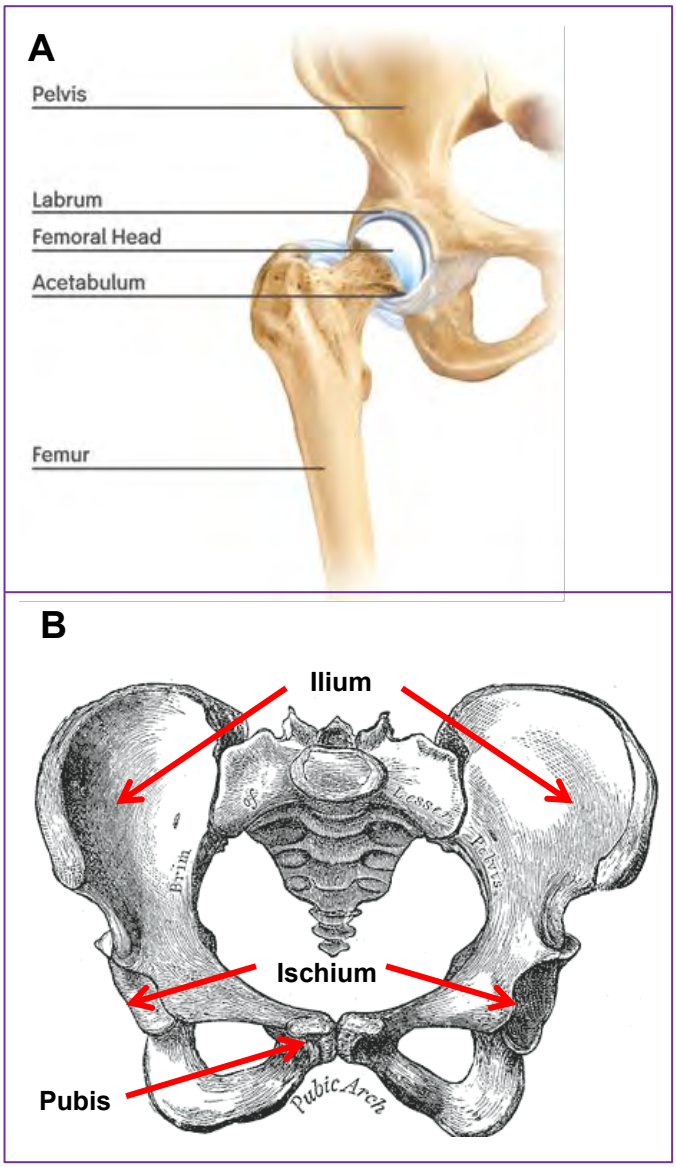

Figure 41. Anatomy of the hip. (A) Available at: Wikimedia Commons Basic Anatomy of the Hip Joint. (B) Available at: Wikimedia.

LOWER EXTREMITY IMAGING — THE HIP

Anatomy of the Hip

The hip joint carries more weight by far than other any joint of the body. Overuse through sports activity as well as degeneration caused by the normal aging process results in various pathologies for a large segment of the population.

The hip is a relatively stable articulation as the femoral head is constrained within the deep osseous acetabulum. Several soft tissue structures including the labrum, muscles, and tendons contribute additional dynamic support to the hip (**Figure 41**).

The three bones that combine to construct the pelvis — the ilium, ischium, and pubis — also form the acetabulum. Into the acetabulum fits the rounded head of the femur, the largest and strongest bone in the body. The proximal portion of the femur is comprised of the head, neck, greater trochanter, and lesser trochanter. The greater trochanter serves as the insertion site for several tendons. The lesser trochanter is the insertion site for the iliopsoas (**Figure 42**). All normal tendons are low in signal on all imaging sequences.

The hyaline articular cartilage is located along the femoral head. Around the acetabulum, the hyaline articular cartilage is only about 3mm thick, is semilunar in configuration, and is intermediate in signal on imaging sequences. The deep surface of the acetabulum is not covered by hyaline articular cartilage. The acetabular labrum deepens the acetabular fossa, providing additional coverage of the femoral head. The usual shape of the labrum is triangular and should be low in signal when normal.

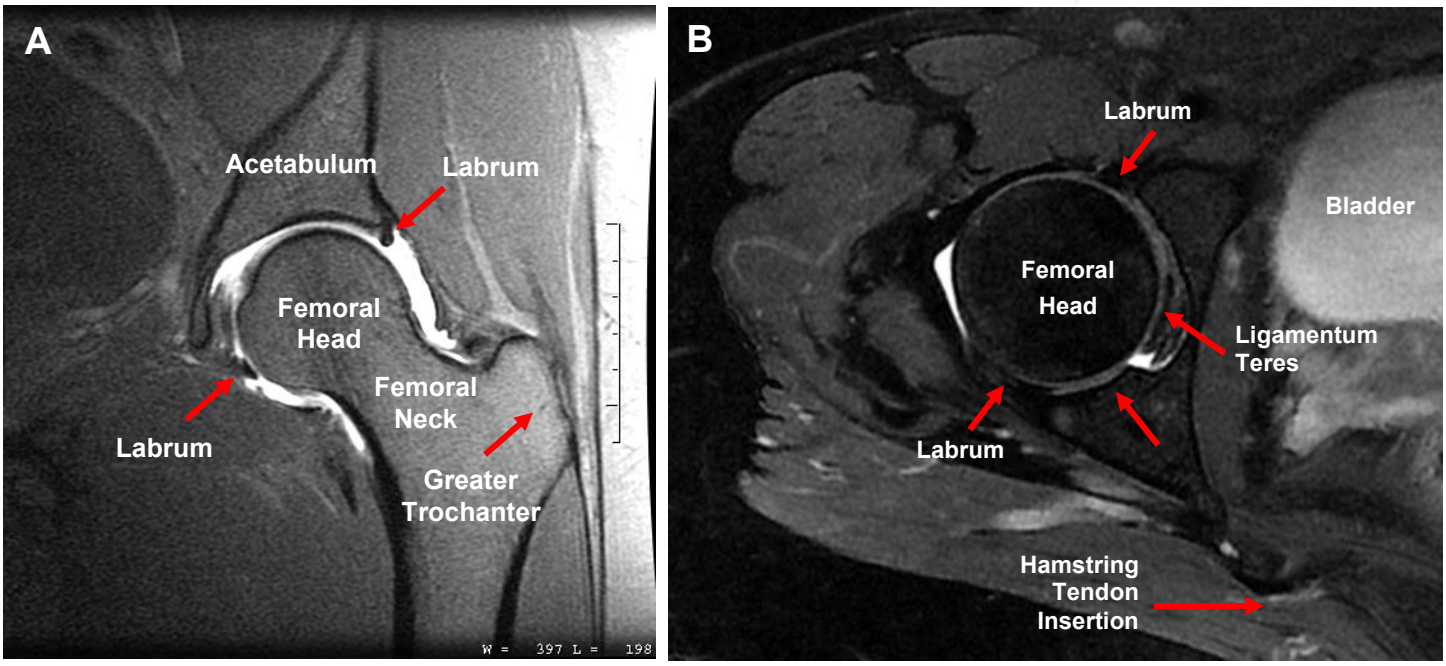

Figure 42. (A) Coronal fat-suppressed view of the left hip. (B) Axial fat-suppressed image of the right hip.

The hip is enveloped by twenty muscles that are divided into four compartments. The anterior compartment contains the primary hip flexors; the posterior compartment contains the primary hip extensors (hamstrings); the medial compartment muscles are the primary **adductors** of the hip; and the lateral compartment muscles **abduct** and rotate the hip.

The pelvis is composed of the sacrum posteriorly and the iliac bones forming the back and side of the pelvis. The ilium and pubic bones form the remainder of the anterior portion of the pelvis. The sacroiliac joints are posteriorly located and have a fibrous connection at the superior margin and a **synovial joint** at the inferior portion. The pubic symphysis is a joint filled with a dense fibrous band.

Hip and Bony Pelvis Positioning

Positioning for the hip is straightforward but nonetheless important. Place the patient supine and straight on the table with the toes pointed inward. If securing the feet in this position is required, tape the feet together but with a wedge sponge placed between the ankles. Pointing the toes inward rotates the femoral heads into the same plane, also allowing the patient to completely relax the feet (**Figure 43**).

The positioning for the bony pelvis is the same as positioning for the hip. Note that a clear distinction is required between imaging of the soft tissue pelvis — for example, the uterus, prostate gland, and bladder — and the bony pelvis for imaging the bony pelvic girdle as in the setting of bony metastasis or **avascular necrosis** (AVN).

Positioning a phased-array surface coil is required for obtaining diagnostic hip and pelvic images. Phased-array surface coils used in pelvic imaging usually have a posterior half that is fitted to the table and an anterior half that provides some flexibility by offsetting its position on the body. For hip imaging, optimal placement of the anterior half of the phased-array coil is over the affected hip and not centrally over the body.

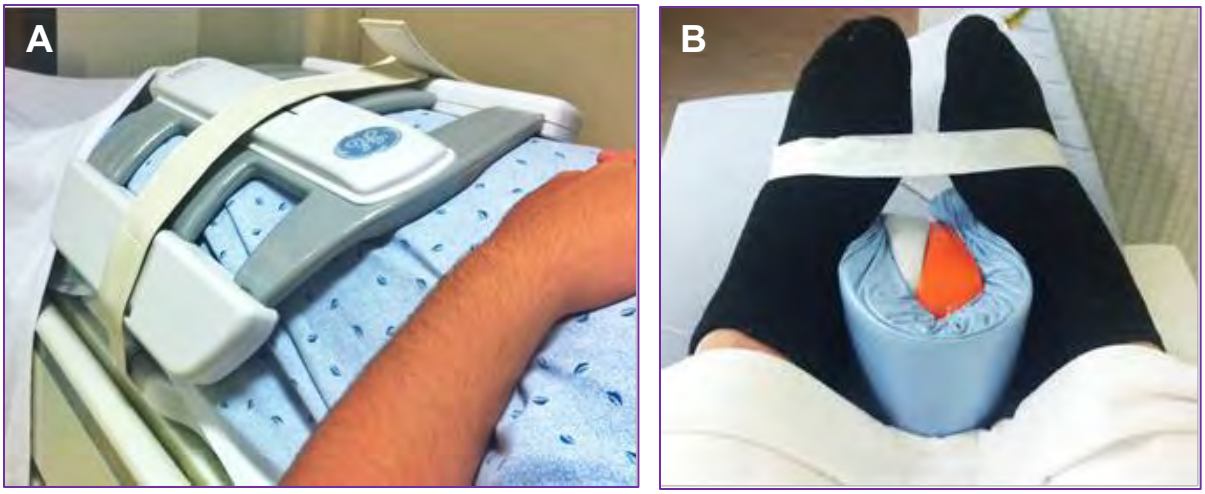

Figure 43. Hip positioning. (A) Place the anterior portion of the phased-array coil over the affected hip. Placing the coil in this position provides the most uniform signal coverage and may also reduce the risk of aliasing effects on larger patients. (B) Place a sponge to separate the ankles and tape the toes together to place the hip joint in the optimal alignment.

Planes of Acquisition

Imaging of the hip should always be unilateral. The spatial resolution required to fully visualize the hip labrum is very high, and therefore the FOV must be small (~20-24cm). Along with a high matrix and thin slices, a phased-array coil is not only required but optimally should be a high-element phased-array coil. Typically, planes of acquisition for the hip include the axial, coronal, sagittal, and oblique-sagittal planes (**Figure 44**). The axial plane usually consists of one large-FOV, fat-suppressed series that covers the entire bony pelvis from the iliac crest through the symphysis pubis superior-to-inferior (S/I) and from greater trochanter of one hip through the greater trochanter of the other. This series provides a wide survey of the entire bony pelvis to rule out any pathology outside the hip that may be a possible cause of symptoms such as **osteomyelitis** or metastasis.

Small-FOV axial imaging of the hip is prescribed orthogonally S/I but may require a slight degree of obliquity in the anterior-to-posterior (A/P) direction if the patient is not lying flat on the MRI table. Patients with severe hip pain often are unable to lie perfectly flat but instead favor the painful side by not putting as much weight on it. In the axial plane, typically two series are run: a T1W or PDW series and an intermediate-weighted TE/long TR fat-suppressed series (TE: 45-50msec; TR: >2500msec). Coverage is from above the acetabulum down through the greater trochanter.

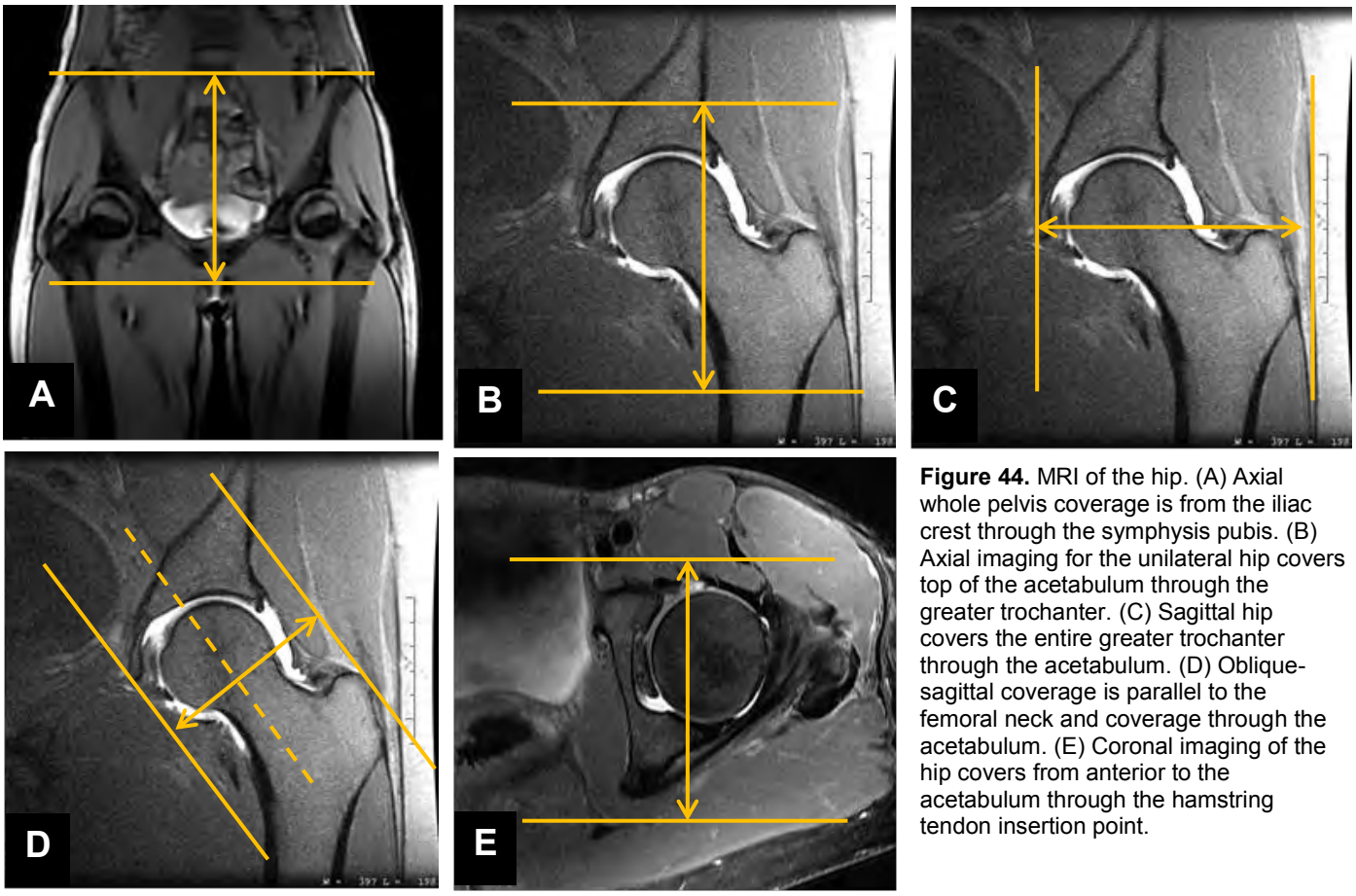

Figure 44. MRI of the hip. (A) Axial whole pelvis coverage is from the iliac crest through the symphysis pubis. (B) Axial imaging for the unilateral hip covers top of the acetabulum through the greater trochanter. (C) Sagittal hip covers the entire greater trochanter through the acetabulum. (D) Oblique-sagittal coverage is parallel to the femoral neck and coverage through the acetabulum. (E) Coronal imaging of the hip covers from anterior to the acetabulum through the hamstring tendon insertion point.

Coronal slice orientation is orthogonal to the plane of the pelvis. Like the axial series prescription, the coronal plane may need to be obliqued slightly in the A/P direction. Like the axial plane, in the coronal plane a T1W or PDW series as well as an intermediate-weighted TE/long TR fat-suppressed series are performed. Thin slice imaging is important in the coronal plane as visualization of the labrum is essential. Typical slice thickness is less than 4.0mm in the coronal plane. Coverage in the coronal plane in the A/P direction is from anterior of the acetabulum through the hamstring insertion at the ischial tuberosity.

The sagittal plane is an orthogonal sagittal acquisition running from the greater trochanter through the acetabulum in both T1W and intermediate-weighted TE/long TR fat-suppressed sequences.

In addition to the imaging discussed above, an oblique series is typically run parallel to the femoral neck. Depending on the degree of obliquity, this series can be viewed as either an oblique-axial or an oblique-sagittal view. This series is typically only done as an intermediate-weighted TE/long TR fat-suppressed series and covers the entire acetabulum.

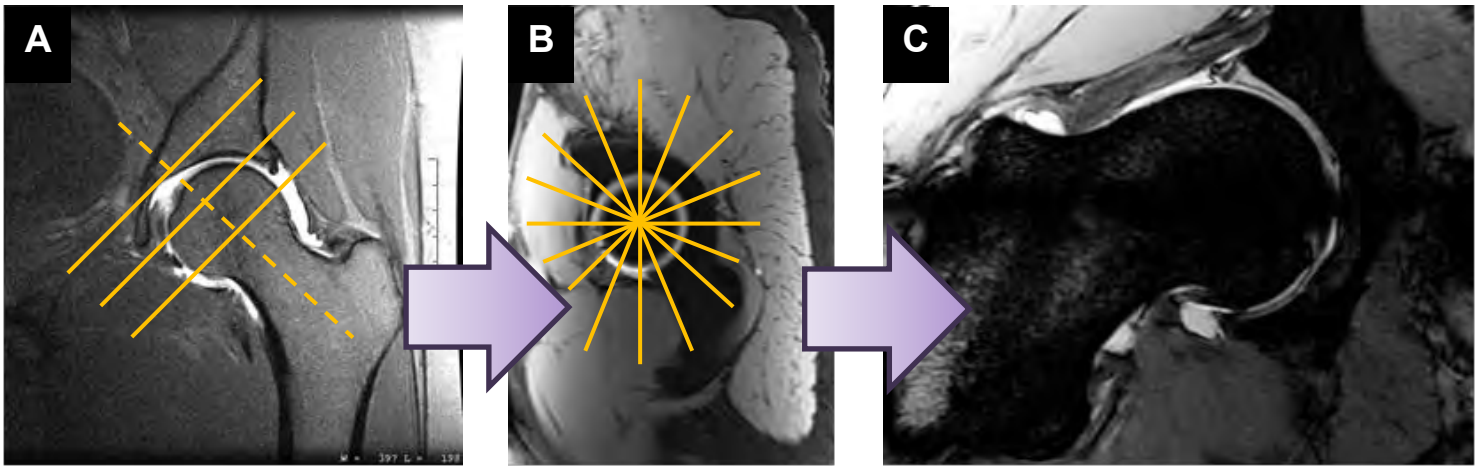

Figure 45. MR hip arthrogram radial fat-suppressed series. (A) Localize 3-5 slices that are perpendicular to the plane of the femoral neck. (B) From this series, localize the radial series off a slice closest to the acetabulum. (C) An image from the series.

MR Hip Arthrography

MR arthrography is the preferred modality for evaluating the acetabular labrum for abnormalities such as micro labral tears. MR hip arthrography comprises most of the imaging sequences of a routine hip but also includes T1W fat-suppressed imaging in the coronal and axial planes (**Figure 45**) as well as a radial fat-suppressed series in the same manner as the MR arthrogram of the shoulder. The addition of a dilute gadolinium injection into the joint increases the sensitivity of the radial series in visualizing small labral tears, and the hyaline articular cartilage can be difficult to identify without fluid in the joint. Once contrast has been administered, the difference in signal intensity of gadolinium (hyperintense) versus the signal of the cartilage (isointense) allows cartilage defects to be more easily identified (**Figure 46**).

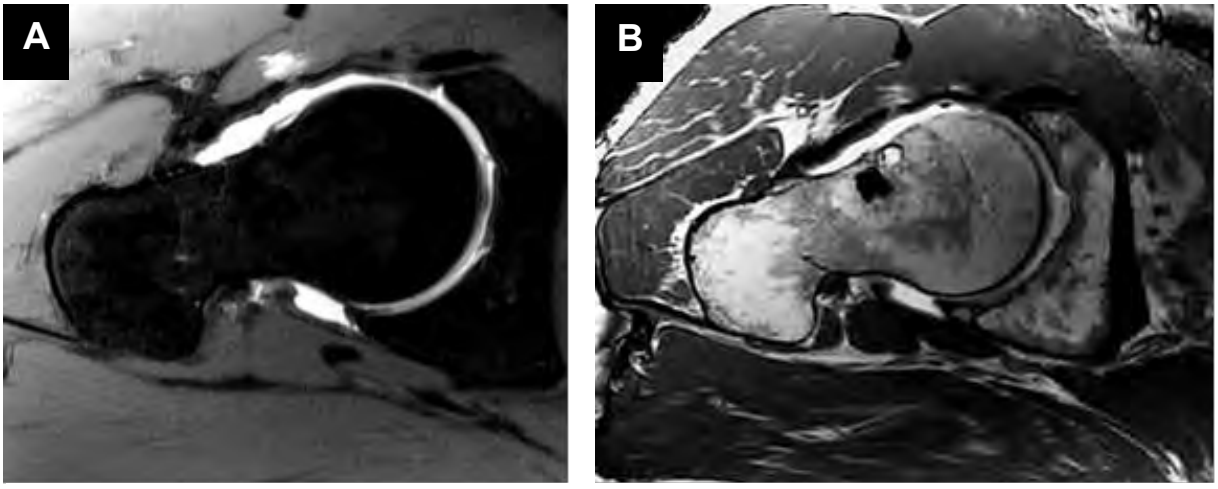

Figure 46. MR hip arthrogram oblique-sagittal series. (A) 2D oblique-sagittal T1W 3.0mm thick slice with chemical fat suppression. (B) 3D FIESTA acquired at 1.6mm thickness in the axial plane. The data have been reformatted into an oblique-sagittal plane.

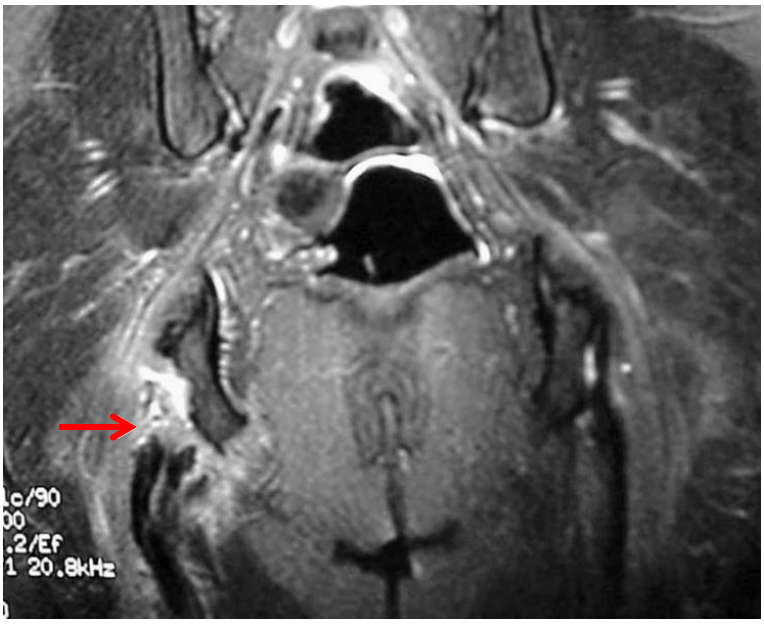

Figure 47. Hamstring tear. Coronal T2W image shows avulsion of hamstring from ischial tuberosity (arrow).
Courtesy of Nancy Major, MD.

Figure 48. 32-year-old male with avascular necrosis (AVN) of the femoral head of the right hip. High-resolution coronal 2.8mm T1W demonstrates hypointensity and indication of AVN (circle).

Common Pathology

Several different abnormalities can be identified on MR imaging of the hip, including muscle injuries, abnormalities in the bone, and intra-articular abnormalities. Muscle abnormalities are identified when abnormal signal is seen within the muscle or tendon. Abnormal high signal can indicate either a full thickness tear — if the tendon is surrounded by fluid — or a muscle strain if the tendon or muscle remains intact but has abnormal signal within the structure (**Figure 47**).

Fractures can occur in all portions of the pelvis and hip and are diagnosed when a linear area of low signal is surrounded by high signal that represents bone marrow edema. In older or **osteoporotic** patients, **insufficiency fractures** can occur, commonly located in the sacrum, pubic bones, and the femoral head, neck, and intertrochanteric region.

Evaluation of avascular necrosis is a common indication for MR imaging, typically revealing an irregular area of hypointense signal in the subchondral location. A tell-tale sign of AVN is when bone marrow edema can be identified in the bones around the pelvis and hips as hypointense signal on T1-weighted images and markedly hyperintense on T2-weighted fat-suppressed images (**Figure 48**).

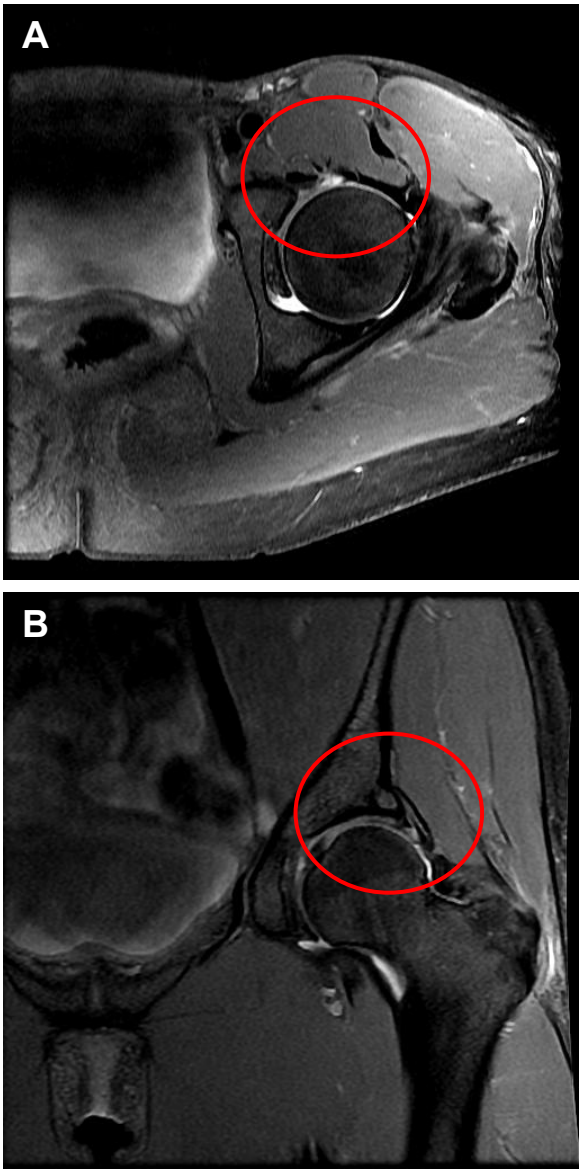

Figure 49. 32-year-old female with a large tear of left acetabular labrum in the anterosuperior quadrant of the left hip. (A) Axial intermediate TE PDW with chemical fat suppression. (B) Coronal intermediate TE PDW with chemical fat suppression.

The labrum is normally adherent to the acetabulum, and labral detachments occur when the labrum is separated from the acetabulum and are diagnosed by the appearance of fluid between these two structures. MR arthrography can reveal if the labrum configuration is deformed, indicating labral pathology. Without arthrography, signal abnormalities within the labrum can be appreciated, but tears through the labrum and labral detachments are much more difficult to identify (**Figure 49**).

LOWER EXTREMITY IMAGING — THE KNEE

Anatomy of the Knee

MR examination of the knee is the most requested musculoskeletal examination. MRI has proven to be highly accurate for diagnosing pathology of the anterior cruciate ligament (ACL) and menisci, both important anatomic structures for normal function.

The knee joint is comprised of a network of ligaments that hold the bones of the knee in place and consist of the distal femur, proximal tibia, proximal fibula, and the sesamoid.

The distal femur has two condyles, the medial (larger) and the lateral. Anteriorly, a groove is present between the condyles known as the trochlea. The condyles and the trochlea are lined by hyaline articular cartilage.

The proximal tibia makes up the other side of the joint space. It has two epicondyles, the medial and lateral, also lined by hyaline articular cartilage.

The proximal tibia has two bony protuberances within the center of the surface that accept the insertion of the cruciate ligaments; this area is not lined by hyaline articular cartilage.

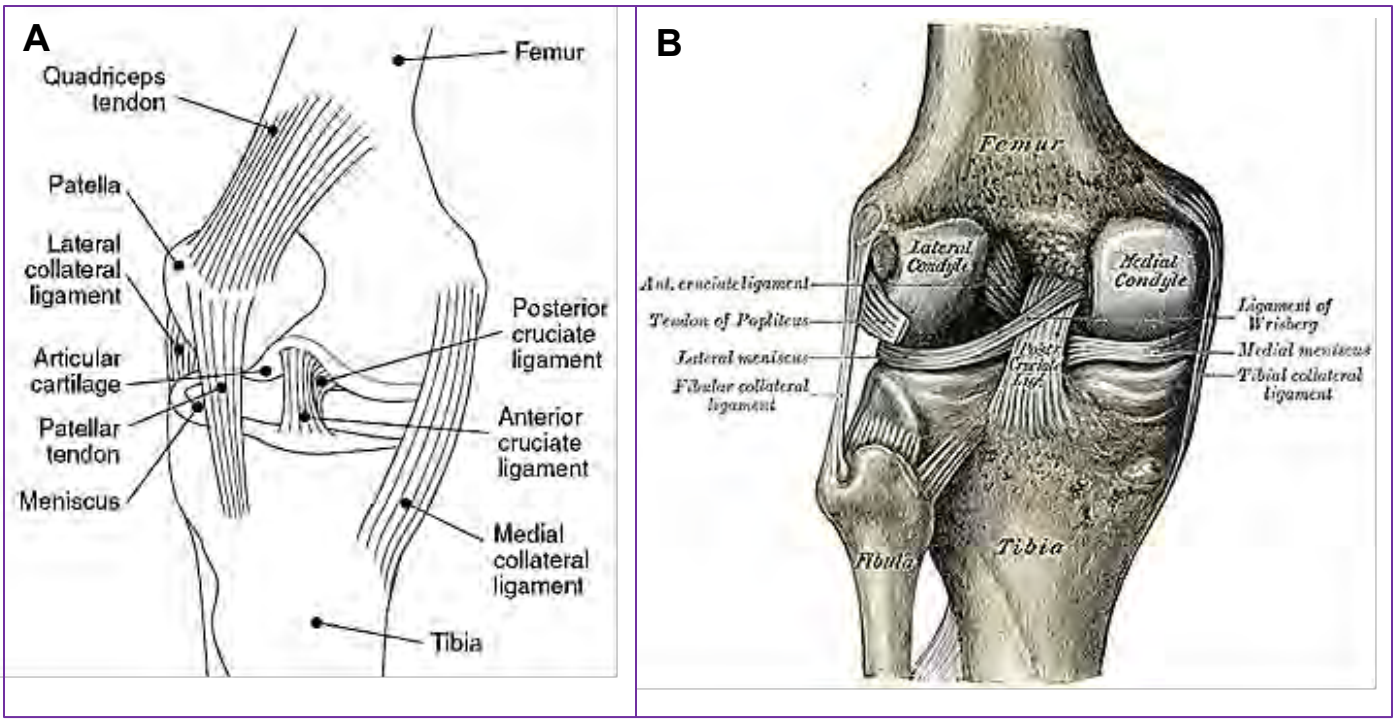

Figure 50. Anatomy of the knee. (A) Available at Wikimedia Commons Knee Medial View. (B) Available at: Wikimedia Commons.

The proximal fibula is the fourth bone located at the knee joint; it acts as an insertion site for one of the hamstring tendons (biceps femoris). The tibia and fibula articulate, but the fibula does not articulate with the femur (**Figure 50**).

The sesamoid-shaped bone is called the patella, the largest sesamoid bone in the body and serves as an insertion site for the quadriceps tendon and is the origin of the patella tendon/ligament; 'sesamoid' and 'patella' are used interchangeably. The dorsal (posterior) patellar surface is lined by hyaline articular cartilage. The patella articulates with the trochlea of the femur, sliding up and down with extension and flexion of the knee joint (**Figure 51A**).

The bones are kept in an organized orientation by the ligaments, which allow the knee to bend without dislocating any of the bones (**Figure 51A**). At the outer aspect of the joint are the collateral ligaments. The medial collateral ligament (MCL) arises on the medial aspect of the medial femoral condyle and inserts at the medial aspect of the proximal tibia. The lateral collateral ligament (LCL) complex is comprised of three distinct structures: the biceps femoris tendon, which inserts on the proximal aspect of the fibula; the fibulocollateral ligament, which arises at the lateral aspect of the lateral femoral condyle and inserts onto the fibula, occasionally with the biceps femoris tendon; and the iliotibial band located anteriorly. The iliotibial band is the only lateral collateral ligament complex structure that inserts on the tibia; the insertion point is located on a small bony tubercle called **Gerdy's tubercle**.

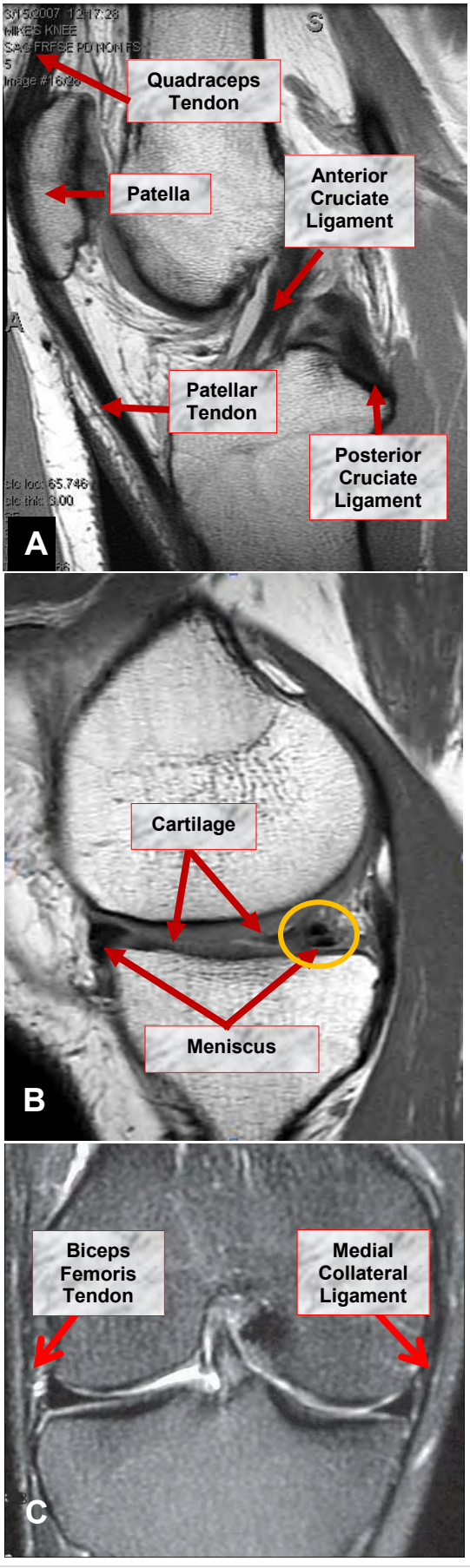

Within the notch (center of the knee) are located two cruciate ligaments. The ACL arises from the wall of the lateral femoral condyle and inserts on the medial spine of the tibia. The posterior cruciate ligament (PCL) arises from the medial femoral condyle and inserts on the lateral tibial spine. When normal, all ligaments and tendons should be low in signal on all imaging sequences (**Figure 51A**).

Within the knee joint itself are two C-shaped fibrous cartilage structures, the medial and lateral menisci (**Figure 51B**). These function as the shock absorbers by dissipating force across the knee. The meniscus ultimately protects the hyaline articular cartilage from being destroyed and fragmented, which would lead to cartilage loss and osteoarthritis.

Understanding of the anatomy of the meniscus is crucial if meniscal pathology is to be accurately diagnosed. The first two or three images of the meniscus in the sagittal plane should resemble a rectangular-shaped, low-signal structure. After these slices, the meniscus should take on the appearance of an elongated triangle; these triangles are referred to as the anterior and posterior horn. The best and most accurate diagnosis of meniscal pathology is arrived at by having thorough knowledge of the shape of the meniscus and then choosing the correct imaging protocol (**Figure 51C**).

Figure 51. Anatomy of the knee. (A and B) Sagittal PDW. (C) Coronal T2W. Note the meniscal tear in image B (circle). *(C) Courtesy of Nancy Major, MD.*

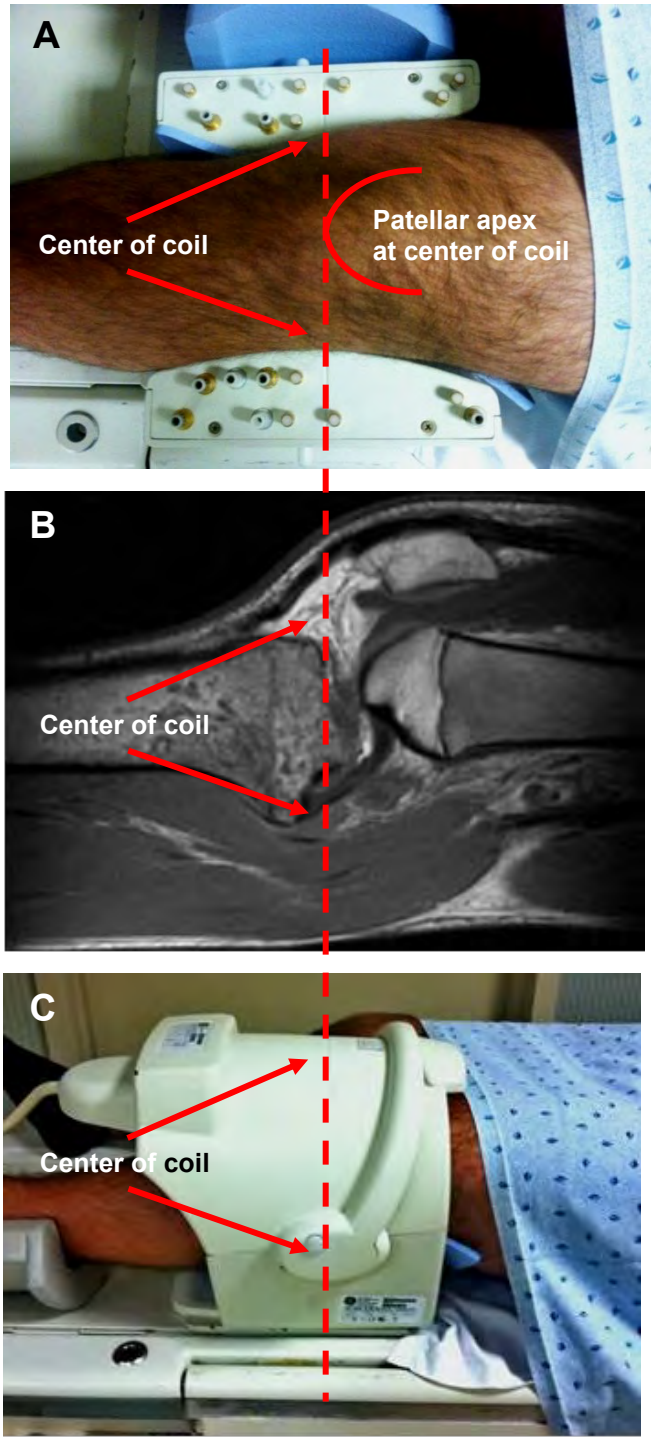

Figure 52. Knee positioning. (A and B) Place the apex of the patella at the center of the knee array coil. (C) Support the ankle and foot for patient comfort and joint stability to reduce the risk of motion.

Knee Positioning

Positioning of the knee is straightforward. Place the knee in a comfortable, straight position. Many current knee phased-array coils have a convex curvature that allows a slight bend to the knee, preventing the cruciate ligaments from being too taut (**Figure 52**). It is *not* necessary to internally rotate the knee 5^0 - 15^0, as was once common, to place the anterior cruciate ligament into an orthogonal-sagittal plane. This technique was often employed before advances in MR technology permitted high SNR ultra-thin slice thickness with high-resolution 2D and/or 3D pulse sequences that show the ligament in its entirety within a single acquired slice.

Planes of Acquisition

Imaging of the knee consists of imaging in all three planes using two differing contrasts in each plane. For non-fat-suppressed imaging, either T1W or proton density-weighted imaging is used. The PDW series provides higher SNR than the T1W series and provides excellent contrast in the joint space, making visualization of small mensical tears more conspicuous. For fat-suppressed imaging, intermediate weighted-TE/long TR imaging is used.

Axial imaging provides good visualization of the patellar-femoral articulation as well as the quadriceps tendon and the patellar ligament. Sagittal imaging provides excellent visualization of the lateral and medial menisci and the anterior and posterior cruciate ligaments. Coronal imaging yields excellent visualization of the menisci as well as the medial and lateral collateral ligaments (**Figure 53**).

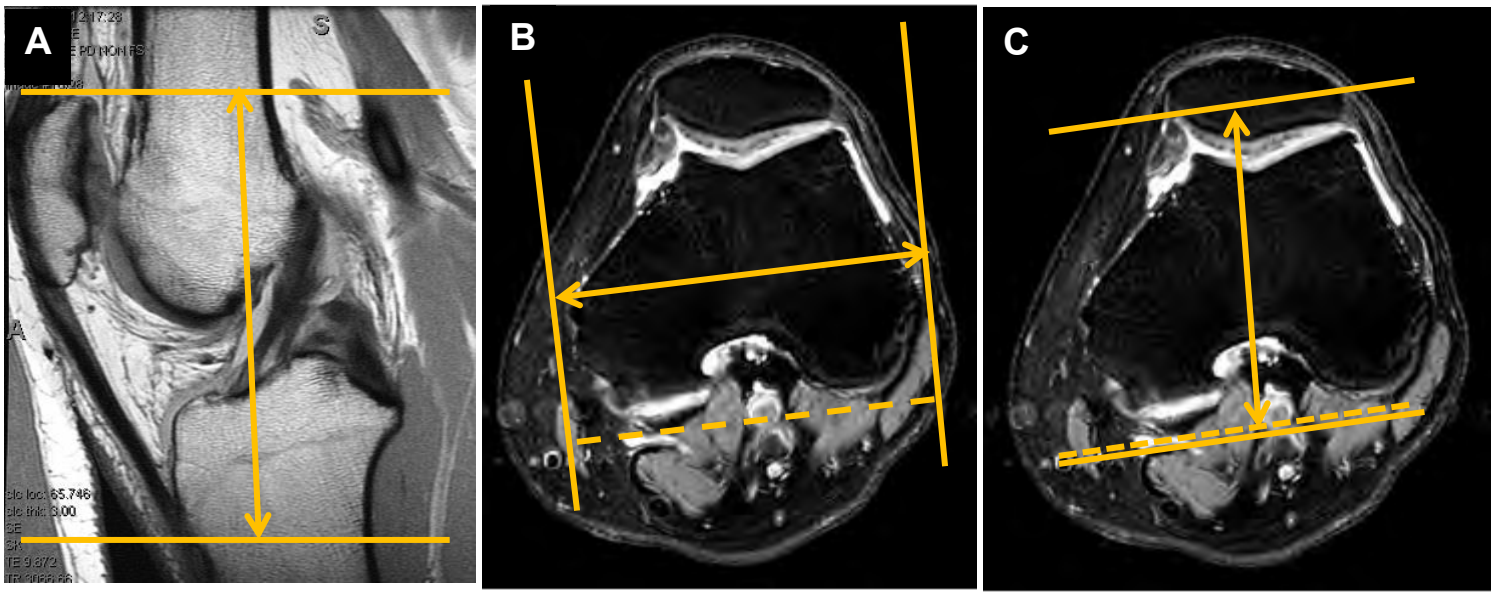

Figure 53. MRI of the knee. (A) Axial coverage includes the top of the patella through the patellar tendon insertion. (B) Oblique-sagittal imaging is perpendicular to the plane of the posterior femoral condyles. (C) Oblique-coronal coverage is parallel to the plane of the femoral condyles.

The axial imaging sequences are orthogonal to the long axis of the distal femur and proximal tibia. Coverage in the axial plane covers the entire patella from its superior base to the insertion point of the patellar ligament into the tibia.

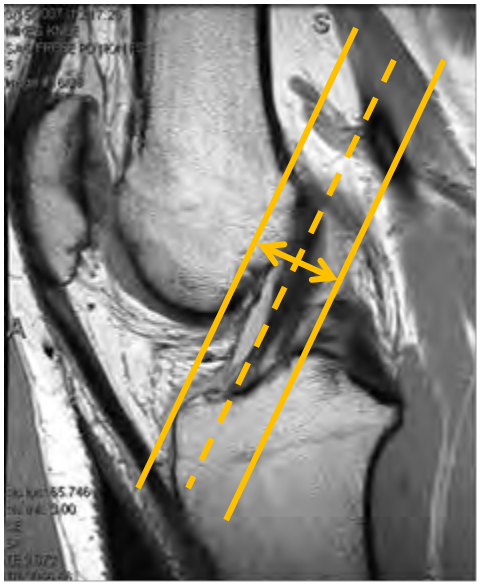

Figure 54. Optional oblique-coronal imaging is parallel and through the anterior cruciate ligament.

The coronal plane is parallel to the plane of the posterior femoral condyles. The coverage in the coronal plane is through the entire knee joint from posterior condyles to the patella.

Sagittal imaging is exactly perpendicular to the coronal plane, which is perpendicular to the plane of the posterior femoral condyles. Coverage in the sagittal plane is entirely through the knee from the medial condyle to the lateral condyle.

For further evaluation of anterior cruciate ligament, an oblique-coronal series is done that runs parallel to the long axis of the ACL in the sagittal plane. It is best to prescribe a single slice precisely through the center of the ACL and then prescribe 5-7 slices on either side. These slices should be less than 3.0mm in thickness (**Figure 54**).

MR Knee Arthrography

MR arthrograms of the knee are rare. The image quality of standard non-contrast knee imaging, particularly when using a 3.0T system, is so great that the use of intra-articular contrast is of little added value. When MR arthrography of the knee is requested, the typical imaging protocol is virtually the same as a standard non-contrast knee but with the addition of T1W fat-suppressed imaging in the axial and sagittal planes (**Figure 55**).

Figure 55. 36-year-old female with a 1.2cm ganglion cyst. Coronal T1W chemical fat-suppressed knee MR arthrogram demonstrates a 1.2cm cyst insinuated into the anterior cruciate ligament (circle).

Common Pathology

An orthopaedic surgeon can usually evaluate the ACL without the need for imaging, but occasionally the examination is confounded by the presence of a very large effusion, or the patient may be in such pain that examination is difficult. When the ACL tears, it can avulse from the femoral or tibial locations, but it most often tears within the substance of the ligament itself, requiring the need for imaging. High signal will replace the normal linear low signal of the ACL (**Figure 56**).

The PCL does not tear in the same manner as the ACL, becoming slightly thicker than normal and thus intermediate rather than high in signal. Again, short TE images are necessary to make the diagnosis of a torn PCL. The PCL can also avulse from the bones, either at the femoral origin or the tibial insertion.

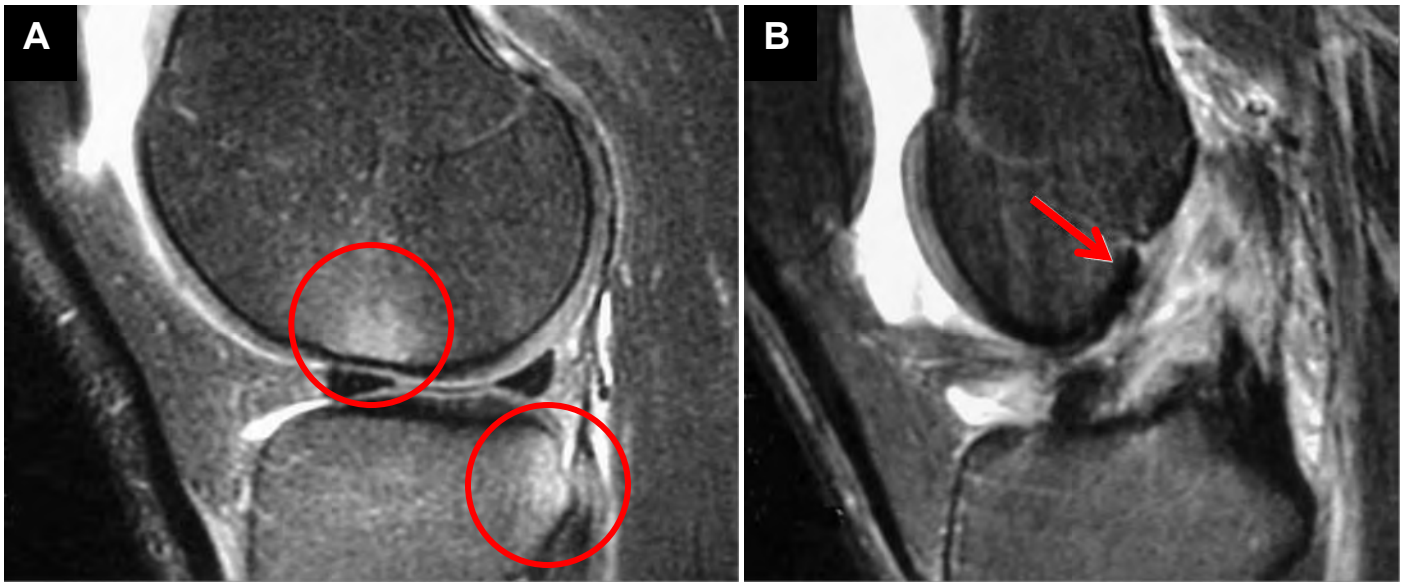

Figure 56. Anterior cruciate ligament tear. (A) Sagittal T2W shows abnormal signal representing bone marrow edema on the lateral femoral condyle and posterior lateral tibial plateau (circles). (B) High signal in the notch replacing ACL (arrow). *Courtesy of Nancy Major, MD.*

Meniscal tears can occur in a variety of configurations, including bucket handle tears through the body and anterior or posterior horn, radial tears, parrot beak tears, and peripheral tears. All of these meniscal tears will show an abnormally-shaped meniscus. One of the more commonly encountered tears is an oblique tear through the posterior horn of the meniscus, and high signal will be noted in an oblique direction that extends to the articular surface either superiorly or inferiorly (**Figure 57**).

Figure 57. Meniscal tear. Sagittal PDW image shows an oblique meniscal tear (arrow). *Courtesy of Nancy Major, MD.*

The collateral ligaments can also tear. The MCL can be completely or partially torn, as in a sprain. The MCL does not require surgical repair when it is the only ligament torn. However, the LCL complex must be repaired when torn. Assessing the integrity of these structures is imperative. If the LCL is torn along with the ACL or PCL, the knee is unstable and repair of the cruciate ligament alone will fail if the structures of the LCL are not also addressed. Similarly, in a multi-ligament injury involving the MCL, surgery is often required to increase overall knee stability.

The patellar tendon can also be injured either chronically or acutely. High signal, partially due to the edema surrounding the injury, is identified in the patellar tendon adjacent to the patella, as is increased thickness of the tendon. These findings have been termed “jumper’s knee” because of the tendency to see continual damage to the patellar tendon in athletes like basketball players. Complete tears are diagnosed when the tendon is ruptured and surrounded by fluid.

The patella can also become dislocated, which always occurs laterally. Bone contusions on the lateral femoral condyle result from patellar dislocation. Identification of a loose body that may have been sheared off from cartilage during the dislocation is important. When the patella dislocates, the medial retinaculum, which aids in keeping the patella normally located, becomes torn, and high signal will be seen throughout this structure. In most cases, the patella **reduces** to a normal location without intervention.

LOWER EXTREMITY IMAGING — THE ANKLE AND FOOT

Anatomy of the Ankle and Foot

There are three bones that comprise the ankle joint: the distal tibia, the talus, and the fibula. The distal tibia has a medial protuberance called the medial malleolus. The fibula at the ankle is called the lateral malleolus, and the talus at the ankle is referred to as the talar dome. Hyaline articular cartilage lines the articulating surfaces of the tibia and talar dome; the cartilage is quite thin at the ankle joint (**Figure 58**).

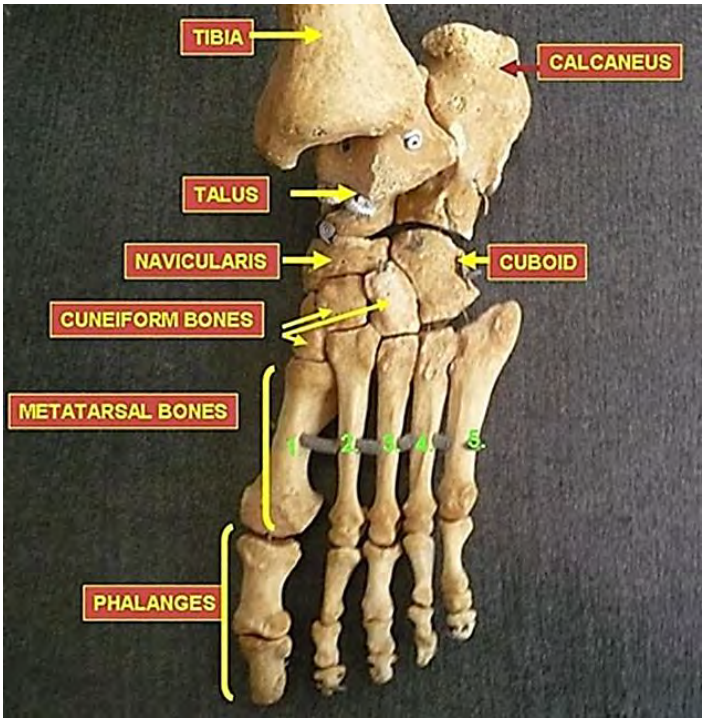

Figure 58. Bones of the foot.

*Courtesy Anatomist90.*Available at: Wikimedia Commons.

At first glance, the anatomy of the tendons of the ankle and foot seems quite complex. However, when divided into quadrants — anterior, posterior, medial, and lateral — the anatomy is straightforward (**Figure 59**).

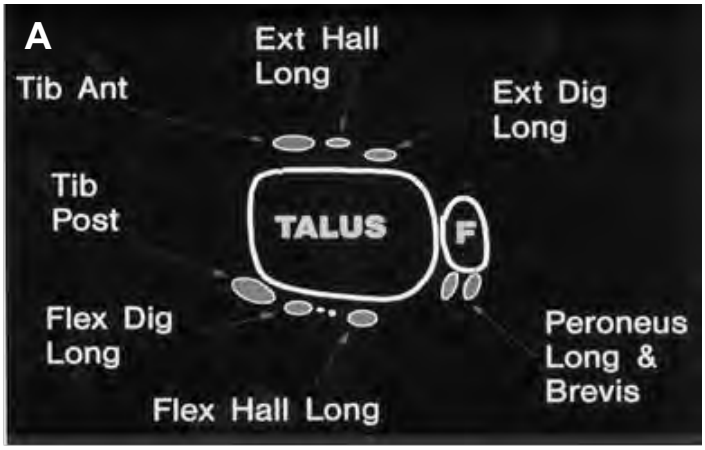

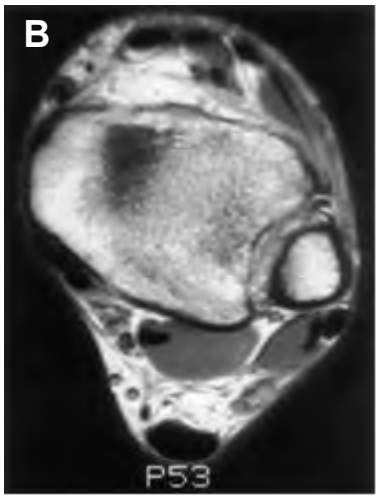

Figure 59. Anatomy of the ankle. (A) Schematic defining anatomy. (B) Axial T1W image at same perspective as schematic. *Courtesy of Nancy Major, MD.*

The extensor tendons are located anteriorly, the largest of which is the tibialis anterior. The Achilles tendon is located posteriorly. A small tendon called the plantaris tendon is often seen inserting into the Achilles tendon. The Achilles tendon does not have a tendon sheath and therefore slips of connective tissue can become trapped within the tendon, giving it a striated appearance (**Figure 60**).

Medially located are the flexor tendons: the posterior tibial tendon (PTT), flexor digitorum longus (FDL), and flexor hallucis longus (FHL). The PTT is crucial for ankle function and stability. This tendon runs along the medial malleolus to insert onto the navicular and is responsible for helping form the arch of the foot.

At the lateral aspect of the ankle are the peroneal tendons, longus, and brevis. These tendons should all be low in signal when normal. Ankle imaging is typically straightforward; however, challenges may arise in eliminating magic angle effects. Magic angle is often a problem when imaging the foot and ankle because many of the tendons can be coursing 55º to the bore of the magnet. Positioning the foot to avoid magic angle effects will be discussed later.

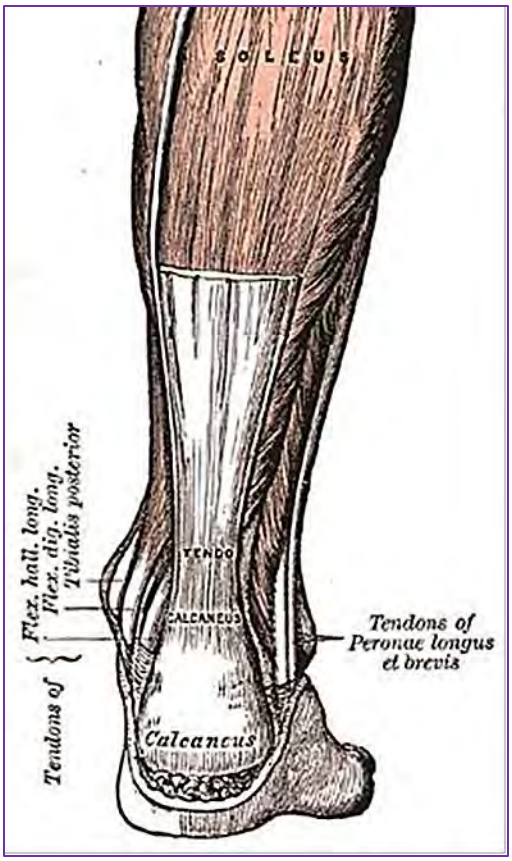

Figure 60. Achilles tendon and supporting tendons. Available at: Wikipedia.

The ligaments in the ankle consist of a complex of structures that help the ankle function as a hinge joint. Above the ankle joint located laterally are the anterior and posterior tibiofibular ligaments. Below the ankle joint are the anterior and posterior talofibular ligaments and the calcaneofibular ligament. At the medial side of the joint is the deltoid ligament. All these ligaments should image as low signal structures when normal, except the deltoid which occasionally demonstrates linear areas of intermediate signal through its fibers.

Ankle Positioning

One of two approaches may be taken when positioning the ankle for MRI evaluation: the patient is supine with the ankle flexed to a near 90^0 angle, or the patient is supine or prone with the foot extended to approximately 45^0 (**Figure 61**).

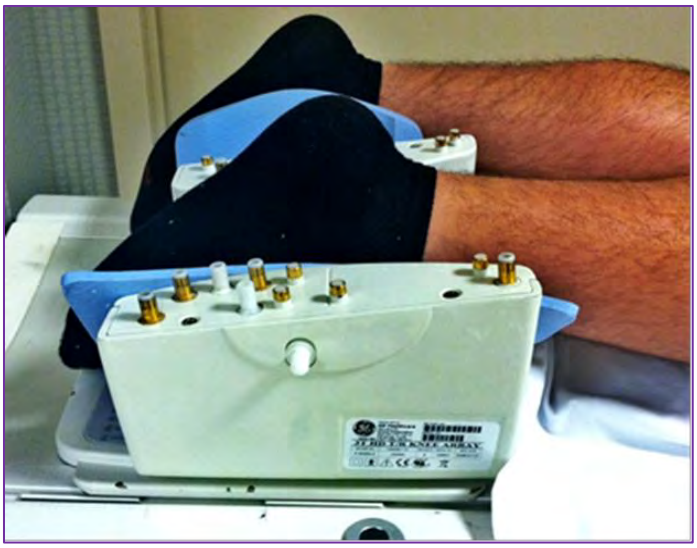

Figure 61. Ankle positioning. To avoid "magic angle" effects extend the ankle ~45° in the supine or prone position (prone shown here). This will eliminate magic angle effects on longer-TE sequences in the peroneal and posterior tibial tendons.

The decision about which positioning method to use is determined by the necessity to avoid the phenomenon of "magic angle." Recall that magic angle is a well-described hyperintense signal appearance in tendons or ligaments with well-organized collagen fibers that run in a single direction. When aligned at approximately 55^0 of the z-axis of the main magnetic field, these collagen fibers act in an anisotropic manner in much the same way the white matter tracts of the brain.[9]

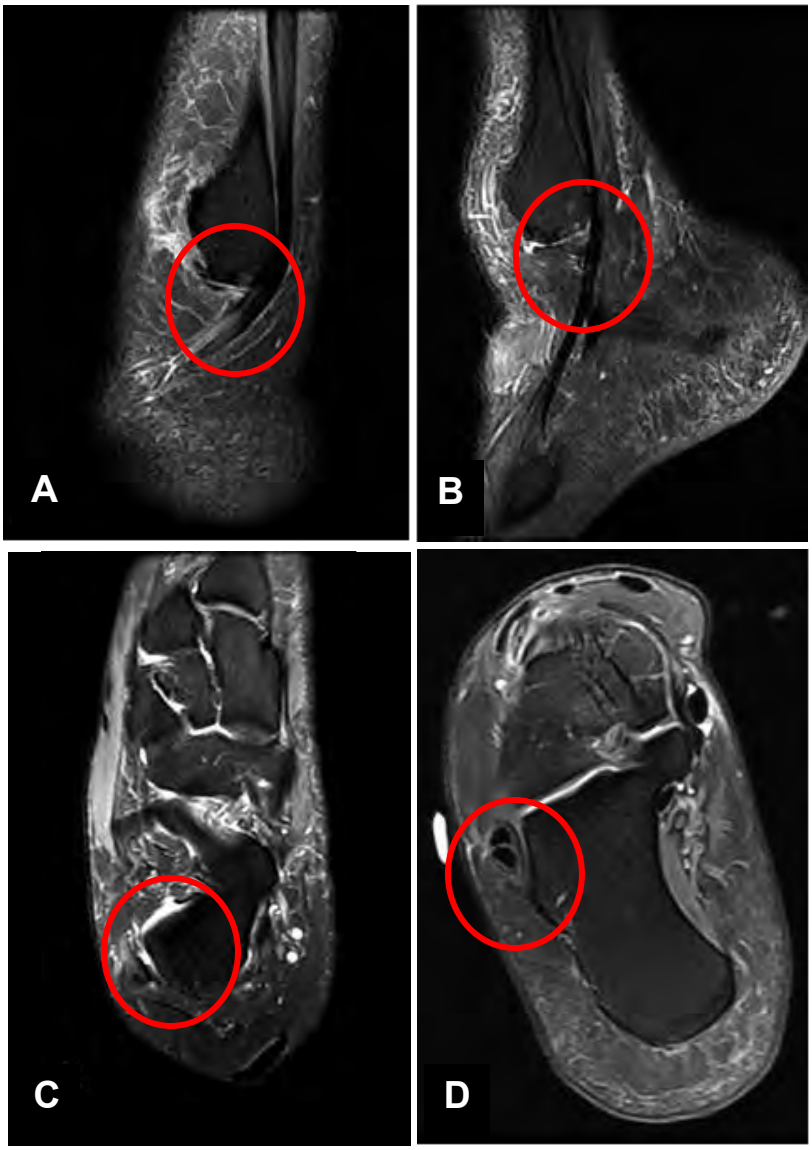

Figure 62. Magic angle effect. (A) Oblique-sagittal ankle and (C) Oblique-axial ankle exhibit the magic angle effect with hyperintense signal in the normal peroneal tendon as a result of positioning the ankle flexed to a 90° angle. (B) and (D) Corresponding images demonstrate the absence of the magic angle effect accomplished by repositioning the ankle to an angle less than 90°.

With short-TE pulse sequences (T1 or PDW), the result is hyperintense signal along the tendon or ligament that mimics inflammation when in fact the tissue is completely normal (**Figure 62**).

The peroneal and posterior tibial tendons of the ankle are highly susceptible to the magic angle phenomenon. When the ankle is positioned in a near-90^0 flexion, the peroneal and posterior tibial tendons have a significant portion aligned at near-55^0 to the z-axis and thus will exhibit magic angle signal characteristics. To avoid the magic angle effect, the foot should be extended to approximately 45^0. However, when evaluating the Achilles tendon, which is not particularly sensitive to magic angle effects, it is important to keep the foot and ankle in a near-90^0 position in order to stretch the Achilles tendon for best visualization (**Figure 63**).

Planes of Acquisition

Imaging of the ankle typically requires all three planes of imaging with short TE non-fat-suppressed imaging (T1W or PDW) and fat-suppressed imaging with intermediate TE/long TR imaging (~ 45-50msec TE/>2500msec TR).

Axial imaging is orthogonal and covers from the distal tibia through the calcaneus. The tendons can be followed contiguously on axial images, and lateral ankle ligaments are also seen to best advantage. Note that if a rupture of the Achilles tendon is apparent, axial imaging must cover sufficiently superiorly toward the insertion of the tendon into the gastrocnemius muscle.

Figure 63. Magic angle is not a concern when imaging the Achilles tendon and planar fasciitis. For these pathologies, position the ankle as close to 90 °as possible. Place support sponges under the calf and knee to provide comfort and leg stability.

Likewise, if plantar fasciitis is suspected, axial imaging must cover the entire soft tissue of the foot inferiorly (**Figure 64**).

Coronal imaging is obliqued to run parallel with the anterior/posterior plane of the talus bone. Slice coverage in the coronal plane is from the calcaneus through the navicular bone.

Like the coronal plane, the sagittal plane is also oblique but perpendicular to the coronal plane. For the oblique-sagittal, the obliquity is set to be parallel with the lateral/medial plane of the talus bone. Coverage in the sagittal plane is completely through the ankle, including the entire lateral malleous of the fibula through the medial malleous of the tibia (**Figures 65 and 66**).

Figure 64. Axial imaging of the ankle covers from the distal tibia/fibula through the calcaneus. NOTE: For plantar fasciitis, coverage is through the entire soft tissue of the bottom of the foot.

Common Pathology

The posterior tibial tendon can be partially or completely torn. When partially torn, there is alteration in the thickness of the tendon — either thicker or thinner — as well as abnormally high signal within the tissue. When completely torn, the tendon will be discontinuous and may have fluid around it. A diagnosis of **tenosynovitis** can be made when fluid is identified within the tendon sheath of any of the tendons around the ankle.

There are two exceptions to this diagnosis. If an ankle effusion is present, then fluid in the tendon sheath of the flexor hallucis longus should not necessarily be considered pathologic because the tendon sheath is contiguous to the joint.

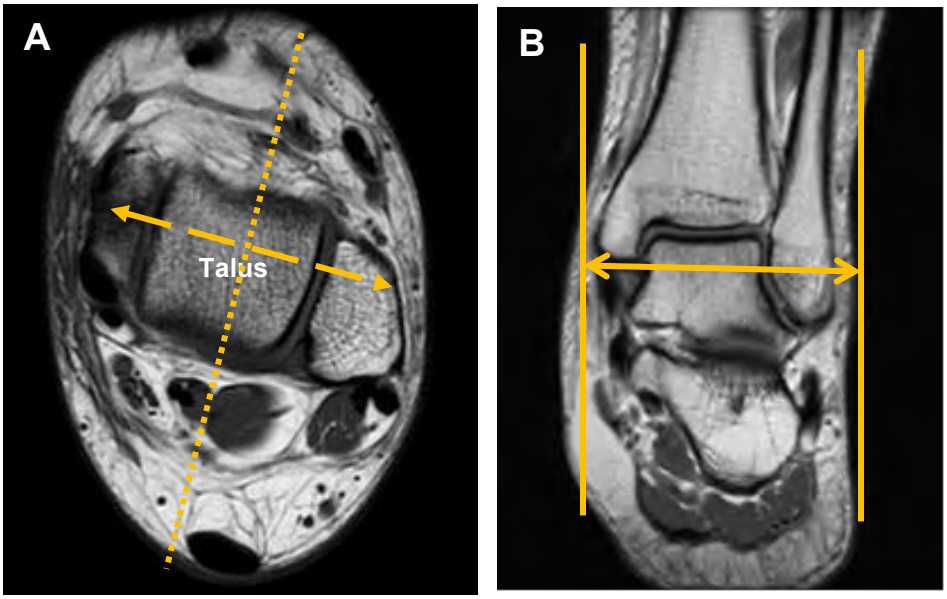

Figure 65. Oblique-sagittal imaging of the ankle. (A) The image is obliqued to the axis of the talus bone.(B) Coverage is from the medial malleolus through the lateral malleolus.

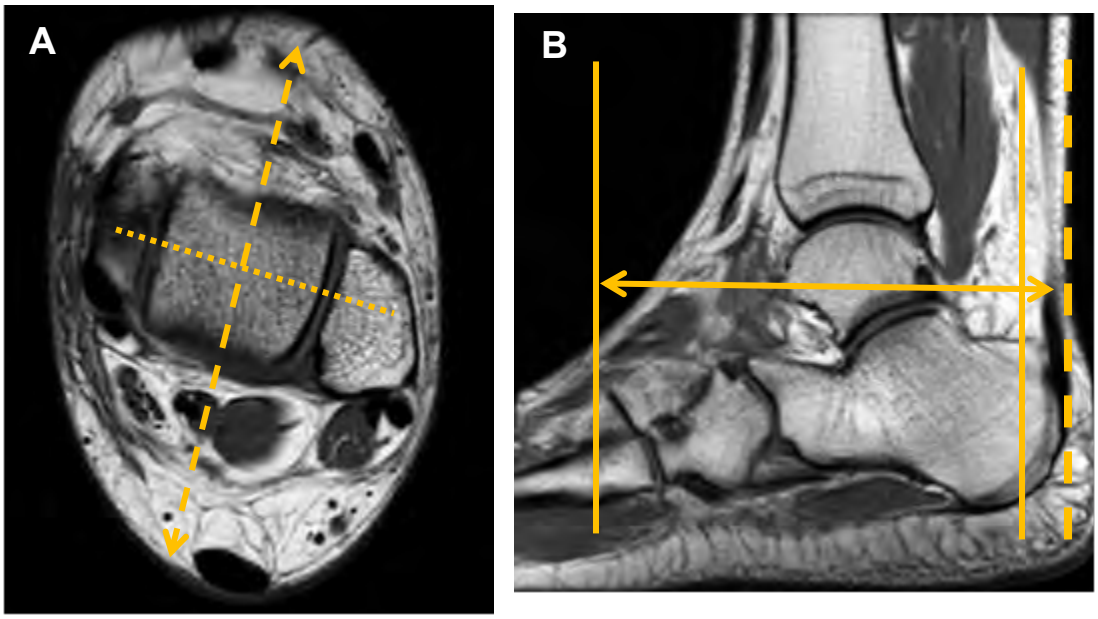

Figure 66. Oblique-coronal imaging of the ankle. (A) The image is obliqued to the axis of the talus bone perpendicular to the oblique-sagittal plane. (B) Coverage is from the mid-posterior calcaneous through the navicular bone. Note: if calcaneous pathology is suspected, the entire calcaneous is included in coronal imaging (dotted line in image B).

The other exception is the Achilles tendon, which does not have a tendon sheath. The Achilles tendon can become abnormal in thickness with partial tears and also have increased signal within the tendon, but a **paratenonitis** is the diagnosis made when increased signal is identified in the pre-Achilles fat and along the tendon.

The anterior talofibular ligament is often torn during an ankle sprain. This diagnosis is made when the ligament is not seen in its proper location. The calcaneofibular ligament and posterior talofibular ligament are much more difficult to tear. However, sprains can cause **fibrosis** and scarring, resulting in a thicker or thinner than normal ligament.

Osteochondral injuries can occur to the talar dome. MR imaging is particularly helpful in determining if there is a loose body and cartilage defect associated with the bone abnormality. T2-weighted images are especially useful with the application of fat suppression, allowing visualization of the cartilage and the bone marrow edema associated with these lesions (**Figure 67**).

When the plantar fascia is injured, abnormal signal can be seen within the fibers. Increased signal can be seen in the heel pad of the foot (subcutaneous tissue) adjacent to the fat pad. The plantar fascia can be completely torn and a gap in the fascia can be visualized (**Figure 68**).

Figure 67. Osteochondral lesion of talus. Coronal T2W image demonstrates an osteochondral lesion along talar dome (arrow). *Courtesy of Nancy Major, MD*

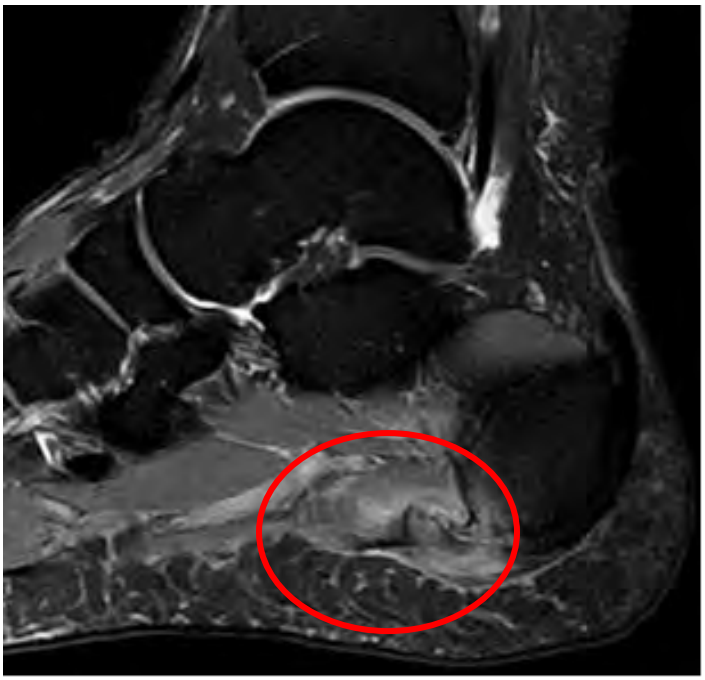

Figure 68. 48-year-old-male with severe plantar fasciitis of the right foot. 2.0mm sagittal PDW image with chemical fat suppression demonstrates a high-grade tear of the plantar fascia at its origin at the calcaneous (circle).

SUMMARY

MSK MRI is not only a demanding but exacting evaluation. A combination of strict adherence to high spatial resolution standards along with exact positioning and slice plane acquisitions will ensure highly diagnostic exams. Continuing education in the advances of MR imaging of the musculoskeletal system is essential for providing a safe and comfortable patient exam and diagnostic images that will guide patient management and treatment.

An intimate knowledge of the anatomy and physiology of the joints is an important factor for proper and timely musculoskeletal imaging. A technologist with intricate knowledge of bony anatomy and physiology becomes a true working partner with the radiologist.

REFERENCES

1. Congressional Research Service website. The Changing Demographic Profile of the United States. Available at: http://www.fas.org/sgp/crs/misc/RL32701.pdf. Accessed May 8, 2013.

2. The Children's Hospital of Philadelphia Health Information website. Sports Safety – Injury Statistics and Incidence Rates. Available at: http://www.chop.edu/healthinfo/sports-safety-injury-statistics-and-incidence-rates.html. Accessed June 12, 2013.

3. Centers for Disease Control and Prevention website. Sports-Related Injuries Among High School Athletes - United States, 2005-06 School Year. Available at: http://www.cdc.gov/mmwr/preview/mmwrhtml/mm5538a1.htm. Accessed June 12, 2013.

4. Centers for Disease Control and Prevention website. Inpatient Surgery data. Available at: http://www.cdc.gov/nchs/fastats/insurg.htm. Accessed May 8, 2013.

5. American Medical News website. Hip, knee replacement surgery rates skyrocket over 7 years. Available at http://www.amednews.com/article/20080505/health/305059956/6/. Accessed June 12, 2013.

6. Koch KM, Brau AC, Chen W, et al. Imaging Near Metal with a MAVTIC-SEMAC Hybrid. *Magn Reson Med*. 2011;65:71-82.

7. ibid

8. ibid

9. Peh WC, Chan JH. The magic angle phenomenon in tendons: effect of varying MR echo time. *Br J Radiol.* 1998;71:31-36.

10. American College of Radiology MRI Accreditation Program Clinical Quality Guide v2.

PROTOCOLS

NOTE: The following protocols are meant as a suggested guideline as individual site preferences result in varied protocols. Where applicable, the American College of Radiology basic requirements for designated MSK imaging parameters are noted[10].

UPPER EXTREMITY

SHOULDER

PLANE	WEIGHTING	SLICE THICKNESS	TE	FOV	FAT SUPPRESSION
3-Plane Scout	NA	5-7mm	minimum	26cm	none
Axial	proton density (PD)	ACR: 4.0mm Rec: 3.0mm	25msec	13cm	none
Axial	intermediate PD	ACR: 4.0mm Rec: 3.0mm	45msec	13cm	chemical saturation
Oblique-Coronal	PD	ACR: 4.0mm Rec: 3.0mm	25msec	13cm	none
Oblique-Coronal	intermediate PD	ACR: 4.0mm Rec: 3.0mm	45msec	13cm	chemical saturation
Oblique-Sagittal	intermediate PD	ACR: 4.0mm Rec: 3.0mm	45msec	13cm	chemical saturation

SHOULDER ARTHROGRAM
Routine shoulder plus:

PLANE	WEIGHTING	SLICE THICKNESS	TE	FOV	FAT SUPPRESSION
Axial	3D FIESTA/ TrueFISP	1.2-1.6mm	in phase	14cm	none
Oblique-Coronal	T1	ACR: 4.0mm Rec: 3.0mm	minimum	13cm	none
Radial	T1	ACR: 4.0mm Rec: 3.0mm	minimum	13cm	chemical saturation
Oblique-Sagittal ABER view	intermediate PD	ACR: 4.0mm Rec: 3.0mm	45msec	13cm	chemical saturation

PROTOCOLS

NOTE: The following protocols are meant as a suggested guideline as individual site preferences result in varied protocols. Where applicable, the American College of Radiology basic requirements for designated MSK imaging parameters are noted.

ELBOW

PLANE	WEIGHTING	SLICE THICKNESS	TE	FOV	FAT SUPPRESSION
3-Plane Scout	NA	5-7mm	minimum	20cm	none
Axial	PD	ACR: 4.0mm Rec: 3.0mm	25msec	12cm	none
Axial	intermediate PD	ACR: 4.0mm Rec: 3.0mm	45msec	12cm	chemical saturation
Oblique-Coronal	PD	ACR: 3.0mm Rec: 2.0mm	25msec	14cm	none
Oblique-Coronal	intermediate PD	ACR: 3.0mm Rec: 2.0mm	45msec	14cm	chemical saturation
Oblique-Sagittal	PD	ACR: 3.0mm Rec: 2.0mm	25msec	14cm	none
Oblique-Sagittal	intermediate PD	ACR: 3.0mm Rec: 2.0mm	45msec	14cm	chemical saturation

ELBOW ARTHROGRAM

Routine elbow plus:

PLANE	WEIGHTING	SLICE THICKNESS	TE	FOV	FAT SUPPRESSION
Axial	T1	ACR: 4.0mm Rec: 3.0mm	minimum	12cm	none
Oblique-Coronal	T1	ACR: 4.0mm Rec: 3.0mm	minimum	14cm	chemical saturation

PROTOCOLS

NOTE: The following protocols are meant as a suggested guideline as individual site preferences result in varied protocols. Where applicable, the American College of Radiology basic requirements for designated MSK imaging parameters are noted.

WRIST

PLANE	WEIGHTING	SLICE THICKNESS	TE	FOV	FAT SUPPRESSION
3-Plane Scout	NA	5-7mm	minimum	14cm	none
Axial	T1	ACR: 3.0mm Rec: 3.0mm	25msec	10cm	none
Axial	intermediate PD	ACR: 3.0mm Rec: 3.0mm	45msec	10cm	chemical saturation
Oblique-Coronal	PD	ACR: 3.0mm Rec: 1.6-2.0mm	25msec	9cm	none
Oblique-Coronal	intermediate PD	ACR: 3.0mm Rec: 1.6-2.0mm	45msec	9cm	chemical saturation
Oblique-Sagittal	PD	ACR: 3.0mm Rec: 1.6-2.0mm	25msec	9cm	none
Oblique-Sagittal	intermediate PD	ACR: 3.0mm Rec: 1.6-2.0mm	45msec	9cm	chemical saturation

WRIST ARTHROGRAM

Routine wrist plus:

PLANE	WEIGHTING	SLICE THICKNESS	TE	FOV	FAT SUPPRESSION
Oblique-Coronal	T1	ACR: 4.0mm Rec: 3.0mm	minimum	9cm	none
Oblique-Coronal	T1	ACR: 4.0mm Rec: 3.0mm	minimum	9cm	chemical saturation

PROTOCOLS

NOTE: The following protocols are meant as a suggested guideline as individual site preferences result in varied protocols. Where applicable, the American College of Radiology basic requirements for designated MSK imaging parameters are noted.

LOWER EXTREMITY

UNILATERAL HIP

PLANE	WEIGHTING	SLICE THICKNESS	TE	FOV	FAT SUPPRESSION
3-Plane Scout	NA	7mm	minimum	48cm	none
Axial Whole Pelvis	Intermediate PD	ACR: NA Rec: 6.0mm	45msec	35-40cm	chemical saturation
Axial Hip Only	Intermediate PD	ACR: 4.0mm Rec: 3.0mm	45msec	20cm	chemical saturation
Oblique-Coronal Hip Only	T1	ACR: 4.0mm Rec: 3.0mm	minimum	20cm	none
Oblique-Coronal Hip Only	Intermediate PD	ACR: 4.0mm Rec: 3.0mm	45msec	20cm	chemical saturation
Sagittal Hip Only	Intermediate PD	ACR: 4.0mm Rec: 3.0mm	45msec	20cm	chemical saturation
Oblique-Sagittal Parallel to Femoral Neck	Intermediate PD	ACR: 4.0mm Rec: 3.0mm	45msec	20cm	chemical saturation

UNILATERAL HIP ARTHROGRAM
Routine Hip Plus

PLANE	WEIGHTING	SLICE THICKNESS	TE	FOV	FAT SUPPRESSION
Axial	3D FIESTA/ TrueFISP	1.2-1.6mm	in phase	18cm	none
Radial	T1	ACR: 4.0mm Rec: 3.0mm	minimum	18cm	chemical saturation

PROTOCOLS

NOTE: The following protocols are meant as a suggested guideline as individual site preferences result in varied protocols. Where applicable, the American College of Radiology basic requirements for designated MSK imaging parameters are noted.

PROSTHETIC HIP

PLANE	WEIGHTING	SLICE THICKNESS	TE	FOV	FAT SUPPRESSION
3-Plane Scout	NA	7mm	minimum	48cm	none
Coronal Whole Pelvis	STIR	ACR: NA Rec: 6.0mm	45msec	35-40cm	IR fat suppression
Axial Hip Only	T1	ACR: NA Rec: 6.0mm	minimum	20cm	none
Axial Hip Only	STIR	ACR: NA Rec: 6.0mm	45msec	26cm	IR fat suppression
Axial Hip Only	PD	ACR: NA Rec: 4.0mm	25msec	20cm	none
Coronal Hip Only	PD	ACR: NA Rec: 4.0mm	25msec	20cm	none
Sagittal Hip Only	PD	ACR: NA Rec: 4.0mm	25msec	20cm	none

PROTOCOLS

NOTE: The following protocols are meant as a suggested guideline as individual site preferences result in varied protocols. Where applicable, the American College of Radiology basic requirements for designated MSK imaging parameters are noted.

KNEE

PLANE	WEIGHTING	SLICE THICKNESS	TE	FOV	FAT SUPPRESSION
3-Plane Scout	NA	7mm	minimum	24cm	none
Axial	intermediate PD	ACR: 4.0mm Rec: 3.0mm	45msec	16cm	chemical saturation
Sagittal	PD	ACR: 4.0mm Rec: 2.0-3.0mm	25msec	14cm	none
Sagittal	intermediate PD	ACR: 4.0mm Rec: 2.0-3.0mm	45msec	14cm	chemical saturation
Oblique-Sagittal	intermediate PD	ACR: NA Rec: 1.8-2.6mm	45msec	14cm	chemical saturation
Coronal	PD	ACR: 4.0mm Rec: 3.0mm	25msec	14cm	chemical saturation
Coronal	Intermediate PD	ACR: 4.0mm Rec: 2.0-3.0mm	45msec	14cm	none

UNILATERAL KNEE ARTHROGRAM
Routine Knee Plus:

PLANE	WEIGHTING	SLICE THICKNESS	TE	FOV	FAT SUPPRESSION
Sagittal	T1	ACR: 4.0mm Rec: 2.0-3.0mm	minimum	14cm	chemical saturation
Coronal	T1	ACR: 4.0mm Rec: 2.0-3.0mm	minimum	14cm	chemical saturation

PROTOCOLS

NOTE: The following protocols are meant as a suggested guideline as individual site preferences result in varied protocols. Where applicable, the American College of Radiology basic requirements for designated MSK imaging parameters are noted.

ANKLE

PLANE	WEIGHTING	SLICE THICKNESS	TE	FOV	FAT SUPPRESSION
3-Plane Scout	NA	7mm	minimum	18cm	none
Axial	T1	ACR: NA Rec: 3.0mm	minimum	14cm	none
Axial	intermediate PD	ACR: NA Rec: 3.0mm	25msec	14cm	chemical saturation
Oblique-Sagittal	PD	ACR: NA Rec: 2.0-3.0mm	25msec	14cm	none
Oblique-Sagittal	intermediate PD	ACR: NA Rec: 2.0-3.0mm	45msec	14cm	chemical saturation
Oblique-Coronal	PD	ACR: NA Rec: 3.0mm	25msec	14cm	chemical saturation
Oblique-Coronal	intermediate PD	ACR: NA Rec: 3.0mm	45msec	14cm	none

UNILATERAL ANKLE ARTHROGRAM
Routine Ankle Plus:

PLANE	WEIGHTING	SLICE THICKNESS	TE	FOV	FAT SUPPRESSION
Sagittal	T1	ACR: 4.0mm Rec: 2.0-3.0mm	minimum	14cm	chemical saturation

PROTOCOLS

NOTE: The following protocols are meant as a suggested guideline as individual site preferences result in varied protocols. Where applicable, the American College of Radiology basic requirements for designated MSK imaging parameters are noted.

FOREFOOT

PLANE	WEIGHTING	SLICE THICKNESS	TE	FOV	FAT SUPPRESSION
3-Plane Scout	NA	7mm	minimum	18cm	none
Axial (short axis to foot)	T1	ACR: 3.0mm Rec: 3.0mm	minimum	12cm	none
Axial (short axis to foot)	intermediate PD	ACR: 3.0mm Rec: 3.0mm	25msec	12cm	chemical saturation
Sagittal	PD	ACR: 3.0mm Rec: 2.0-3.0mm	25msec	12cm	none
Sagittal	intermediate PD	ACR: 3.0mm Rec: 2.0-3.0mm	45msec	12cm	chemical saturation
Oblique-Coronal (long axis to foot)	PD	ACR: 3.0mm Rec: 3.0mm	25msec	12cm	none
Oblique-Coronal (long axis to foot)	intermediate PD	ACR: 3.0mm Rec: 3.0mm	45msec	12cm	chemical saturation

GLOSSARY OF ABBREVIATIONS

ABER	abduction external rotation (view)
AC	acromioclavicular (joint)
ACL	anterior cruciate ligament
A/P	anterior-to-posterior
AVN	avascular necrosis
DJD	degenerative joint disease
ETL	echo train length
FDL	flexor digitorum longus
FHL	flexor hallucis longus
FSE	fast spin-echo
FOV	field of view
GRE	gradient-echo
LCL	lateral collateral ligament
LUCL	lateral ulnar collateral ligament
MARS	metal-artifact-reduction sequence
MAVRIC	multi-acquisition variable resonance imaging combination
MCL	medial collateral ligament
mm	millimeter
msec	millisecond
MSK	musculoskeletal
NSA/NEX	numbers of signal averages/number of excitations
PCL	posterior cruciate ligament

GLOSSARY OF ABBREVIATIONS

PDW	proton density-weighted
PIP	proximal interphalangeal
PTT	posterior tibial tendon
RBW	receive bandwidth
RF	radiofrequency
SE	spin-echo
SEMAC	slice-encoding metal artifact correction
S/I	superior-to-inferior
SNR	signal-to-noise ratio
STIR	short-tau inversion recovery or short-T1 inversion recovery
T	tesla
T1W	T1-weighted
T2W	T2-weighted
T2'	T2 prime
T2*	T2-star
TE	echo time
TFCC	triangular fibrocartilage complex
TR	repetition time; time to recovery
TSE	turbo spin-echo
VAT	variable angle tilt

GLOSSARY OF TERMS

abduct/adduct
an abductor muscle draws a limb away from the midline or median plane of the body; an adductor muscle pulls the limb toward the midline

abscess
a collection of pus accumulated within tissues, organs, or confined spaces due to inflammation or infection

anisotropic/anistrophy
in diffusion-weighted imaging, the diffusion of water in a non-random, preferred pathway

antevert
to displace an organ or part by tilting it forward

arthrography
a series of joint images acquired after injection of a mixture of saline, radiopaque contrast material, and a diluted gadolinium-based contrast agent are injected directly into the joint under X-ray guidance; can be acquired via X-ray, CT, or MRI

arthroscopy/arthroscopic surgery
minimally invasive surgical procedure used to evaluate and/or repair many orthopaedic conditions

articulation, joint
the location at which two or more bones connect

artifact
in the science of imaging, a substance or structure not naturally present in living tissue but which appears in an image

atrophy, muscle
partial or complete wasting away of the muscle due to lack of use or disease

avascular necrosis (AVN)
cellular death (necrosis) of bone components due to interruption of blood supply where the bone tissue dies and the bones collapse; especially common in the hip joint, which may result in total hip replacement

avulsion/avulse
in medicine, an injury in which a body structure is detached from its normal point of insertion by trauma or surgery

bone marrow
flexible tissue found in the interior of bones where red blood cells are produced

cartilage
a flexible gel-like connective tissue found in the joints between bones, the rib cage, ear, nose, bronchial tubes, and intervertebral discs; classified into three types: elastic, hyaline and fibrocartilage

cervical
in MSK, the neck, or region of the neck

chemical shift
the difference in between resonant frequencies of any two signals

collagen
a naturally-occurring protein found especially in the connective tissue: tendon, ligament, cartilage, and bone as well as in other body areas

contrast, image
differences in signal intensity between two adjacent areas on an MR image

cortical bone
also known as compact bone, cortical bone forms the cortex, or outer shell, of most bones

cyst
an abnormal fluid-filled, closed cavity within the body

echo time (TE)
time interval between the initial RF pulse to the first echo of a pulse sequence, also echo delay time

edema
the accumulation of fluid within tissue spaces

effusion
seeping of fluid into a body cavity or space

extra-articular
occurring within a joint as opposed to intra-articular, which occurs within the joint

fascia
a layer or band of fibrous tissue that connects and/or supports muscles or organs

fibrosis
formation of excess fibrous connective tissue or organ tissue in a reparative or reactive process; can be reactive, benign, or pathological and similar to the process of scarring

field of view (FOV)
the area of tissue/anatomy to be imaged

fossa
depression or hollow in a bone or other part of the body

frequency-selective fat suppression
the application of a RF pulse at the resonant frequency of fat

gadolinium (Gd)
a rare earth element that when chelated is used as a paramagnetic contrast agent in MRI

Gerdy's tubercle
the insertion point of the LCL complex on a small bony tibial tubercle

gradient
a magnetic field that changes in strength along a given direction

gradient-moment nulling
reduces constant velocity motion and distortion in a pulse sequence

hematopoietic
the formation of blood or blood cells

homogeneity
the presence of uniformity; in MRI, magnetic field homogeneity is the most critical element in obtaining high image quality

hyaline articular cartilage
the most abundant type of cartilage in the human body; hyline covers the articular surfaces of bones in synovial joints, reducing friction and acting as a shock absorber; also found in the ribs, nose, ear, trachea, larynx, and smaller respiratory tubes

hyper/hypointense
in MRI, a hyperintense image shows the appearance of bright tissue against a dark background, as contrasted to hypointense, the appearance of dark tissue against a lighter background

insufficiency fracture
occurs when thin, weak, osteoporotic bone cannot support the normal load of the body

interleave
arrangement of the order of slice acquisitions so that the slices located next to each other are excited as far apart in time as possible

isocenter
the 3-dimensional exact center of the main magnetic field; isocenter is where the magnet is most homogeneous

isointense
intermediate signal intensity, showing neither hyper- nor hypointensity but a medium contrast against the background

isotropic
of equal physical properties along the x, y, and z axes, for example, a 0.5x0.5x0.5mm voxel

labrum
a lip or rim of cartilage around the edge of a bone

Larmor frequency
the frequency at which magnetic resonance is produced in a sample of hydrogen nuclei or other types of nuclei used in MRI; the frequency at which the hydrogen nuclei precess when disturbed from their alignment in the B_0 magnetic field

lesion
a wound, injury, or structural tissue change of traumatic or pathologic origin

ligament
fibrous tissue that connects bone to other bones

magic angle
a spurious increase in signal intensity of collagen fibers that course 55^0 to the z direction of the MR magnet on a short TE imaging sequence

magnetic susceptibility
the degree to which a tissue can be magnetized in the MR system

motion artifact
an artifact or signal not naturally present in living tissue, but which appears on MRI film due to movement of muscle or fluid or motion of any body part

magnetic resonance angiography (MRA)
a form of magnetic resonance imaging used to study blood vessels and blood flow, particularly for detection of abnormalities in the arteries and veins throughout the body

magnetic resonance imaging (MRI)
a method of visualizing tissues of the body by applying an external magnetic field that makes it possible to distinguish between hydrogen atoms in different environments

myxoid
resembling mucus

neurography
In MR, imaging specific to the nerves of the extremities

null point
the time from inversion of the longitudinal magnetization to –z until the longitudinal magnetization of *a particular tissue* crosses the midpoint between –z and +z where no net magnetization exists

osteochondral injury
injury to the smooth surface on the end of bones, ranging from a small crack to a piece of bone breaking off inside the joint

osteoporosis/osteoporotic
occurs when the creation of new bone does not keep up with the removal of old bone, resulting in weak and brittle bone. Can cause osteoporosis-related fractures, which most commonly occur in the hip, wrist, and spine; osteopenia is the risk for developing osteoporosis

osteomyelitis
inflammation or infection of the bone or bone marrow

paratenonitis
inflammation of the covering of the Achilles tendon, usually due to overuse, repeated movements, or ill-fitting shoes; frequently seen in marathon runners

phased-array coil
a type of surface coil composed of several coils and receivers that are linked together; signals from each of the coils and receivers are subsequently united to produce an image with high SNR

radiofrequency (RF)
the range of frequencies of electromagnetic radiation between 10 kilohertz and 100 gigahertz; used for radio communication

radiopaque
unable to be penetrated by x-rays or other forms of radiation

receive bandwidth (RBW)
a range of sequences accepted by the receiver to sample the MR signal; has a direct relationship to signal-to-noise ratio and depends on the frequency-encoding gradient and the data sampling rate

reduce
in orthopaedics, the moving of the dislocated bone back to its original place; dislocated or sprained bones can reduce on their own or be manipulated into place by the clinician or, in severe cases, by surgery

repetition time/time to recovery (TR)
the time interval between the beginning of one pulse sequence to the beginning of the next; TR determines the amount of T1 recovery permitted in any given pulse sequence

short-T1 inversion recovery or short-tau inversion recovery (STIR)
a fat suppression technique with an inversion time set to the null point of fat

signal-to-noise ratio (SNR)
amount of true signal relative to the amount of random background signal (noise) on an image

spatial resolution
determines image sharpness and detail and is the product of the number and sizes of the voxels in that range; the smaller the voxel size, the higher the spatial resolution, and the higher the spatial resolution, the sharper the anatomic detail

spin-echo (SE)
MR signal that appears due to the rephasing of spins by a 180° RF pulse that follows the initial 90° RF pulse in a spin-echo pulse sequence; spin-echo is also a pulse sequence name used to describe a pulse sequence that begins with a 90^0 slice excitation pulse followed by a 180^0 RF refocusing pulse

synovial
a synovial joint is the most common and most moveable type of joint in the body; what distinguishes a synovial joint from others joint types, eg, cartilaginous or fibrous, is the existence of capsules surrounding the articulating surfaces of the joint and the presence of lubricating synovial fluid within those capsules

synovitis
inflammation of the synovial membrane that lines the joints

tendon
tough band of fibrous connective tissue that usually connects muscle to bone; made of collagen, like ligaments

tendon sheath
a layer of membrane around a tendon that permits the tendon to move; the sheath's two layers are comprised of the synovial sheath and the fibrous tendon sheath

tendinopathy
tendon injuries that involve larger-scale acute injuries accompanied by inflammation

tendinosis
chronic tendon injury with damage to the tendon at a cellular level absent of inflammatory response

tenosynovitis
inflammation of the fluid-filled synovium (sheath) that surrounds a tendon; includes pain, swelling, and difficulty moving the joint

Tesla (T)
the preferred (SI) unit of magnetic flux density. One tesla = 10,000 gauss, the older (CGAS) unit; current range for patient images is 0.3T – 3.0T. Named for "The Father of Physics," Nicola Tesla (1856 – 1943) from Croatia, for his contributions to the field of electricity and magnetism

T1
time constant that characterizes the rate of longitudinal relaxation; time for 63% of a tissue's longitudinal magnetization to recover

T1-weighting (T1W)
generation of MR images under conditions that highlight differences in T1 between tissues

T2
time constant that characterizes the rate of transverse relaxation in a perfectly homogeneous magnetic field; time for 63% of a tissue's transverse magnetization to decay

T2-weighting (T2W)
generation of MR images under conditions that highlight differences in T2 between tissues

T2' (prime)
the dephasing of spins in the transverse plane due to local field susceptibility effects; when in combination with "true" T2 dephasing, anatomy will display T2* (star) contrast

T2* (star)
Signal decay of a transverse spin due to the combination of T2 and T2' (prime) contributions

TI
time to inversion; inversion time
time interval between a 180^0 inversion pulse and 90^0 excitation pulse

TR
repetition time; time interval between two RF excitation pulses in an MRI pulse sequence; also time to recovery or recovery time